OPTIMAL SIZING AND LOCATION OF ENERGY STORAGE SYSTEMS

by
ARYA SEVGEN

Submitted to Sabancı Graduate School Business
in partial fulfilment of
the requirements for the degree of Doctor of Philosophy

Sabancı University
December 2021

OPTIMAL SIZING AND LOCATION OF ENERGY STORAGE SYSTEMS

Approved by:

Date of Approval: December 16, 2021

Arya Sevgen 2021 ©

All Rights Reserved

ABSTRACT

OPTIMAL SIZING AND LOCATION OF ENERGY STORAGE SYSTEMS

ARYA SEVGEN

Ph.D. Dissertation, December 2021

Dissertation Supervisor: Prof. Abdullah Daşcı

Keywords: Energy storage, renewable energy generation, storage sizing, storage siting, island systems

Energy storage systems (ESSs) play an important role in the rate of renewable energy adoption. Because, in addition to their higher costs, renewable energy sources are also disadvantaged due to their highly variable and intermittent nature. Therefore, it is almost impossible to adopt renewable energy at a meaningful level without a well placed ESS infrastructure. Unfortunately, ESSs too may be quite expensive, which makes these infrastructure decisions even more important. Due to its popular nature, one might mistakenly believe that these ESSs are nothing but battery energy storage systems (BESS) placed at the sites of the renewable generation units. However, the most economical ESSs are those of pumped hydro storage (PHS) units that are dispersed across the geographies that are served by large electricity networks.

The subject of this dissertation is to study siting and capacity decisions of ESSs in electricity transmission networks. We consider systems where electricity generation units from renewable and conventional sources are already established. For such systems our purpose is to find the location and capacities of ESSs and transmission line capacities to minimize the total system costs. Perhaps the greatest challenge in finding optimal solutions of these set of structural decisions is the incorporation of operational decisions which influence as well as are influenced by these structural decisions. In fact, optimal resolution of operational decisions alone is a daunting task even in the smallest networks because these decisions must be dynamically made while considering the uncertainties in electricity demand and supply. Therefore, we are compelled to adopt a sample average approximation (SAA) approach in the incorporation of those operational decisions.

This dissertation has four main chapters. The introduction, apart from the overall motivation for this study, also presents a review of current technological and economical properties of wide variety of ESS alternatives. This section allows us to identify appropriate ESS alternatives that can be used in our models and their realistic cost estimates. The second chapter presents our problem in an island electricity system, which is commonly studied in energy literature for their simple transmission networks and small size. In our island system, there is only one generation unit, which is a wind farm, one demand node, and two alternative storage systems; one PHS with a known location and one BESS to be located at the site of the wind farm. Whenever there is a shortage, the demand is satisfied from diesel at the demand node. Hence, the structural decisions to be found are the capacities of ESSs and the transmission lines to minimize the total cost of investments, operations and maintenance, and diesel costs. We must also remark that capacity of an ESS is a pair of variables; one for the maximum energy storage and one for the maximum energy flow, which are commonly referred as the energy rate and power rate, respectively. By deploying two different storage types at different places, we investigate the circumstances where installation decisions change. Stochastic renewable energy generation and demand are taken into account by scenarios that are reproduced based on real data. The third chapter extends the mathematical model to a small grid system with 13 nodes that consist of various generation units and demand centers. Despite being far smaller than many realistic grid systems, the problem has shown to be far beyond resolution with the existing computational resources. Therefore, we have developed a two-stage algorithm, which determines the investment decisions in the first stage, followed by the second stage operational decisions. Finally, the fourth chapter revisits the island system with solar power instead of the wind power, to investigate how differences in the intermittent feature of the two most common renewable sources affect the optimal structural decisions.

ÖZET

ENERJI DEPOLAMA SISTEMLERI IÇIN EN IYI BOYUTLANDIRMA VE KONUMLANDIRMA

ARYA SEVGEN

Doktora Tezi, Aralık 2021

Tez Danışmanı: Prof. Abdullah Daşcı

Anahtar Kelimeler: Enerji depolama, yenilenebilir enerji üretimi, depolama boyutlandırma, depolama konumlandırma, ada sistemleri

Enerji depolama sistemleri (EDS'ler), yenilenebilir enerjinin benimsenme oranında önemli bir rol oynamaktadır. Halen yüksek olan maliyetlerine ek olarak, yenilenebilir enerji kaynakları, oldukça değişken ve kesintili yapıları nedeniyle de dezavantajlıdır. Bu nedenle, iyi yerleştirilmiş bir EDS altyapısı olmadan yenilenebilir enerjiyi anlamlı bir düzeyde benimsemek neredeyse imkansızdır. Ne yazık ki, EDS'ler de oldukça pahalı olabilir ki bu da bu altyapı kararlarını daha da önemli hale getirir. Popüler doğası nedeniyle, bu EDS'lerin yenilenebilir üretim birimlerinin bulunduğu yerlere yerleştirilmiş pil depolama sistemlerinden başka bir şey olmadığı yanılgısına düşülebilir ancak en ekonomik EDS'ler, coğrafyalara dağılmış pompalı hidro depolama (PHD) birimleridir.

Bu tezin konusu, EDS'lerin elektrik iletim şebekelerinde yerleşim ve kapasite kararlarını incelemektir. Halihazırda kurulu olan çeşitli yenilenebilir ve konvansiyonel kaynaklardan elektrik üretiminin yapıldığı ve talep profillerinin bilindiği sistemleri ele alıyoruz. Ancak, iletim hattı kapasitelerini EDS'lerin kararlarına ek olarak alınacak kararlar olarak görüyoruz. Belki de bu yapısal kararların optimal çözümlerini bulmadaki en büyük zorluk, bu yapısal kararları etkileyen ve aynı zamanda onlardan etkilenen operasyonel kararların dahil edilmesidir. Aslında, tek başına operasyonel kararların optimal çözümü en küçük ağlarda bile göz korkutucu bir iştir, çünkü bu kararlar, elektrik arz ve talebindeki belirsizlikler göz önünde bulundurularak dinamik olarak alınmalıdır. Bu nedenle, bu operasyonel kararların dahil edilmesinde stokastik yaklaşım methodu benimsemeye mecburuz.

Bu tez çalışması dört ana bölümden oluşmaktadır. Giriş, bu çalışmanın genel motivasyonunun yanı sıra, çok çeşitli ESS alternatiflerinin mevcut teknolojik ve ekonomik özelliklerinin bir konsolidasyonunu da sunmaktadır. Bu bölüm, modellerimizde kullanılabilecek uygun EDS alternatiflerini ve bunların gerçekçi maliyet tahminlerini belirlememizi sağlar. İkinci bölüm, basit iletim ağları ve küçük boyutları nedeniyle enerji literatüründe yaygın olarak incelenen bir ada elektrik sistemindeki için olan problemimizi sunmaktadır. Ada sistemimizde tek üretim birimi rüzgar santralidir, bir talep düğümü ve iki alternatif depolama sistemi, bilinen bir konuma sahip bir PHS ve rüzgar çiftliği sahasına yerleştirilecek bir batarya vardır. Talep bir kıtlık olduğunda, talep merkezinde bulunan dizelden karşılanır. Dolayısıyla, bulunması gereken yapısal kararlar, toplam yatırımı, işletme ve bakım maliyetini ve dizel maliyetlerini en aza indirgemek için EDS'lerin ve iletim hatlarının kapasiteleridir. Bir EDS'nin kapasitesinin bir çift değişken olduğunu da belirtmeliyiz; biri maksimum enerji depolaması için diğeri ise genel olarak güç oranı olarak adlandırılan maksimum enerji akışı için. İki farklı depolama türünü farklı yerlere konuşlandırarak kurulum kararlarının değiştiği durumları araştırıyoruz. Stokastik yenilenebilir enerji üretimi ve talebi, gerçek verilere dayalı olarak yeniden üretilen senaryolarla dikkate alınmaktadır. Üçüncü bölüm, matematiksel modeli, çeşitli üretim birimleri ve talep merkezlerinden oluşan 13 düğümlü küçük bir ızgara sistemine genişletir. Birçok gerçekçi grid sisteminden çok daha küçük olmasına rağmen, problemin mevcut hesaplama kaynaklarıyla çözümün çok ötesinde olduğu görülmüştür. Bu nedenle ilk aşamada yatırım kararlarını, ardından ikinci aşamada operasyonel kararları belirleyen iki aşamalı bir algoritma geliştirdik. Son olarak, dördüncü bölüm, en yaygın iki yenilenebilir kaynağın kesintili özelliğindeki farklılıkların optimal yapısal kararları nasıl etkilediğini araştırmak için rüzgar enerjisi yerine güneş enerjisine sahip ada sistemini yeniden gözden geçirmektedir.

ACKNOWLEDGEMENTS

I would like to express my sense of gratitude to Dr. Abdullah Daşcı who gave me the opportunity to do and accomplish my dissertation which enabled me to conduct plenty of research and I came to know about a lot of new things. During my doctoral studies, I always felt his utmost support and guidance in every manner, which was more than valuable. I consider myself very fortunate to be able to work under his supervision.

Additionally, I would like to offer my special thanks to Dr. Raha Akhavan-Tabatabaei who constantly encouraged me by giving advice and helping on my academic and particularly teaching development since the beginning of my PhD program. Working as her teaching assistant gave me the opportunity to get to know her and she became one of the most valuable people that Sabanci University added to me.

I would also like to thank Dr. Mümtaz Karataş for his contributions to the organization of the latest version of my dissertation.

I am also thankful to the members of dissertation the committee: Dr. Raha Akhavan- Tabatabaei, Dr. Mümtaz Karataş, Dr. Alper Şen and, Dr. Kemal Kılıç for their valuable time and helpful suggestions.

Finally, I would like to extend my deepest gratitude to my parents for their never ending support and understanding.

To my mom and dad...

TABLE OF CONTENTS

LIST OF TABLES

LIST OF FIGURES

1. INTRODUCTION

Electricity is generated by using renewable and non-renewable sources. Traditionally, non-renewable sources such as coal and natural gas have been dominating the global electricity generation. In 2019, they accounted for around 60% of the electricity generation according to BPEnergy [2021]. In addition, natural gas has a considerable share in the global electricity generation, with 23%. Nuclear power plants, whereas, started to generate electricity in the 1950s, and the global share of this generated electricity recently reaches to 11%. Global shares of the other main sources are shown in Figure 1.1.

However, fossil fuels can bring harmful environmental problems like water and air pollution, global warming, and public health problems. Therefore, these issues are the significant drivers of the shift towards renewable energy sources usage. The major renewable electricity sources are solar, wind, biomass, hydropower, tidal, wave, renewable waste, and geothermal energy. Among the renewable sources, hydro power and wind power contribute the most to the electricity generation. Based on the report prepared by RenGSR , renewable sources have enough capacity to provide 26.5% of the global electricity demand where 16.5% comes from hydro power, and 7.5% represents wind and solar by the end of 2017. Even though hydropower is still the leader globally, wind and solar capacity doubled themselves in the last decade. In EU, however, electricity generation from wind overtakes hydropower in 2017, as depicted in Figure 1.2. Moreover, solar power has become the trend in the last years. The shares of wind and solar power in renewable sources are 35.9 % and 12.2%, respectively, for the EU countries by 2018 [Statista, 2018].

Wind power is used to generate electricity in more than 90 countries where China is the leading country with almost 200 GW installed capacity. Wind farms can be located both onshore and offshore, while onshore means to place the wind turbines on land, the term offshore is used when wind turbines are established on the water.

According to U.S. Energy Information Administration (EIA) electricity is produced from solar energy by two different methods, which are photovoltaic (PV) cells and

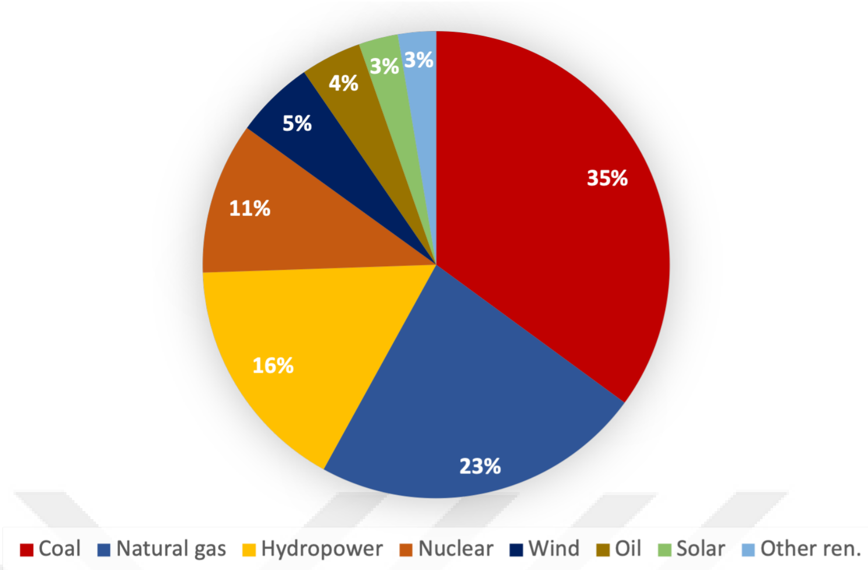

Figure 1.1 World electricity production by source, 2019: (Source: [BPEnergy, 2021])

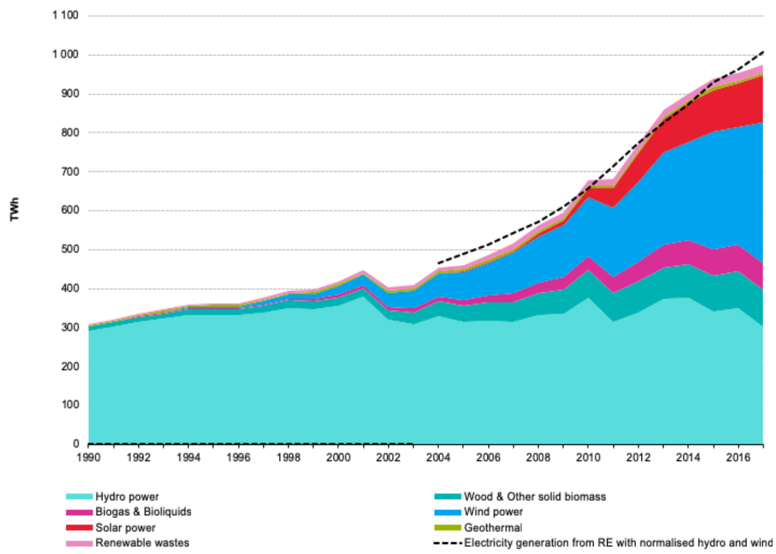

Figure 1.2 Gross electricity generation from renewable sources of EU-28 between 1990-2017, Source: [Statista, 2018]

thermal. Concentrated solar power (CSP) is also used to generate electricity by focusing the sunlight from a large area by using mirrors. Almost half of the installed capacity of CSP belongs to Spain. While thermal energy is mostly used for buildings or water heat, PV cells convert the sunlight into electricity in PV power plants, and this electricity is then distributed for the general usage of electricity. PV cells can be even placed into small electronic devices like calculators. China, the USA, Japan, and Germany are the top countries based on the installed PV capacity.

1.1 Electricity Consumption

Electricity is vital to our daily life since it is used for many purposes, such as heating, cooling, lighting, and all electrical devices in our homes. Electricity is consumed by residential, commercial, industrial, and transportation sectors. According to U.S. Administration [2020], 3.8 trillion kilowatt-hours (kWh) electricity is consumed in the United States in 2020, of which 38.9%, 34.8%, and 25.1% of the consumption belong to residential, commercial, and industrial, respectively. Also, electricity consumption share of transportation is 0.2% in the same year but may be expected to rise with the more widespread use of electric vehicles (EV).

Residential consumers consist of single or multi-family homes, which use electricity for heating, cooling, lighting, and electronic appliances such as refrigerators, dishwashers, computers, and televisions. Air conditions have the largest share in the consumption of residential. Commercial sectors include government and other public or private sectors. Some of the commercial sectors are health care, education, service, and mercantile. Industrial consumers are using the electricity for manufacturing, mining, producing, processing, construction, and assembling where 54% of the delivered electricity is consumed by them world-wide [Conti et al., 2016].

The transportation sector has been using fossil fuels for energy; however, rapid growth in the electric vehicle's usage results with an increase in electric consumption. According to National Renewable Energy Laboratory, electricity consumption for the transportation sector might increase considerably by 2050 [Mai et al., 2018]. The annual past and projected electricity consumption for different sectors are presented in Figure 1.3.

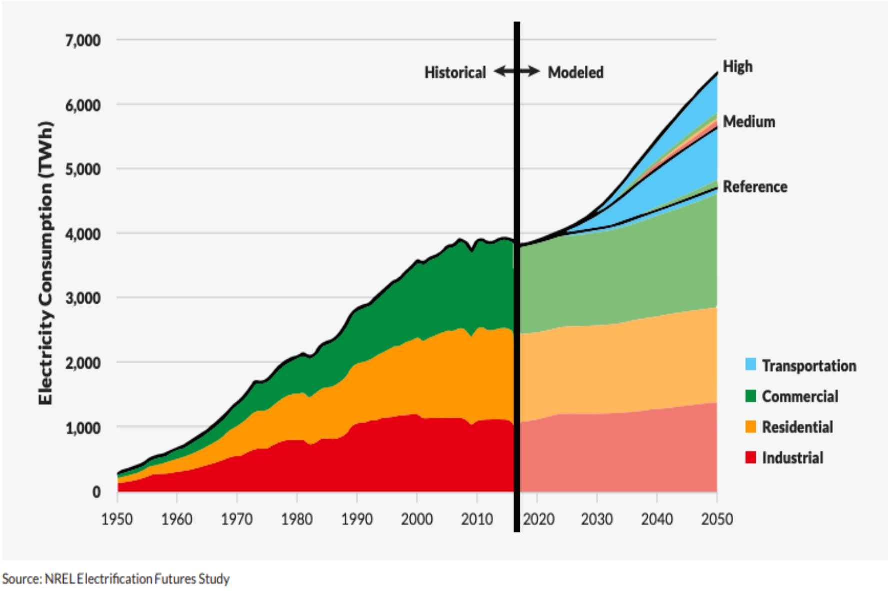

Figure 1.3 Historical and projected annual electricity consumption

1.2 Electricity Transmission and Distribution

Melhem [2013] states that, "a power transmission and distribution (T&D) system is that portion of the power system that moves power from where it is produced to where it is consumed". The term grid corresponds to T&D systems as a whole according to Eyer and Corey [2010]. In the traditional system, the electricity is generated only by a few large central stations and distributed to consumers. Load centers solely depend on large power stations. The generated electricity is carried through transmission lines to the distribution lines which carries electricity to consumers in a city or a region can reach the electricity via the distribution lines. Recently, many relatively small generation plants have begun to be placed. Governments, companies, and factories could produce their own electricity. Even individuals might generate electricity on their own with renewable energy sources like solar or wind energy. These generators which are placed near to the load centers are also feeding the electricity system in addition to large power plants. This type of power system is called the distributed power system where it brings both pros and cons. Small generators are mostly closer to the load center than the large power plants, hence transmission losses and costs are expected to reduce. However, reliability is one issue that should be taken into consideration when the distributed system is in use [Melhem, 2013].

Bulk energy is distributed over the long distances with high voltages to avoid the losses. Throughout the system, the voltage is reduced level by level by using transformers. The levels of the T&D system consist of transmission, sub-transmission, substation, primary feeder, service transformers, and the secondary and service level. Transmission and sub-transmission are generally formed as a network that has loops, where if one of the paths fails, the other one continues to send the electricity, whereas, substations are formed radially which consist of only one path. Power is sent to the substation via transmission and sub-transmission where the voltage level is dropped by transformers. Sub-transmissions transfer the electricity with relatively lower voltage and shorter distances than transmission lines. The service transformers finalize the voltage level and electricity is sent through these transformers either directly to the end customer or to secondary systems.

High voltage alternating current (HVAC) and high voltage direct current (HVDC) are differentiated by their geographic constraints, voltage conversation, and transmission losses. Although HVAC is a more common technology for transmitting the bulk power over long distances, HVDC has started to be used in many countries which was introduced by Sweden where a commercial HVDC transmission is constructed named Gotland 1 in 1954 [Rudervall et al., 2000]. Later on, China set the longest HVDC transmission line with 3000 km from Northwest to Eastern China in 2016 ABB. One of the most well-known installations of HVDC line is set between Oregon and California in the US which called Pacific Intertie [Gonen, 2011]. Likewise, the electricity is sent by means of DC voltage to Vancouver Island, Canada [Gonen, 2011]. Early on, DC was commonly used in the transmission systems, however, it was not efficient to send the power via DC at the time. That is why HVAC is still the dominant transmission technology today. After technological advancements, HVDC has become more economically and environmentally competitive compared with HVAC. Transmitting electricity with DC voltage is cheaper after a specific distance called also break-even point, before that point HVAC is more cost effective to construct since DC transmission requires many converters throughout the line. However, DC converters are quite expensive and the conversion process is subject to a loss of around 0.8-1% of the power [Melhem, 2013], where these costs directly affect the determination of the break-even distance. HVDC results in fewer losses and more power quality. On the top of that DC has no length limitation where AC does. Transmission could happen via underwater power cables since DC needs less isolation. For example, HVDC transmission lines are used for connecting the offshore wind farms to the grid with the sea cables where a company constructed an HVDC transmission to a wind farm called Dan Tysk which placed in the German North Sea [Garus, 2014].

As mentioned, the electricity generations mostly rely on bulk generators, however, it was not the case at the first years of the electricity distribution where the first electricity generation, which was Pearl St. Station, provided lightening over the Pearl St. in New York City. The generators were formerly using DC voltage and located near to the cities where they could supply electricity only to a few houses close to the generators. After the invention of AC voltage, electricity could be transmitted over long distances; thus, large-scale generators have been developed since then. Nevertheless, nowadays, small-scale generators are in demand, called distributed generator (DG), and located near to the load centers like the early ones. According to Fraser [2002], DGs have become common simply because the increase on demand, difficulties on constructed new transmission lines, and increasing concerns on climate change. DGs supply the electricity directly to the local distribution network where some examples could be renewable sources such as PV, biomass, wind, and geothermal or small turbines and fuel cells. Some wind turbines might not be accounted for DG since they could be placed in rural areas and require transmission system so that the wind power can be reachable by the load centers. Distributed power (DP), however, includes storage technologies besides generator units which are described in Section 1.5. The term distributed energy resources (DER) is a more broad term that includes both DG and DP together. Thus, DER could consist of either only DGs or a hybrid system (e.g., a PV panel and a battery storage system). Storage systems provide great potential to support the grid for distributed systems that consist of relatively small generators. There are plenty of benefits that storage technologies provide, and they also help to meet the general concerns about the system.

Although benefits of low voltage direct current (LVDC) systems for the distribution systems are being discussed, AC system is still being used in the last step of the electricity distribution. So, DG units should either provide AC load or convert DC into AC before dispatching the electricity. Even though each DGs' technologies are different, in the last step DC/AC converter is generally used to have an AC output. For example, PV panels generate DC outputs, however, it first uses DC/DC converter to regulate the voltage level, then the DC/AC converter is used for achieving the final AC output [Melhem, 2013].

1.3 System Characteristics

- Real power: Real power is (also called as true power, active power, and useful power) generally represented by P and measured in watts where the real power is the actual power that is consumed and transferred to the load.

- Reactive power: Reactive power is (also called as use-less power) generally represented by Q and in a unit of Volt-Amps-Reactive (VAR). Reactive power is only defined for AC systems. "The portion of electricity that establishes and sustains the electric and magnetic fields of alternating-current equipment [Akhil et al., 2015]."
- Apparent power: Apparent power is a combination of reactive and real power that is represented by S and measured in the unit of Volt-Amps (VA).
- Power factor: Power factor is real power over apparent power where apparent power is a combination of reactive and real power.
- Power rate: It is "the rate at which the storage system can discharge energy [Eyer et al., 2005]."
- Durability: Durability is the expected a lifetime of storage. It can be measured by the number of cycles (fully charged to empty) or the age of the storage.
- Discharge duration: Discharge duration is the amount of time that storage discharged at a rated power according to Akhil et al. [2013]. Discharge time may vary from seconds to months depending on the storage system. While double-layer capacitors, superconducting magnetic, and flywheels have short discharge duration time, seconds to minutes, battery types like lead-acid, Li-ion and sodium sulfur (NaS) have medium discharge times of minutes to hours. The flywheel could have both small and medium discharge duration depending on the storage capacities. The duration times of pumped hydro, compressed air, and redox flow are relatively longer than other storage systems IEC.
- Response time: Response time is the amount of time needed for storage system to reach and supply energy at its full rated power.
- Ramp rate: Ramp rate is the rate at which power can increase or decrease which are generally expressed as % per minute.
- Self-discharge: Stored energy can be dispersed as a consequence of some chemical actions [Eyer and Corey, 2010]. The rate of self-discharge depends on the storage system.
- Round trip efficiency: "The amount of electric energy output from a given storage plant/system per unit of electric energy input [Eyer and Corey, 2010]."
- Power conditioning: Power conditioning is a subsystem that storage types in-

clude which called power conditioning unit (PCU). PCUs transform the voltage and the form of the current (AC or DC) [Eyer and Corey, 2010].

1.4 Application Areas of ESSs

Based on DOE [2019] database, energy time-shift, supply capacity, frequency regulation, renewables capacity firming, supply capacity, and voltage support are the applications most deployed ones so far. ESSs can be classified into three main categories: Generation, Transmission and Distribution (T&D), and End-User applications.

1.4.1 Generation Applications

Combining renewable sources or power plants with ESSs has many benefits, both economically and environmentally. Energy storage could be used as a back-up in case of emergency situations like failures, which is also called as *reserve augmentation* [Committee, 2008]. Mainly to meet the peak-time demand or in case of growth in electricity demands, power plants may need to buy or rent new central plant stations. To defer or decrease these needs, storage systems could be used as the supply capacity.

More specifically, *spinning reserve* is an ancillary service which is defined as "the unused capacity which can be activated on decision of the system operator and which is provided by devices which are synchronized to the network and able to affect the active power [Rebours and Kirschen, 2005]." Spinning reserves are the primary sources that are ready to serve in case of outages or contingency incidents on the transmission or generator side, and must respond within 10 minutes. Spinning reserves are online; however, they are not being used at full capacity. Storage technologies can be used as spinning reserves.

Another ancillary services like *area regulation* or *regulation* is also beneficial and could be considered as an ESS application. The main aim of this service is to balance the difference between supply and demand, thus, maintain the system frequency [Eyer and Corey, 2010]. The generation units which have capability to increase or decrease the power output instantly do not need any external technology to maintain the frequency. However, especially for renewable sources, the regulation is a crucial issue since their power outputs are intermittent, and it leads to some problems with matching the supply and demand. In that case, storage could provide this regulation service. Another example is for large thermal generation units since they cannot respond to sudden changes immediately, storage can be used to provide regulation with charging and discharging the storage. The storage is charged to down the regulation by absorbing the excess demand from the grid and up the regulation by releasing the energy from the storage to fulfill the excess grid supply [Akhil et al., 2013]. Storages should have a rapid response; in other words, they should have a fast ramp rate. In this regard, flywheels and some battery types are suitable for regulation [Eyer and Corey, 2010].

Energy time-shift is also known as buy-low/sell-high transaction [Committee, 2008]. This application relies on storing energy whenever the energy usages and the value is low. The stored energy is then released and distributed to the grid with high prices and value at peak times. Since the aim is mostly to charge and discharge the energy at most for several hours (at most 6 hours), CAES and pumped hydro are appropriate storage systems for this application. For instance, both CAESs in Germany and the USA are storing the energy at off-peak times and release the energy at peak times during the day IEC.

Diurnal renewable levelizing is the application which aims to store the energy while there is excess load and use it at on-peak load hours. Likewise, *weekly renewable levelizing* and *seasonal renewable levelizing* focus on storing the energy for using it on-peak weekdays and on-peak seasons. For weekly storage systems, pumped hydro is appropriate with more than 48 hours of discharge duration, whereas, hydroelectric facilities store the energy more than months [Committee, 2008].

One of the application areas for renewable sources is *renewable capacity firming*. Capacity firming is postponing or reduce the needing for rent or purchase new generation sources [Eyer and Corey, 2010]. Renewable source output is smoothed with the existence of storage systems, which helps to mitigate intermittency as well as the ramping challenge.

1.4.2 (T&D) Applications

Due to the growth in electricity demand, especially in peak times, the capacity of transmission or distribution lines are not enough to meet the demand. It needs to be invested in line upgrades, which leads to high costs. In particular times (e.g., some specific day in a year or specific hour in a day), the lines are over the capacity, so even if new an infrastructure would be constructed, they would not in use all the time. *T&D upgrade deferral* is applied to avoid the high investment infrastructure costs by using energy storage that can be appropriately located downstream. Even small-sized storage can help to meet the demand in most of the time.

Similarly, in peak times, congestion on the lines occurs, and the electricity should be sent across other transmission lines or incur additional costs like congestion charges. The congestion could occur due to the outdated transmission lines. *Transmission congestion relief* is being applied with a storage system in which the storage is placed downstream [Eyer and Corey, 2010]. The energy can be stored when there is no congestion, in other words, off-peak times, and released during peak times to use the line capacity efficiently.

Another transmission line problem is associated with wind farms. They are generally installed where the wind is abundant and flow continuously, but these places are mostly rural areas that are far from the load centers and do not have transmission infrastructure. Transmission line construction should be jointly considered while a wind farm is being installed; otherwise, the line capacity might be less than or greater than the wind output depending on the weather conditions. Wind output could be curtailed because of the capacity limit. Therefore, in some situations where it might not be cost-effective to construct lines with some capacity, it could be supported with the ESSs instead.

Energy storage supports the T&D system by reducing the disturbances and balancing the system. Some of the applications of *T&D supporting* are voltage control and stability and reducing the load shedding. This kind of application requires very low response time (at most 20 seconds) and high charge-discharge cycles [Eyer and Corey, 2010]. Energy storage could provide reactive power, where they can both absorb the reactive power from the grid and release it to back to ensure that voltage levels are between required intervals.

The substations are also benefiting from the energy storage during the outages which supply power to the switching components and other equipment in the substation. Batteries are suited for this application where more than 100.000 storage system is placed at substations in the U.S. [Eyer and Corey, 2010]. Most particularly, lead-acid batteries are being used for this application.

Load leveling decreases the losses as well as defers to construct new lines at the transmission and distribution phase. In addition to transmission and distribution lines, storage also contributes to supply power on the peak demand intervals, which results in a decrease in resistive loss of the system. "Since T&D losses are proportional to the square of the load current, shifting any amount of load from peak to off-peak results in a net reduction of T&D losses [Nourai et al., 2008]."

1.4.3 End-User Applications

End-users include residential, commercial, and industrial customers who generally meet their entire electricity demand from the grid. The ones who possess a renewable energy system, on the other hand, could buy electricity from the grid partially or even do not buy any as soon as the generated electricity is sufficient. The end-users are charged by the utilities which are responsible for the distribution of the electricity.

Time of use (TOU) is the energy price that the customers are charged if they use the energy during a specific hour a day, a day in a week, or a season [Akhil et al., 2013]. *Load leveling* is applied by end-users such as households, factories, schools, and research institutes, hospitals, office buildings, etc, IEC. The target of the load-leveling is to decrease the load, which is supplied from the grid at on-peak times, thus reducing the TOU price. Load leveling is done by time-shifting. Since the electricity generally tends to be expensive at peak times, it could be supplied from storage, which is filled at off-peak times rather than the grid. NaS batteries are widely used for load leveling; almost 50% of consumers who built NaS battery storage system are using them explicitly for load leveling IEC.

Demand charge is one of the parts of the electric bill of commercial and industrial customers who are charged according to the highest load that they use it over a period. This amount is usually measured in 15-minute intervals. As long as the highest flow achieved, no matter if it is reached in one 15-minute interval or more, the charge will be the same. Supplying this energy constantly requires additional resources and additional costs as a consequence of investment for generators. So, this price is reflected in the electric bills. Demand charges apply not only the peak time of the day but also any time during the day. *Demand charge management* is concerned with reducing these high amounts of prices. Storage systems provide the potential to reduce these costs, especially for commercial users or the facilities, who consume electricity at some constant rate. They could store the energy, preferably off-peak times, and use it to reduce the demand charge price.

By nature, storage systems can be used as a backup for all types of customers in case of outages. Especially for commercial customers, storage systems provide power in emergency situations, particularly the ones in the hospitals.

1.4.4 Renewable integration

Regardless of the end-user type, storage systems help with *smoothing* the power output since the ramp-up and ramp-down frequently occurs in renewable sources. It helps maintain the voltage level and about the reliability issues [Kempener and Borden, 2015]. Battery technologies are suitable for this application since their response times are quite fast.

For residential users, storage systems are becoming more crucial since the widespread use of renewable sources like rooftop PV panels. End-users can save excess energy to use it later when the weather conditions are not favorable for producing electricity from renewables. They can also save their electricity to avoid high grid costs with time shifting at a smaller scale.

1.5 Energy Storage Systems

ESSs have been used for a large variety of applications and will be used for many other applications soon. According to DOE [2019], the USA, Japan, and China are the global leaders, respectively, in terms of installed storage capacity and the number of installed storage plants. ESS technologies are classified as electrical, mechanical, electrochemical, chemical, and thermal. An extensive categorization of the various storage types is shown in Figure 1.4. The technical characteristics of the main storage systems retrieved from Council [2016] are shown in Table 1.1.

Bulked storage systems are considered as the large-scale systems which have some

Table 1.1 Technical comparison of ESSs

	Power rating (MW)	Discharge time	Cycles, or lifetime	Self-discharge	Energy density (Wh/l)	Power density (W/l)	Efficiency	Response time
Pumped Hydro	100 – 2500	4 – 16h	30 – 60 years	~ 0	0.2 – 2	0.1 – 0.2	70 – 85%	10 s – min
Compressed Air	10 – 1000	2 – 30h	20 – 40 years	~ 0	2 – 6	0.2 – 0.6	40 – 70%	min
Flywheels	0.001 – 20	sec – min	20000 – 100000	1.3 – 100%	20 – 80	5000	70 – 95%	< sec
Li-ion battery	0.05 – 100	1 min – 8h	1000 – 10000	0.1 – 0.3%	200 – 400	1300 – 10000	85 – 95%	< sec
Lead-acid battery	0.001-100	1 min – 8h	6 – 40 years	0.1 – 0.3%	50 – 80	90 - 700	80 – 90%	< sec
Sodium-sulphur battery	10 – 100	1 min – 8h	2500 – 4500	0.05 – 20%	150 – 300	120 – 160	70 – 90%	< sec
Flow battery	0.1 – 100	hours	12000 – 14000	0.2%	20 – 70	0.5 – 2	60 – 85%	< sec
Superconducting Magnetic	0.1 – 1	ms – sec	100000	10 – 15%	~ 6	~ 2600	80 – 95%	< sec
Supercapacitor	0.01 – 1	ms – min	10000 – 100000	20 – 40%	10 – 20	40000 - 120000	80 – 95%	< sec
Hydrogen	0.01 – 100	min – week	5 – 30 years	0 – 4%	600 (200bar)	0.2 – 20	25 – 45%	sec - min
Synthetic Natural Gas	1 – 100	hour – week	30 years	Negligible	1800 (200bar)	0.2 – 2	25 – 50%	sec - min
Molten Salt (latent thermal)	1 – 150	hours	30 years	n/a	70 – 210	n/a	80 – 90%	min

Excludes technologies with limited experience to date from multiple sources. Sources: Bradbury, K. (2010), "Energy Storage Technology Review"; IEC (2011), "Electrical Energy Storage. A White Paper"; Schlumberger Business Consulting (2013), "Leading the Energy Transition: Electricity Storage." Schlumberger Business Consulting Energy Institute, FactBook Series, World Bank ESMAP Technical Report 006/15 'Bringing variable renewable energy up to scale: Options for grid integration using natural gas and energy storage', and contributions from WEC Energy Storage Knowledge Network participants.

distance to the load centers. Pumped hydroelectric storage (PHS) and compressed air energy storage (CAES) are accounted for as a bulk storage technology where PHS is the most installed storage type, while CAES is the distant second with a few numbers of installations worldwide. On the contrary, distributed energy storage (DES) is located near to load centers, which could be flow batteries and high-temperature batteries, flywheels, and supercapacitors. DES has a wide range of application areas such as "voltage support, transmission congestion relief, T&D upgrade deferral, TOU energy cost management, demand charge management, electric service reliability, electric service power quality, renewables capacity firming, and wind generation grid integration [Eyer and Corey, 2010]". Load leveling, spinning reserve, peak shaving, contingency service, and area regulation are being provided by bulk storage systems [Ferreira et al., 2013].

One of the most preferred technology is PHS, which belongs to the mechanical category and has dominated energy storage systems for a long time. It represents 99% of installed storage capacity all over the world, which is equivalent to 3% of overall energy production IEC. PHS systems have two reservoirs; upper and lower. Reservoirs could be natural or human-made, which are dams, seas, or rivers. Water is pumped from lower reserve to upper reserve for storing energy when there is excess energy and then released downwards to generate electricity when it is needed. In general, water is pumped up when the electric price is low and released on-peak times. The selection of the PHS plants strictly depends upon the geographical locations, which accounts for the significant disadvantage of this technology.

Pumped hydro plants could be up to 4000 MW in capacity, and the efficiency varies

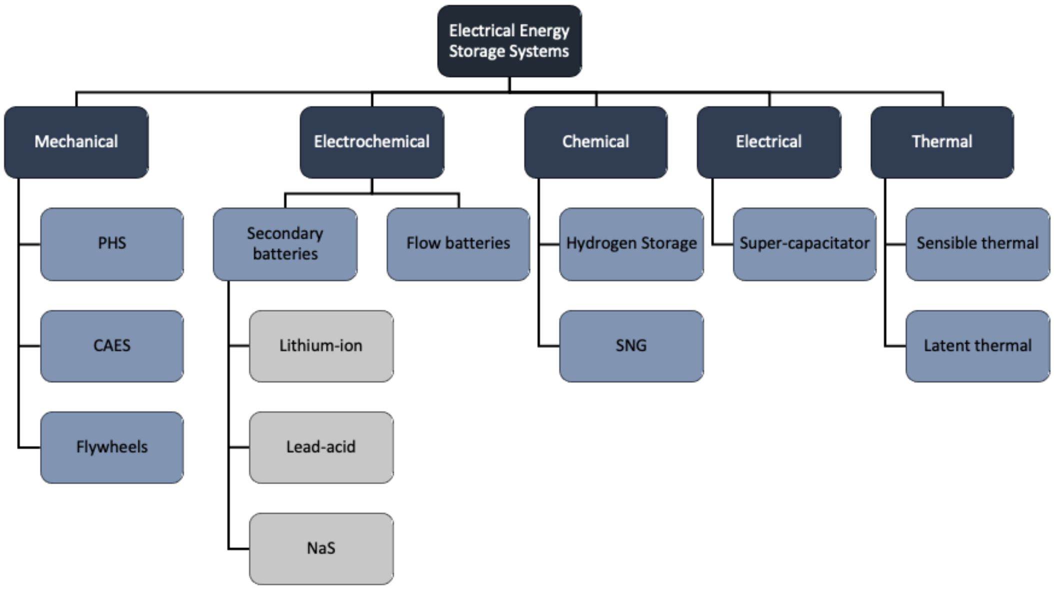

Figure 1.4 Electrical energy storage systems

between 76% - 85%. Compared to the other storage systems, their lifetimes are relatively long, with an average of 50-60 years. They can react to the changes quite fast. Discharge duration varies between 4-16 hours based on power rating. For instance, Rocky Mountain pumped hydro plant has more than 10 hours of discharge time with 1095 MW according to Akhil et al. [2013].

First PHS plants are constructed in Italy, Switzerland, and Austria in the 1890s [Rehman et al., 2015]. The USA, Japan, and China are the leading countries in terms of installed pumped hydro plant capacity. United States has more than 10 installed PHS, which are larger than 1000MW capacity.

"CAES utilizes off-peak electricity to compress air, usually at high pressures, for storage in geological structures such as mines or aquifers, salt caverns, and above ground pressure vessels. The compressed air is then released, preheated and used to drive a turbine-generator system to produce electricity when required [Council, 2016]."

Due to the location-constrained characteristics of CAES, which is similar to PHS, only two compressed air plants are constructed worldwide so far. These plants are located in Alabama, USA, and Huntorf, Germany [Akhil et al., 2015, He and Wang, 2018, Luo et al., 2015]. Several new plant projects are either under construction or in the project phase. In spite of the large capacity and ability to store the energy over weeks, CAES plants are operating with quite a low efficiency compared to PHS and other battery-based technologies. Huntorf is operating with 41% round trip efficiency whereas it is 54% for Alabama IEC; the low efficiency is the main barrier of this technology.

A new technology named Advanced Adiabatic CAES (AA-CAES) uses zero-carbon while operating and the aim is to achieve higher efficiencies than traditional CAES. The first AA-CAES is under construction in Saxony-Anhalt, Germany, where the intended efficiency of the plan is around 70% [Luo et al., 2015].

"Though flywheels have been in existence for decades, they have only recently gained attention for large-scale stationary energy storage. They store kinetic energy in rotating discs or cylinders, suspended on magnetic bearings Council [2016]." The flywheel was first used for public transportation called "Gyrobus" in the 1950s in Switzerland and Belgium. Engineers invented this technology to avoid the disadvantages of batteries such as long time charging, low capacity, and low usage time Gyr. Flywheel storage systems could be used for grid support systems. They have been integrated with renewable energy especially with wind farms to reduce the uncertainty. In 2011 and 2014, Beacon power opened two flywheel storage plants in New York and Pennsylvania, USA which have 20 MW capacities. They provide frequency regulation and area control error correction with relatively high efficiencies bea [2014]. One of the key advantages of this storage system is to have high efficiency with almost 90% at rated power. Additionally, flywheel has a pretty fast response time which are a few milliseconds. However, high cost and high self-discharge rates (20% of stored energy per hour) are the major drawbacks of this technology [Hadjipaschalis et al., 2009]. Due to the high self-discharge rates, flywheels are not appropriate storage type for long periods of time. Also, it does not require much maintenance compared with other types. Council [2016].

Most common secondary batteries are lead-acid, Lithium-ion (Li-ion), sodium-sulfur (NaS), and sodium nickel chloride. In contrast to PHS and CAES, batteries have less discharge duration that generally varies between a few seconds up to 6 hours.

The Li-ion battery was invented early in the 1980s and has been one of the promising battery technologies due to their long-life (roughly ten years), fast charging, quick response, and high efficiencies (up to 97%), however, they are more costly than most of the storage systems even though their costs have been decreasing significantly over the last years. Li-ion mostly provides ancillary services to independent system operators (ISO) [Committee, 2008]. Some applications of Li-ion are peak-shaving, frequency regulations, as well as PV and wind integration, served to end-users, utilities, and generators [Akhil et al., 2013]. For example, U.S. AES Energy Storage constructed Li-ion based storage system in New York and West Virginia (wind plant), providing frequency regulation. Li-ion type battery is being utilized by well-recognized car brands, and dominate the hybrid and electric vehicle (HEV and EV) sector.

The oldest secondary battery type is lead-acid, found in 1859. Among the batteries, this type of battery is the most mature one, which has quick response times, low self-discharge rates (<0.3%), and high efficiencies (up to 90%). However, it is not durable as it has approximately two years of cycle life [Luo et al., 2015] and has a weight of approximately three times more than Li-ion batteries. Charging time is relatively slower, varies between 8-16 hours. In addition, they need maintenance occasionally. Despite the significant downsides, they are less costly than Li-ion and NaS batteries. They are being used for a large number of application areas such as spinning reserve, frequency control, load leveling, and renewable integration. "Total consumption of lead-acid batteries for commercial, industrial, and automotive use in the United States is currently $2.9 billion per year and is growing at an annual rate of 8% [Committee, 2008]."

NaS batteries have a long discharge duration (up to 8 hours) and could be used for grid support or renewable source integration. The approximate lifetime is 15 years. NaS battery cells are being charged and discharged under the high temperatures, which should be kept approximately between 300°C to 350°C [Akhil et al., 2015]. So far, the largest storage plant with 216 MW capacity is placed by a wind generator company in Japan that has been using this storage system since 2008 [Akhil et al., 2013]. Some other applications of installed NaS battery are load leveling, integration with renewable sources, and emergency supply IEC.

Flow battery stores electrolyte in an external tank by contrast with the other types of batteries, and electrolyte is pumped between tank and cell stacks during charging or discharging [Eyer and Corey, 2010, Luo et al., 2015]. Self-discharge could be negligible, which is considered as the main advantage for this type of battery system since it has a separate sealed tank [Akhil et al., 2013].

Vanadium Redox Flow Battery (VRB), is one of the most deployed flow battery types, and it has been involving and could be used for many applications like load leveling, mitigating the renewable intermittency, ancillary services, and telecom applications. VRB can operate for more than 10000 cycles; they have quick response times and can reach up to 85% round-trip efficiency. However, the operating cost of redox flow is relatively high, and it demonstrates low energy density [Eyer and Corey, 2010, Luo et al., 2015].

In Hokkaido, Japan, SEI installed a VRB storage system, which is one of the world's largest flow battery-based storage plant, into a substation that gets wind and solar power, where one of them is a 111MW mega solar power plant, for smoothing the renewable output fluctuations Glo, Rou.

Excess electricity could be converted and stored as hydrogen or methane (or synthetic natural gas (SNG)) by means of electrolysis. The round trip efficiencies are very low, but yet it has relatively higher storage capacity than the others, even higher than PHS. Energiepark is a hydrogen storage plant located in Mainz, Germany, in which electricity obtained from both grid and a nearby wind plant's energy is transformed into hydrogen. They provide ancillary services for a local grid [Kopp et al., 2017].

Supercapacitors (or ultra-capacitors) belong to the electrical category and have many advantages over battery types. First, since the supercapacitors do not include chemicals, they can be charged and discharged within seconds, which are much faster than battery types [Hadjipaschalis et al., 2009]. Moreover, their cycle life is more than 500,000 cycles, and they have a high-efficiency rate (85% to 98%). However, they have a high self-discharge rate approximately far above compared to battery according to Hadjipaschalis et al. [2009]. Another drawback of supercapacitors is that they are not an appropriate technology for storing energy for long times, such as hours and days. Like flywheel storage systems, supercapacitors are being applied in frequency regulation and support power quality [Committee, 2008].

Thermal energy storage keeps the energy in a liquid or solid form so that it could be used at a later time, mostly for applications like cooling or heating. Thermal storage systems (TES) are sensible heat storage and latent heat storage [Luo et al., 2015]. The temperature can vary between -40 and 600 °C while TES is working. Sensible heat stores the energy by heating and cooling of the solid and liquid such as water, molten sand, or sand [Sarbu and Sebarchievici, 2018]. Sensible heat type is the most common TES application among the commercial and residential since the usage of the materials are cheap and safe. "Latent heat TES employs Phase Change Materials (PCMs) as the storage media and uses the energy absorption or emission in liquid-solid transition of these PCMs at constant temperature [Luo et al., 2015]."

Nowadays, TES systems are being used mostly for seasonal, which store heat or cold for a season and convert heat or cold to other forms depending on the current season. Nevertheless, applications of thermal-hydro are rare [Alva et al., 2018]. TES is mostly used for district heating and industrial needs. This storage system is one of the most proper storage systems for concentrated solar power plants [Alva et al., 2018].

1.6 Cost Characteristics of ESSs

In this section, cost characteristics of ESS are discussed. The cost evaluations are done by ESS systems and divided into two groups as BESS and non-BESS. Cost components are shown in Figure 1.5. Total project cost for BESSs consists of a power conversion system (PCS), the balance of plant (BoP), capital cost, and construction and commissioning (C&C) [Mongird et al., 2019]. Another cost component is operations and maintenance (O&M) cost and falls into two categories: fixed and variable cost. It should be noted that, especially for BESSs, cost differences could be observed among the storage types depending on the characteristics.

In the study of Mongird et al. [2019], the cost ranges for various storage types for the year 2018 and cost predictions for the year 2025 are provided. In Table 1.2, only for the year 2018 ranges are obtained from Mongird et al. [2019], and the cost ranges are shown by storage types. Among the storage types in Mongird et al. [2019], sodium-sulfur, lithium-ion, lead-acid, pumped hydro and compressed air are investigated. For the battery technologies, the E/P ratio is assumed as 4 hours, while the ratio for PHS and CAES is 16 hours.

- Capital Cost: All storage system types include the capital cost. Specifically for BESSs, the cost is assigned for electrodes, electrolytes, and separators. Caverns and compressors count as capital costs for CAES. PHSs' capital costs mainly consist of two water reservoirs, pumps turbines, generators, and waterways to connect reservoirs.

- Power Conversion Systems: PCSs account only for BESSs and convert the stored energy in storage from DC to AC for the electricity grid. The cost of PCSs includes inverter and packaging. For PHS, PCS cost is included in the capital cost of the system.

- Balance of Plant: BoP costs are assigned for transformers, electrical wiring, and some other equipment that are needed to have a secure and reliable connection from storage to the grid.

- Construction and Commissioning: C&C costs include the planning and design of the project, transportation, and installation costs during the construction phase.

- Fixed Operations and Maintenance Cost: Fixed (O&M) costs includes labor cost and taxes of the system and do not depend on the storage usage, charging,

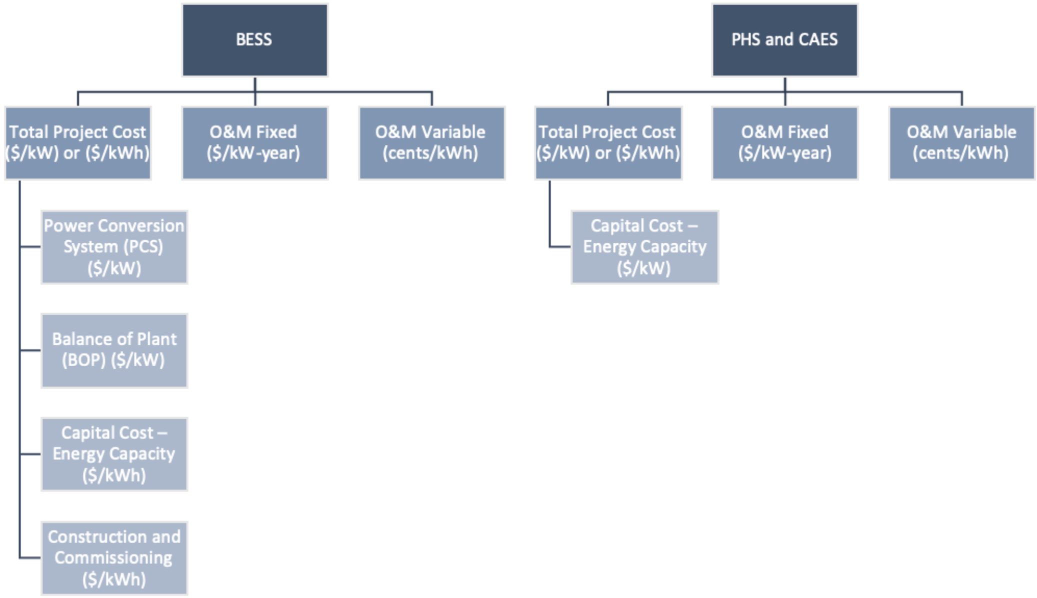

Figure 1.5 Cost components of BESS and non-BESS

Table 1.2 Cost ranges for various ESS technologies

Parameter	Sodium Sulfur	Li-ion	Lead Acid	PHS	CAES
Capital Cost – Energy Capacity ($/kWh)	400-1000	223-323	120-291	1,700-3,200	1,050-2,544
Power Conversion System (PCS) ($/kW)	230-470	230-470	230-470	Included in Capital Cost	
Balance of Plant (BOP) ($/kW)	80-120	80-120	80-120		N/A
Construction and Commissioning ($/kWh)	121-145	92-110	160-192		
Total Project Cost ($/kW)	**2,394-5,170**	**1,570-2,322**	**1,430-2,522**	**1,700-3,200**	**1,050-2,544**
Total Project Cost ($/kWh)	**599-,1293**	**393-581**	**358-631**	**106-200**	**94-229**
O&M Fixed ($/kW-yr)	10	10	10	15	16.7
O&M Variable (cents/kWh)	0.03	0.03	0.03	0.00025	0.21

or discharging energy amounts. It is the fixed cost accounts per year and expresses by the power rate.

- Variable Operations and Maintenance Cost: The annual discharge output is the primary metric to assign the variable O&M cost.

1.7 Problem types on ESSs

ESSs problems include storage-only, producer-oriented, and consumer-oriented applications [Weitzel and Glock, 2018]. Storage-only problems generally try to maximize the storage owner's profit where the storage systems are independent but have a communication with the grid. An electricity generation plant is combined with the storage systems in producer oriented-production. Consumer-oriented applications are mostly combined with a small generator unit like PVs or wind turbines with a storage system. In addition, micro grid systems are considered more complex systems where they could be connected or disconnected to the grid [Weitzel and Glock, 2018].

Some papers focus on finding the optimal storage management policy, where most of them interested in maximizing the profit. Kim and Powell [2011] derive a closed-form expression to find an optimal commitment in a day-ahead energy market for the combined wind plant and a battery storage system. Similarly, Harsha and Dahleh [2014] considered optimal storage management while considering a renewable generator associated with the grid. They formulate stochastic dynamic programming to find the optimal policy of the storage. Some others present bidding strategies for the day-ahead market Kanakasabapathy and Swarup [2010], Steffen and Weber [2016]. For a wholesale electricity market, the arbitrage value of a stand-alone storage system is studied in the work of Sioshansi et al. [2009]. The electricity market is connected with the storage-only PHS system, and they try to maximize storage's cumulative profit by considering the stochastic electricity price by Densing [2013]. They emphasize that there is a dual relation between the applied price-driven dispatch model and the well-known newsvendor problem. The value of a storage system is also discussed in many papers where different combinations of the storage system and the generation plants are taken into consideration.

Determining the optimal size of the storage system is another problem which has been widely studied in the literature. Mathematical programming, analytical and heuristic methods are used to solve the sizing problems [Zidar et al., 2016].

The selection of the appropriate ESS technology is also addressed in the literature by considering and comparing the technical or economic characteristics of the storage systems. For instance, PHS and different types of battery storage types are compared while considering a wind farm in the work of Hayes et al. [2016]. Likewise, genetic algorithm is applied to determine the best battery type, including lead-acid and NaS, as well as finding the optimal size and site for a distribution network [Rangel et al., 2017].

1.8 Outline of the Dissertation

The rest of this dissertation organized as follows. In Chapter 2, we present a electricity system for remote areas and island systems with wind power. A transmission grid is demonstrated in Chapter 3. In Chapter 4, we study an island system with Solar photovoltaic (PV) power. Lastly, we conclude the study and suggest future works in Chapter 6.

2. Remote Areas and Island Systems

Remote areas, geographical islands, or rural areas that generally have low population density can not always be supplied by primary generators, as opposed to the main population areas connected with large grids. These areas are either not connected to the grid or have limited access to it, traditionally relying on diesel generators at a huge cost to generate electricity, mainly due to transportation costs. According to Energy Access Outlook 2017, 1.3 billion people live in such areas that have no access to an electricity network. Therefore, finding cost effective and environmentally friendly energy solutions for almost one-sixth of the world's population is of paramount importance.

As a solution, these areas should be connected to either a central electrical grid or microgrids which are fed by renewables. Also, the accessibility of electricity has been increasing worldwide thanks to technological developments and declining costs of renewables and storage devices. Integration of renewable sources helps in cutting down the dependency on the diesel generators and provides considerable cost savings and also reduces carbon emissions. As a result, storage systems are critical solutions in supporting renewable energy sources for isolated areas.

Hybrid systems seem to be the most feasible solutions to ensure the stability of the remote systems; for instance, hybrid wind/diesel, PV/wind/diesel, wind/hydro or any other possible combination of renewable sources and storage technologies could be used. For example, Alcatraz Island, USA, formerly known for the prison on it, has a hybrid solar PV/batteries/diesel electricity system with 959 PV solar panels (305 kW), 8 power inverters (100 kW each), and 480 batteries (1,920 kW hours of energy storage). Bozcaada, Turkey, generates its entire electricity from PV panels and wind turbines combined with hydrogen storage. Moreover, production is more than 30 times than the consumption of the island, and the excess electricity is sent to the mainland. El Hierro, one of Spain's Canary Islands derives its own electricity from a wind/hydro hybrid system and aims to reach one hundred percent renewable generation. Prior to this system, diesel generators were being used as a primary source; they have now turned into a back-up plan. This is the first Europe's hybrid renewable energy system. Greece's Ikaria Island which is located at the Aegean Sea is the second hybrid renewable energy system in Europe, after El-Hierro Island. This system consists of 2.7 MW wind farm and two hydro plants with an installed capacity of 4.1 MW. Also, Tilos Island, Greece was chosen as the first island in Mediterranean sea to be funded by Horizon 2020 in order to implement renewable hybrid system (wind, solar, and a battery storage system). The aim is to reduce to carbon footprint, as well as reduce the power outages which occurs due to the sent energy from Kos Island via undersea cables. Malalison Island, the Philippines has the solar PV hybrid system with the assistance from Asian Development Bank. Sumba island is located eastern Indonesia and energy cannot be supplied by the national grid so it depends on the diesel generators to reach the energy and most of the inhabitants had no access to electricity. Luckily, this island has a great renewable source potential such as hydro, biogas and solar to be converted to an energy. A project was proposed called Sumba Iconic Island where the aim is to reach 100% renewable energy by 2025. So far, wind turbines, PV solar panels, biomass, and biogas facilities have installed.

2.1 Literature Review on Remote Systems

In this section, the papers which consider only remote areas with storage systems are considered. There are many problems that should be addressed regarding the energy storage and renewables for remote areas. One of the most significant issues is the sizing and operations of the storage systems, as mentioned in Section 1.7. Stochastic optimization is widely used to solve the sizing and operations problems in the literature. For example, a linear programming is formulated to determine the optimal pumped hydro storage reservoir and power capacity for an island system where the load is met by thermal generators, wind, and hydropower by Brown et al. [2008]. In this problem, the authors try to minimize the total investment cost and fuel cost by considering the dynamic security criteria. They generate different scenarios by using fuzzy clustering in order to include the uncertainty of load and renewable electricity generations. The scenarios are generated based on the net load that is the demand unit fulfilled by thermal generators for each time slot. Two-stage stochastic optimization is applied by Abbey and Joós [2008] for the isolated wind-diesel power system to find the optimum size of the energy storage systems while minimizing the investment and operational cost. At the first stage, size of the storage systems is determined in order to satisfy all scenarios. At a second stage, the optimal operation of the whole system, which consists of wind-diesel and storage systems, is found. Stochastic mixed integer programming (SMIP) is solved by using GAMS. The uncertainty of wind and load is considered through 24-hour scenarios. The diesel system's operating is also considered, which could also be shut down. Yang and Nehorai [2014] consider a remote area where the electricity is supplied by diesel generators, renewable sources, and energy storage systems. This work is similar to others and solved using SMIP; however, they consider more than one renewable source and storage types, namely pumped hydro, flywheels, and li-ion batteries, which increase the dimension of the problem. The aim is to determine the optimal portfolio of the power system, where the total investment and operational cost is minimized. A distributed optimization approach is applied to solve the optimization model by dividing the horizon into shorter horizons in order to cope with scenarios due to the uncertain nature of renewable sources and electricity demand. Unlike the other studies, Kuznia et al. [2013] solve a model by SMIP to take operation and transmission lines, renewable sources, and storage system investment decisions. The model is proved to be an NP-hard problem; thus, they develop a Bender's decomposition-based algorithm to solve it. Harsha and Dahleh [2014] formulate a storage investment problem as stochastic dynamic programming from the perspective of the local renewable generator, which supports electricity for the local area and supplied electricity from the primary grid when required. The goal of this study is to minimize the electricity bill of the local area by considering the investment costs of the storage system. The electricity bills only cover the purchased electricity from the main grid and do not include the electricity supplied from renewable generators. This study gives an insight into the optimal storage sizing under some special assumptions. The MILP are constructed for an islanded and grid-connected microgrid (MG) system by Chen et al. [2011] in which the aim is to find the optimal size of the battery system while minimizing the cost and profit for each mode, respectively, considering the spinning reserve requirements. As a solution method, they introduce a specific algorithm to solve two models efficiently, which is applied in AMPL (A Modelling Language for Mathematical Programming). Wind speed and solar radiation are predicted based on real data. The economic benefit of the battery system is addressed in cost-benefit analysis for both islanded and grid-connected MG systems.

Instead of giving only the storage investment decisions, some papers also focus on finding the generator side based decisions for hybrid systems. Malheiro et al. [2015] try to find the number of wind turbines, PV panels, batteries, and diesel generators in the same MILP model while minimizing the total cost for an isolated system.

The demand should be satisfied for all time slots and assumed to be known, which is the same for each day in a year. They solve this problem through GAMS and apply sensitivity analysis based on different scenarios. Some cases have different combinations of components in the hybrid system, and others change depending on the weather conditions. Another study tries to determine the optimal size of a hybrid autonomous wind/PV system with battery technology by considering the system reliability requirements. The model aims to find minimum levelized system cost while meeting the reliability restrictions. Combined wind farm and PHS system are considered by Anagnostopoulos and Papantonis [2007] where electricity is sold to the primary grid. The optimum size of the pumping stations is determined by conducting a 1-year simulation based on three different pumping designs while maximizing the net present value over a period. Alharbi and Bhattacharya [2017] point out that the optimal size of the storage system could be found if and only if the other electricity generation sources operations are considered jointly. They propose a two-stage optimization problem where at the first stage, the optimal sizes of the batteries are found covering all scenarios while the optimum year of installation of batteries is determined based on a new BESS degradation matrix at the second phase. The rise of the demand over the horizon and energy capacity degradation of the battery is also taken into account while finding the optimal installation year. The stochasticity of solar and wind generations and demands are considered in the scenarios where all of the scenarios are represented by a certain probability. The objective is minimizing the sum of the expected net present value of the battery installation cost, operation and maintenance cost and, microgrid operation cost. Microgrid operation costs include the on-off status of the diesel generators and fuel cost and its escalation rate over the years. This problem also ensures the minimum reserve and load shedding requirements in addition to other works.

In the literature, both operating the system and sizing the storage systems are considered under the market conditions. Korpaas et al. [2003] study an isolated network with wind power and storage system. In addition, they also include the transmission line limitations while using the external grid, which could be considered as both source and sink power. They forecast the wind generation through an algorithm based on real data. The problem is solved by a dynamic programming approach where the forecasted generation are treated as deterministic for reducing the computational complexity. A simulation study is carried out by having the load and generation variables as continuous variables to point out the importance of the energy storage sizing for the whole system. Castronuovo et al. [2014] consider a problem that maximizes the day-ahead profit for a wind farm and a PHS where the bidding decisions should be given one-day advance. They use the chance-constraint approach to convert the stochastic model into a deterministic one. It gives an opportunity to evaluate the trade-off between risk and expected revenue.

Some papers only consider optimal scheduling while keeping the size of the storage system as a parameter. Ross et al. [2011] study an isolated system with the wind, diesel, and storage components. An operation scheduling model is proposed to minimize wasted energy, which also results in minimizing the diesel consumption. Moreover, they investigate two cases when diesel sources are continuously working and when there is an on-off option for them.

2.2 Deterministic Problem Formulation

The studies mentioned above mostly consider sizing and operation decisions for one kind of storage system or examine the storage systems from a portfolio. However, deployment of more than one type of storage in a remote area facilitates reducing the total cost of construction and operating of ESSs and also increase the reliability. Depending on the geographical conditions of the specific area, small-scale pumped hydro, CAES, and battery technologies are some of the viable options. Another advantage of using multiple storage types is that it offers more flexibility for placement decisions. For instance, the deployment area of a wind farm and PHS can not always be the same since the expected conditions for the two systems are quite different. While the wind farm should be constructed in a favorable place in terms of wind speed, PHS requires two water reservoirs at different elevations. On the other hand, co-located wind farms with batteries are quite common since they are portable and do not require very specific geological conditions. Hence, depending on the circumstances, different storage types at different locations can be used in the same system.

By deploying two different storage types at different places, we are able to find the values of the storage types and under which circumstances they are superior to one another. Past works have not examined the sizing and decision problem at the same time. For instance, optimizing the size of the storage system was not the aim of this paper and was assumed as a fixed parameter in the work of Kuznia et al. [2013]. However, unlike the other works, the authors provide investment decisions by finding the number of storage devices, the number of renewable sources and, the number of transmission lines. In our study, we propose an integrated model that considers both investment decisions for the storage systems, the capacity of the transmission lines, and the size of the deployed storage systems.

We study an island system that consists of two separate storage systems where the first one is considered as a battery and the second one is considered as a bulk storage technology such as pumped hydro or compressed air storage facility. An island system consists of renewable sources and diesel generators (or will be mentioned just as penalty cost) which are being used as a back-up plan in case of renewable sources and storage levels are not enough to satisfy the demand at any time. While batteries are installed nearby the renewable generators, bulk storage is installed between the load center and renewable generators. Diesel generators are assumed to be at the side of the load center. There are two transmission lines; the first one connects the renewable sources and batteries to the bulk storage system, and the second one connects the bulk storage to the load center. This problem will be referred as the sizing problem of the storage systems where the meaning of sizing is twofold: the first one is the capacity or the energy rate of the storage, and the second one points to the power rate of the storage. The primary aim of this problem is to determine whether the storage systems should be installed, if yes, what should be the size and the power rates of them. There are also operational decisions for all periods. The model determines how much the storage source charges/discharges, how much amount of electricity is generated from the diesel generators, or dumped. The objective of the problem is to find the minimum cost of installation, operation and maintenance cost of the storage systems, and the penalty cost due to the usage of diesel generators. The mathematical model of the sizing problem is the following:

Sets

I: set of storage type ($i = 1, 2$)
T: set of time slots ($t = 1, ..., T$)
K: set of transmission line ($k = 1, 2$)

Parameters

F_1, F_2: Fixed costs of storage types 1 and 2
C_i^e: Energy related investment cost of i^{th} storage
C_i^p: Power related investment cost of i^{th} storage
C_i^{OM}: Operation cost of i^{th} storage
C_k^{TR}: Unit transmission cost of building k^{th} line
G_t: Generation at time t
D_t: Demand at time t
π_t: Penalty at time t

S_{min}: Minimum storage level
η_i^c: Charging efficiency of i^{th} storage
η_i^d: Discharging efficiency of i^{th} storage

Decision Variables
X_i: 1, if i^{th} storage type is constructed and 0 otherwise
S_{it}: i^{th} storage level at time t
S_{it}^{ch}: Charging rate of i^{th} storage at time t
S_{it}^{dis}: Discharging rate of i^{th} storage at time t
E_i: Energy rate for i^{th} storage
P_i: Power rate for i^{th} storage
X_{kt}: Flow at line k at time t
X_k^{max}: max. capacity of k^{th} transmission line
L_{kt}: Dump load at k^{th} line at time t
U_t: Slack variable

P(1)

$$Min \sum_{i \in I} F_i X_i + \left[\sum_{i \in I} C_i^e E_i + C_i^p P_i \right] + \sum_{k \in K} C_k^{tr} X_k^{max}$$

(2.1) $$+ \sum_{i \in I} \sum_{t \in T} C_i^{OM} S_{it}^{dis} + \sum_{t \in T} \pi_t U_t$$

subject to;

(2.2) $X_{1t} = G_t - S_{1t}^{ch} + S_{1t}^{dis} - L_{1t}$ $\quad t \in T$

(2.3) $X_{2t} = X_{1t} - S_{2t}^{ch} + S_{2t}^{dis} - L_{2t}$ $\quad t \in T$

(2.4) $X_{2t} = D_t - U_t$ $\quad t \in T$

(2.5) $X_{kt} \leq X_k^{max}$ $\quad k \in K \quad t \in T$

(2.6) $S_{it} \leq E_i$ $\quad i \in I \quad t \in T$

(2.7) $S_{it} \leq E_{max} X_i$ $\quad i \in I \quad t \in T$

(2.8) $S_{it} = S_{i,t-1} + S_{it}^{ch} \eta_i^c - S_{it}^{dis} / \eta_i^d$ $\quad i \in I \quad t \in T$

(2.9) $S_{it}^{ch} \eta_i^c \leq P_i$ $\quad i \in I \quad t \in T$

(2.10) $S_{it}^{dis} / \eta_i^d \leq P_i$ $\quad i \in I \quad t \in T$

(2.11) $P_{min} \leq P_i \leq P_{max}$ $\quad i \in I$

(2.12) $E_{min} \leq E_i \leq E_{max}$ $\quad i \in I$

(2.13) $S_{it} \geq S_{min}$ $\quad i \in I \quad t \in T$

(2.14) $E_i, P_i, S_{it}, S_{it}^{ch}, S_{it}^{dis}, X_{kt}, X_k^{max}, L_{kt}, U_t \geq 0$

(2.15) $X_i \in \{0,1\}$

The objection function consists of five parts(2.1); the first term denotes fixed costs, which occurs if the storage ith storage is installed. The second term consists of two parts; the first one is the fixed cost per installed energy rate and the second one depends on the installed power rate of the storages. The third term denotes the costs of the transmission lines depending on their capacities. The fourth part is operation and maintenance cost for the storages and depends on the discharge rates. The last one is the total penalty cost incurred due to the diesel usages for all periods. Equation (2.2) is a balance constraint and shows the flow rate from the generation side to the bulk storage. Likewise, Equation (2.3) shows the flow rate from bulk storage to the load center. Equation (2.4) ensures that the diesel generators are in charge if demand cannot be satisfied by the generator or the batteries. A shortage could occur when the transmission lines have not enough capacity to transmit the whole on-hand energy. Also, in this case, diesel generators supply the required electricity. Naturally, the model could decide to use diesel generators instead of using batteries or even instead of generated electricity from renewable sources; however, using diesel generators is more costly than using batteries and renewable generators. So, it might be assumed that the diesel generators are used when the system cannot provide enough energy to satisfy the demand. Transmission capacity constraint is in (2.5). Equation (2.6) ensures that the storage level cannot exceed the energy rate for any period. Any storage type can be filled up to its capacity at most. The maximum physical energy rate capacity is given by (2.7). Storage level is updated for all periods, which depends on the previous level and charge or discharge units in the current period. Equations (2.9) and (2.10) are the power rate capacities for all periods. Minimum and maximum physical capacity restrictions for power and energy rates for storage types are shown in (2.11) and (2.12). The storage level should be greater than a minimum amount for all time slots is given by (2.13). Lastly, variable definitions are given in (2.14) and (2.15).

2.3 Scenario Representation

Electricity production from renewable sources mostly depends on uncertain weather conditions. In addition, electricity demand is random and affected by some external factors such as weather conditions, seasons and any other unpredicted situations. Therefore, incorporating stochasticity into the model is necessary to have a more realistic model. One way to do this is to add different scenarios by reproducing generation and demand time series. Scenarios are represented as hourly based data sets for 365 days. Data sets include wind generation and electricity load.

A tree scenario representation is almost impossible given the potentially massive tree size. Hence, we adopted sample average approximation (SAA) method which is very a common approach for solving the stochastic optimization problems and used by many authors in many different contexts. In this technique, a stochastic optimization problem can be solved as a discrete optimization model by incorporating random samples to the model. Then, the objective function value is approximated by the sample average function.

A set of scenarios is added to the primal model, which is the distinction between the deterministic and stochastic models. Every randomly generated data is associated with a probability. In our model, probabilities are taken as equally likely for all scenarios.

The main decisions are energy and power rate of two storage types, whether they are installed or not, and the capacity of the transmission lines. These decisions are taken independently from the scenarios, whereas operational decisions are based on scenarios. Mixed integer linear programming (MILP) is the following:

Sets
I: set of storage type ($i = 1, 2$)
T: set of time slot ($t = 1, ..., T$)
K: set of transmission line ($k = 1, 2$)
S: set of scenario ($s = 1, ..., S$)
Parameters
F_1, F_2: Fixed costs of storage types 1 and 2
C_i^e: Energy related investment cost of i^{th} storage
C_i^p: Power related investment cost of i^{th} storage
C_i^{OM}: Operation cost of i^{th} storage
C_k^{TR}: Unit transmission cost of building k^{th} line
G_{ts}: Generation at time t for scenario s
D_{ts}: Demand at time t for scenario s
π_t: Penalty at time t for scenario s
S_{min}: Minimum storage level
η_i^c: Charging efficiency of i^{th} storage
η_i^d: Discharging efficiency of i^{th} storage
P_s: Probability of s^{th} scenario

Decision Variables
X_i: 1, if i^{th} storage type is constructed and 0 otherwise
E_i: Energy rate for i^{th} storage
P_i: Power rate for i^{th} storage
X_k^{max}: max. capacity of k^{th} transmission line
S_{its}: i^{th} storage level at time t for scenario s
S_{its}^{ch}: Charging rate of i^{th} storage at time t for scenario s
S_{its}^{dis}: Discharging rate of i^{th} storage at time t for scenario s
X_{kts}: Flow at line k at time t for scenario s
L_{kts}: Dump load at k^{th} line at time t for scenario s
U_{ts}: Slack variable at time t for scenario s

P(1S)

$$
\begin{aligned}
& Min \sum_{i \in I} F_i X_i + \sum_{i \in I} C_i^e E_i + C_i^p P_i + \sum_{k \in K} C_k^{tr} X_k^{max} \\
(2.16) \quad & + \sum_{s \in S} P_s \left[\sum_{i \in I} \sum_{t \in T} C_i^{OM} S_{its}^{dis} + \sum_{t \in T} \pi_t U_{ts} \right]
\end{aligned}
$$

subject to;

$$
\begin{array}{llllll}
(2.17) & X_{1ts} = G_{ts} - S_{1ts}^{ch} + S_{1ts}^{dis} - L_{1ts} & t \in T & s \in S & \\
(2.18) & X_{2ts} = X_{1ts} - S_{2ts}^{ch} + S_{2ts}^{dis} - L_{2ts} & t \in T & s \in S & \\
(2.19) & X_{2ts} = D_{ts} - U_{ts} & t \in T & s \in S & \\
(2.20) & X_{kts} \leq X_k^{max} & k \in K & t \in T & s \in S \\
(2.21) & S_{its} \leq E_i & i \in I & t \in T & s \in S \\
(2.22) & S_{its} \leq E_{max} X_i & i \in I & t \in T & s \in S \\
(2.23) & S_{its} = S_{i,t-1,s} + S_{its}^{ch} \eta_i^c - S_{its}^{dis} / \eta_i^d & i \in I & t \in T & s \in S \\
(2.24) & S_{its}^{ch} \eta_i^c \leq P_i & i \in I & t \in T & s \in S \\
(2.25) & S_{its}^{dis} / \eta_i^d \leq P_i & i \in I & t \in T & s \in S \\
(2.26) & P_{min} \leq P_i \leq P_{max} & i \in I & & \\
(2.27) & E_{min} \leq E_i \leq E_{max} & i \in I & & \\
(2.28) & S_{its} \geq S_{min} & i \in I & t \in T & \\
(2.29) & E_i, P_i, S_{its}, S_{its}^{ch}, S_{its}^{dis}, X_{kts}, X_k^{max}, L_{kts}, U_{ts} \geq 0 & & & \\
(2.30) & X_i \in \{0, 1\} & & &
\end{array}
$$

2.4 Data Description

We use observed wind power production and electricity demand data, which is obtained from a small Spanish island located in Atlantic Ocean. The data includes 8760 hourly based data points. We reproduce wind and load time series from the observed data in order to use the synthetic ones as inputs in the proposed SMIP.

Cost of ESSs, transmission lines, and diesel costs are obtained from literature and annualized. We assume diesel cost is around \$0.25/kWh based on the work of Gioutsos et al. [2018] which investigates electricity systems of six different islands.

The annualized building cost of a transmission line is determined as $\$1/kW$ per *mile* as in the work of Qi et al. [2015].

2.5 Scenario Generation for Load

Load demand changes hour by hour on a specific day, and as it is mentioned earlier, electricity is used by residential, commercial, industrial, and transportation customers. Residential customers are the majority for the chosen island, considering that the island is relatively small, and the industry is not widespread. For residential customers, electricity consumption has a trend in general, depending on human-specific daily routines. For that particular island, it follows a similar pattern in which peak demand occurs in the evening around 10 p.m., seen in Figure 2.3. Although for all months, the load pattern is quite similar based on hourly change, the consumption seems to increase or decrease for time slots on the average depending on the current month. In Figure 2.5 (c), the average load of 24-hour is shown for twelve months. The peak consumption occurs in August, whereas least consumption is observed in December.

After these observations, we try to construct similar scenarios. The scenarios are generated based on their months. The base equation consists of an average of all 24 hours and given by;

Sets
H: set of hours ($h = 1, ..., 24$)
M: set of months ($m = 1, ..., 12$)
$Days$: set of days line ($d = 1, ...Days$)

$$\overline{D_h} = \frac{1}{365} \sum_{m \in M} \sum_{d \in D} D_{mdh} \qquad h \in 24 \tag{2.31}$$

Now, we have an hourly based equation which is also shown in Figure 2.3. Also, hourly averages by their month are found by a similar formula and given by

$$\overline{D}_{hm} = \frac{1}{30}\sum_{y\in Y} D_{mdh} \qquad m \in 12 \qquad h \in 24 \tag{2.32}$$

After having both hourly averages and monthly based hourly averages, we find the differences between $\overline{D_h}$ and $\overline{D}_{hm}$ for all months and hours, defined as Δ_{hm}. Then, the first prediction equation becomes;

$$\chi_{mdh} = \overline{D_h} - \Delta_{hm} \qquad m \in 12 \qquad d \in Days \qquad h \in 24 \tag{2.33}$$

ε_{mdh} indicates the error between the real demand and the predicted demand for all time slots. The errors obtained are fitted to a probability distribution and added to our prediction equation. Then, the prediction equation is determined and given by;

$$\varepsilon_{mdh} = \chi_{mdh} - D_{mdh} \qquad m \in 12 \qquad d \in Days \qquad h \in 24 \tag{2.34}$$

Lastly, the prediction equation is used to estimate the demand for any specific hour of a day in any month. Any time slots can be generated numerous times due to the fitted error probability distribution. For this data set, the prediction error is fitted to a normal distribution. According to Kim [2013], using formal normality tests for the relatively larger data sets (e.g., n>300), may provide unreliable results. The author proposes to consider skewness and kurtosis with the histogram of data set in order to decide whether data is distributed normal. They suggest ranges for absolute values of skewness and kurtosis (skewness>2 and kurtosis>7) for determining substantial non-normality. Thus, normality check is done by histogram, normal probability plot and checking the skewness and kurtosis values of the error data. This data are positively skewed with the value of 0.24 and the kurtosis is 0.11. We see the histogram of the error data in Figure 2.1. Even though it is positively skewed, this figure seems to be normally distributed. Also, PP-plot (Figure 2.2) shows that there are some unexpected points which are greater than 1.5, yet, we can say that this data mostly follows the normal distribution.

The prediction equation is given by;

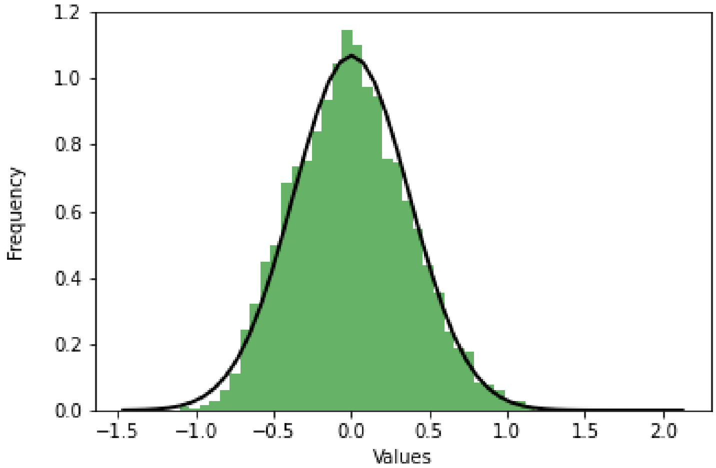

Figure 2.1 Histogram and PDF of error data

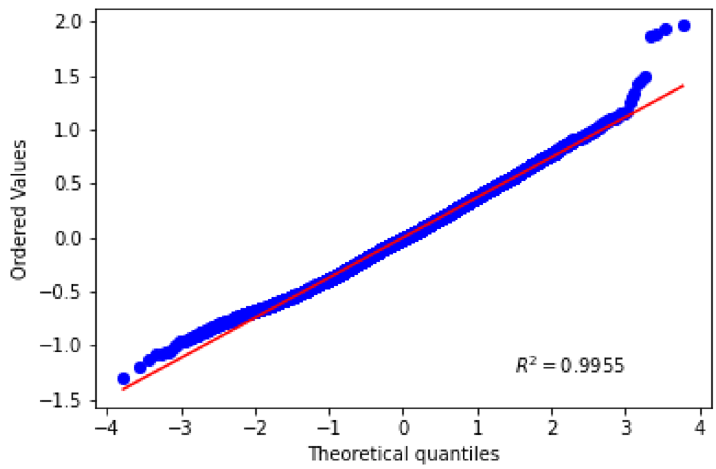

Figure 2.2 PP-plot of error daya

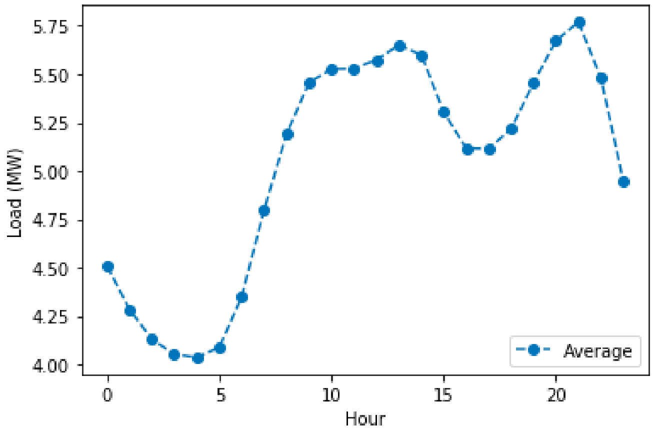

Figure 2.3 Average hourly load for 365 days

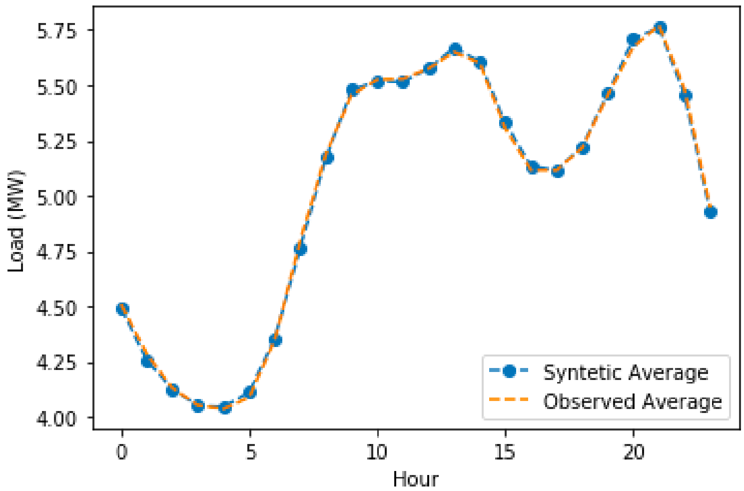

Figure 2.4 Average hourly load, real vs. synthetic

$$(2.35) \qquad Y_{mdh} = \chi_{mdh} + \varepsilon \qquad m \in M \qquad d \in Days \qquad h \in H$$

The generated hourly load time series are compared with the historical time series. In Figure 2.4, average hourly load is shown for two data sets. It is clearly seen that created series closely follows the real data. Similarly, a created hourly averages by month is shown in Figure 2.5 (d). The created data successfully mimics the real data for all months. As a result, this approach produces almost identical data points to the observed series. Thus, it can be considered as a proper approach to generate synthetic electricity load time series.

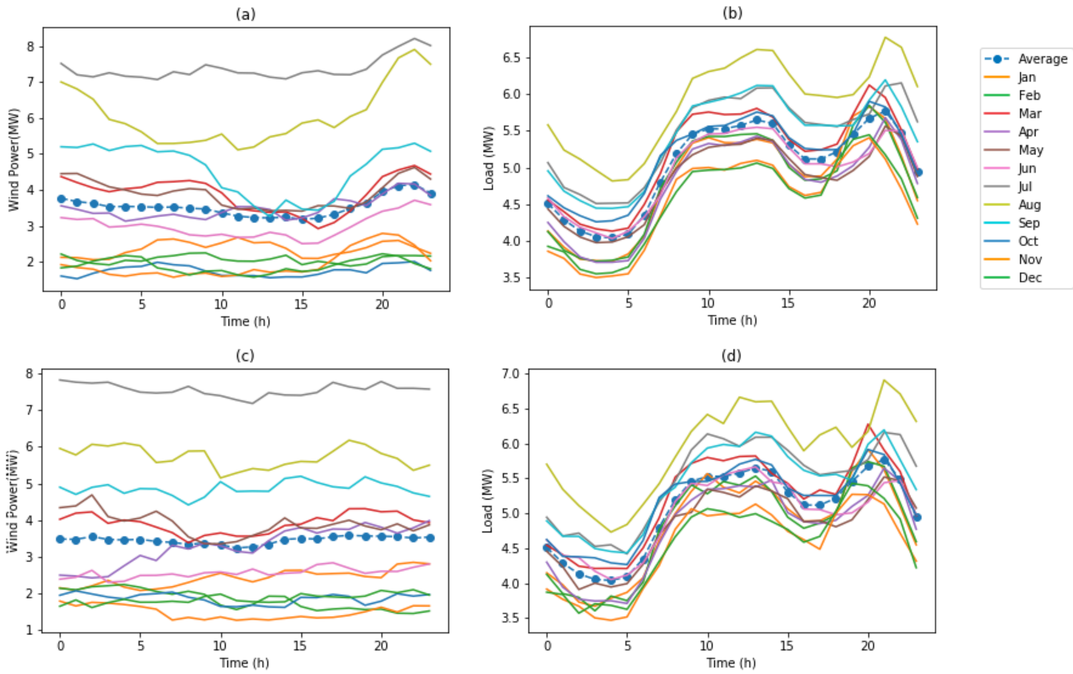

Figure 2.5 Average hourly time series by months
(a)Observed wind power, (b)Observed load, (c)Synthetic wind power, (d)Synthetic load

2.6 Scenario Generation for Wind Power

Wind power hourly averages by months are shown in Figure 2.5 (a); it is clearly seen that wind energy amounts produced vary month to month depending on the climate conditions. While in July, production amounts reach up to 10 MW per hour, during the winter, this amount decreases dramatically.

Wind speed and wind power synthetic data generation have been studied in the literature and various approaches have been proposed. Markov chain process is one of the acceptable methods to generate time series of wind power. Even though most of the papers study on wind speed time series, creating wind power data based on observed data gives more accurate results. Converting the wind speed into the wind power production could include errors since it predicts the power using a power curve function and may result error in up to 9% according to Chen et al. [2009]. Also, unpredictable production issues like failures cannot be included in wind speed data. However, wind power data already includes these problems in it.

The order of the Markov chain concerns the transition from the current state to the nth state. For instance, first-order Markov chain (FOMC) deals with only the previous state. FOMCs are proposed by Sahin and Sen [2001] and Nfaoui et al. [2004] to predict the hourly wind speed. Sahin and Sen [2001] create the states by using mean and the standard deviation of the data. They state that second-order Markov chain (SOMC) can yield better results. Similarly, Shamshad et al. [2005] use the first and second-order Markov models for crating synthetic hourly wind speed time series by using 7-year observed data. They conclude that the second-order Markov model is barely superior to the first-order one in terms of statistical properties like mean, standard deviation, and autocorrelation functions. The first and second-order Markov chain is also used by Carpinone et al. [2015], based on wind power data to predict wind power for a very short-term horizon. In the work of Hocaoglu et al. [2008], a study is conducted to emphasize the importance of the state size of a Markov chain. They construct a probability matrix with 13 and 26 states to compare them. They conclude that when state size increases, the accuracy of the model also increases. Two new improvement methods are proposed in the work of Tang et al. [2015]. The first one includes a new state characterization which benefits from empirical distributions of the wind speed. Second, they suggest using empirical distributions for the states with a large number of elements instead of using a common distribution. By this method, they try to avoid assigning an inappropriate distribution to the states.

Brokish and Kirtley [2009] address the potentially dangerous aspects of applying Markov based model to create wind speed or power time series. Using less than 15 to 40 minutes of time steps may lead to inappropriate results.

We try various orders and the number of states of the Markov chain models. We train the entire data to construct synthetic series with first and second-order Markov chains with several state sizes. Even though it shows similarity with the probability distribution of the observed series, the model fails to reproduce other aspects of the real data. First, it fails to capture the monthly seasonality as it can be expected. This problem would misguide us while deciding the size of the energy storage technologies. Second, when the entire data is used, the autocorrelation function of the created data seems to fall rapidly, where autocorrelation is one of the most important statistical characteristics. To overcome these problems, months are considered separately. However, the main drawback of constructing monthly models is the decrease in the length of time series from 8760 to 740 hours, on the average. At this stage, FOMC gives more accurate results since SOMC suffers from lack of data. It is noted that higher-order Markov chain models mostly yield better results if enough observed data can be obtained. The other critical point is the time step used. Although we also have 10-minutes periods of wind power data, hourly based data is used as it is suggested by Brokish and Kirtley [2009].

Synthetic wind power generation by using the Markov chain can be divided into four main steps:

Step 1: Categorize the states
First, all continuous data values are assigned to a state, where the states are uniformly discretized (e.g., $0-0.5, 0.5-1, .., 10, 10.5$). In the original time series, minimum wind power is 0, and maximum wind power is 10.3; hence, 21 states are constructed with an increment scale of 0.5.

Step2: Constructing a transition matrix
After assigning all values to a state, 21x21 transition matrices are derived. In this process, We then have 12 matrices for all months. Let p_{ij} is the probability of passing from i^{th} state at time t to j^{th} state at time $t+1$ where the p_{ij} should be between 0 and 1 and all row summation has to be 1. First-order 21x21 transition probability matrix $P_{t,t+1}$ is;

$$p_{t,t+1} = \begin{bmatrix} p_{1,1} & p_{1,2} & \cdots & p_{1,21} \\ p_{2,1} & p_{2,2} & \cdots & p_{2,21} \\ \vdots & \vdots & \vdots & \vdots \\ p_{21,1} & p_{21,2} & \cdots & p_{21,21} \end{bmatrix}$$

Let m_{ij} represents the observed frequencies that state i is followed by state j. Then, p_{ij} could be estimated by;

$$p_{ij} = \frac{m_{ij}}{\sum_j m_{ij}} \quad i,j = 1,2,\ldots,21$$

Step3: Simulation
In this step, synthetic values are generated. Before finding the exact values, we first need to determine the states. Let p_{ik} represents the cumulative probability in ith row at state k. New states are determined by the cumulative matrix which is calculated as

$$p_{ik} = \sum_{j=1}^{k} p_{ij} \quad i = 1,2,\ldots,21$$

Transition probability matrices for all twelve months are converted to cumulative matrices in order to assign new states by using random numbers where this probability varies between 0 and 1, for all rows. For instance, let's assume that we are at time t at the nth state. At $t+1$, we determine the new state by using the cumulative probabilities at the nth row. Depending on the random number which is also between 0 and 1, we can easily assign the new state by using the nth row cumulative probabilities. Next state assignment is now based on the state which is determined at time $t+1$. This procedure continues until 8760 states are created.

Before we start to create states, the initial state is determined by assigning a random state, depending on the probability of occurrences of the states from the real data. Once the initial state is determined, data is simulated until the end of the month. This procedure applies for twelve months.

Step4: Conversation of the states into values
In this step, the states which are created at the Step 3 are converted into values. Wind power is assigned mostly by using uniform distribution within the range of the current state. When the states are investigated, uniform distribution mostly approximates the elements in the states. However, other distributions may represent some of the intervals better, especially the states with few members which are proposed in the work of Nfaoui et al. [2004].

A stationary test should be applied to be sure that the Markov chain is a valid approach for the particular data set. Augmented Dickey-Fuller Test is done to be sure that the series is stationary and concluded that the historical time series is stationary and appropriate to use a Markov chain-based model.

Autocorrelation functions (ACF) for observed and generated wind time series are created with fifty lags, which checks if there is a correlation between the first data point up to the fiftieth data point, as shown in Figure 2.6. The initial lags have similarities; however, the autocorrelation is weaker in the created time series. Nonetheless, monthly generated series performs much better than both FOMC and SOMC models created with the entire data.

One created scenario is picked to compare real and synthetic time series averages, as shown in Figure 2.5 (c). Based on hourly averages of wind power, real and synthetic time series have similarities. For instance, synthetic time series able to capture the monthly variability. Depending on the randomly assigned initial values, these averages may be slightly different for other scenarios. Another crucial question is whether the synthetic time series follows the observed one. Figure 2.7 shows that it generally follows the same distribution. Likewise, it is based on one scenario and could differ more or less for the others.

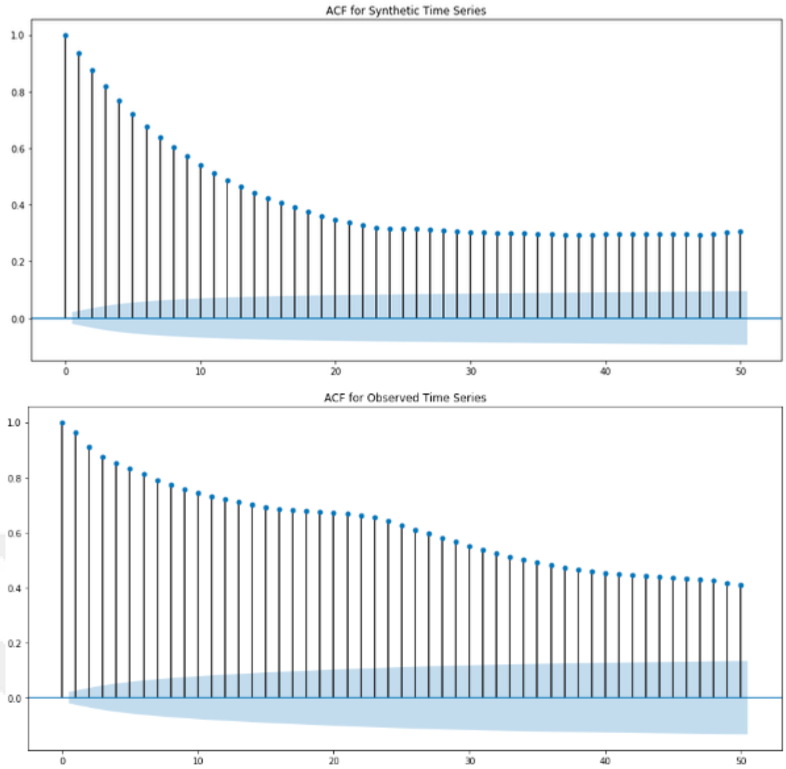

Figure 2.6 Autocorrelation function with 50 lags for synthetic and observed time series

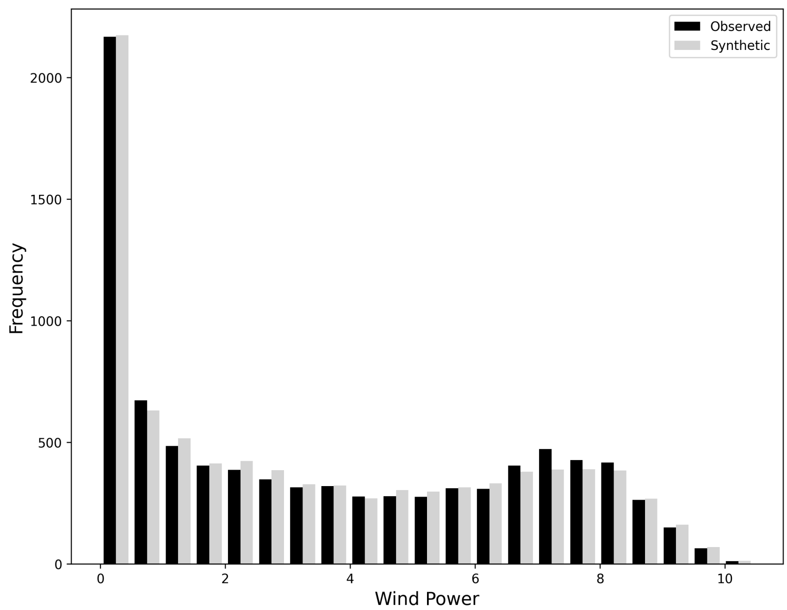

Figure 2.7 Observed vs synthetic data

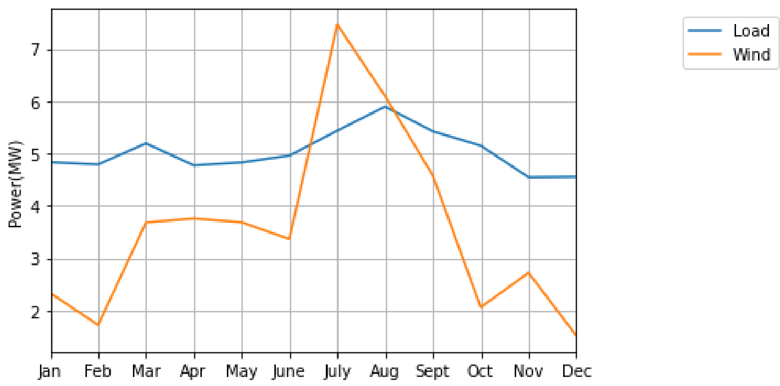

Figure 2.8 Average monthly power of load and wind

2.7 Experimental Results

Li-ion and PHS are chosen as battery and bulk storage systems, respectively. The mathematical model represented in Section 2.3 is solved using different instance sets. Table 2.1 represents the cost parameters of different instances where minimum, moderate, and maximum investment costs of ESSs are taken from Table 1.2 and annualized.

First, created wind and load data are investigated. While the average of the wind power is 3.60 MWh, average of the electricity demand is 5.03 MWh. Monthly averages show that electricity demand is greater than the supply except for two months, also shown in Figure 2.8. In order to balance the demand and the supply, we decrease the demand and create three load profile as low, moderate, and high with the averages 3.40 MWh, 3.60 MWh, and 3.80 MWh, respectively. By applying this balance, we are able to analyze and interpret the storage investments and decisions properly, otherwise the analysis is dominated by diesel cost as the average demand is greater than average supply.

As it is known, the operating cost of the batteries is quite expensive, especially compared to PHS. Considering the technological advances in batteries and the potential price drop in the future, we have added two relatively lower costs to our data set, in addition to the current operating cost, which is 0.03 \$/kWh. Besides the operating cost, two lower investment costs have also been created based on the maximum annual cost, as shown in Table 1.2.

Figure 2.9 shows the problem setting in which there are two transmission lines, where the first line connects the wind farm and the battery to the bulk storage. The second line connects the bulk storage to the load center. If the model decides

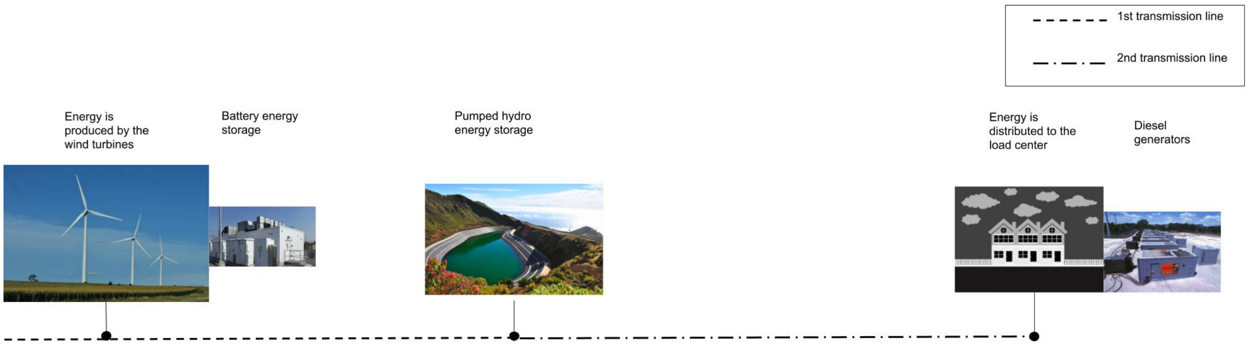

Figure 2.9 Proposed island system

not to construct bulk storage, then the transmission line is assumed to be a straight one from generation to load center. Since we consider a geographically small island, the total length of the transmission line is considered as 30 miles, roughly about 50 kilometers. To assess importance of the location of PHS, we determine five different places that PHS might be located. These points are obtained by dividing the line in five equal distances.

To investigate the effect of some of the parameters on the system model, an experimental analysis is performed. Instance sets are generated by changing five different problem parameters, namely investment costs of ESSs, location of the PHS on the transmission line, battery operating cost, and electricity load profile. For both ESSs, power and energy-related investment costs are calculated as a minimum, moderate, and maximum costs (for battery, we have 2 additional costs), which is shown in Table 1.2. There are fifteen different investment decisions for ESSs, five candidate locations for PHS, three operating costs for battery, and three load profile. In total, 675 instances are created.

In addition, 45 cases are also investigated, in which only battery installation is allowed. Electricity is directly sent through the straight transmission line to the load center as there is no PHS in any of those cases. Five different investment costs and three different operating costs of battery and three load profile are determined as the parameters, which has the same values as the previous model setting that includes two different types of ESSs.

Table 2.1 Sets of ESSs energy and power rate

Technology		Cost				
		Minimum	Moderate	Maximum	Maximum/3	Maximum/10
Li-ion	Power ($/kW-yr)	78.5	97.3	116.1	38.7	11.61
	Size ($/kWh-yr)	19.65	24.35	29.05	9.68	2.905
PHS	Power ($/kW-yr)	34	49	64	-	-
	Size ($/kWh-yr)	2.12	3.06	4	-	-

Table 2.2 Sets of other parameters

	Li-ion	PHS
Variable O&M ($\kWh)	0.03, 0.001, 0.003	0.00025
Round-trip Efficiency (%)	95	85
Diesel Cost ($\kWh)	0.25	
Transmission line ($\kW-mile)	1	

2.7.1 Battery and PHS Installation

We observe some of the results to understand the effect on parameter changes. Investment decisions of ESSs, invested energy and power rates, invested transmission line capacity, and total annual costs are analyzed. Also, cost elements are investigated separately, which are total diesel consumption cost, total investment cost, including transmission line and investment of ESSs, and total operating cost of ESSs.

Out of 675 instances, battery and PHS are invested in 140 and 590 instances, respectively. In 55 instances, both battery and PHS are invested. In the vast majority of cases with battery placement, we observe that the battery investment cost is the lowest among the parameter set. However, PHS is invested for all of the instances except the ones with some of the lowest investment cost for battery and some of the two highest investment costs for PHS among the parameter set. Both battery and PHS are invested when both investment costs of both ESSs are at their minimum level. Another significant point is at least one of the ESS types is invested for all instances. It brings us to a notable finding; constructing ESSs helps to reduce the total system cost within this or similar generation-load time series. It is also clear that investment decisions are made mostly depend upon the investment costs, rather than the other cost parameters.

Total cost is affected by the total invested energy rate of ESSs, which is shown in Figure 2.10. As the total invested energy rate decreases, total cost increases for all load profiles. The main reason for this is the increasing diesel consumption and the corresponding cost of it. Thus, it can be said that, while total investment energy rate decreases, diesel cost increases, which results in an increase of the total cost, for most of the instances. Also, we observe that the total cost and the diesel cost has a strong relation, in which a linear trend between two costs are shown in Figure 2.11.

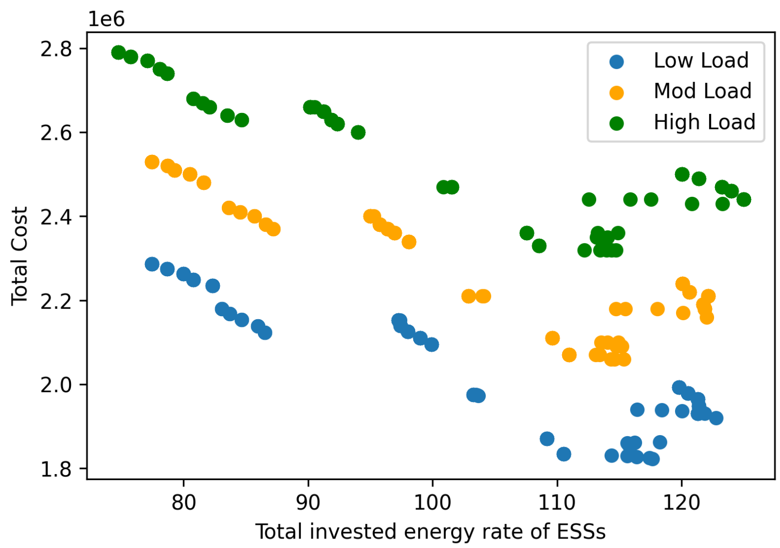

Figure 2.10 Effect of sum of battery and PHS energy rate on total cost

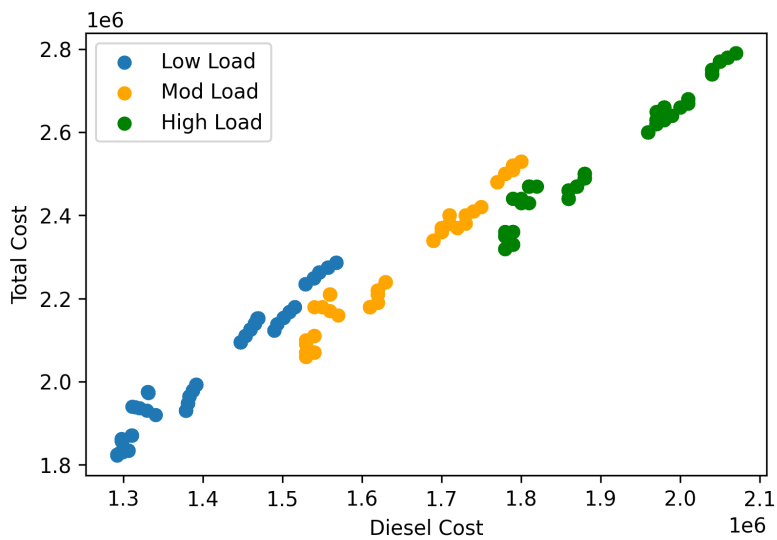

Figure 2.11 Diesel cost effect on total cost

Figure 2.12 depicts all cost components by instances. First 225 instance has a low load, the latter 225 represents the moderate load, and last 225 shows the high load profile. Total system cost and diesel cost follow almost the same pattern for all instances, which means the increment on the total cost strictly depends on the diesel cost. In Table 2.3, average of the costs according to load profiles is shown. We can also see similar results, where the total cost increases as the load profile scale up, even though the battery and PHS investments yield pretty similar values. Since the wind generation and corresponding storage level are similar over the load profiles, ascending energy need inclines to diesel consumption in order to fulfill this increased demand. Average O&M cost for battery is higher than the average O&M cost for PHS, as all of the three parameters we used in the analysis are way greater than the O&M cost for PHS. Also in Figure 2.12, O&M cost shows a sharp increase for all load profile at some specific instances. This increase happen when battery storage systems is invested and mostly dominate the total invested EES energy rate where battery investment decisions are made at its lowest investment cost and highest O&M cost. We can also see two less remarkable increases on the same figure, in which only different parameter is O&M cost of battery which are 10 and 3. At these points, transmission line investment also decreases as the PHS is not constructed or constructed with very small sizes. This leads to a decrease on especially first transmission line.

On average, 19.33MWh and 82MWh energy rates are invested for battery and PHS with 0.9MW and 3.125MW power rates, respectively. Thus, the average investment cost of PHS is greater than the investment cost of battery. Finally, the investment cost of the transmission line increases as the electricity demand increases, since more investment is needed to satisfy the demand and reduce the total system cost.

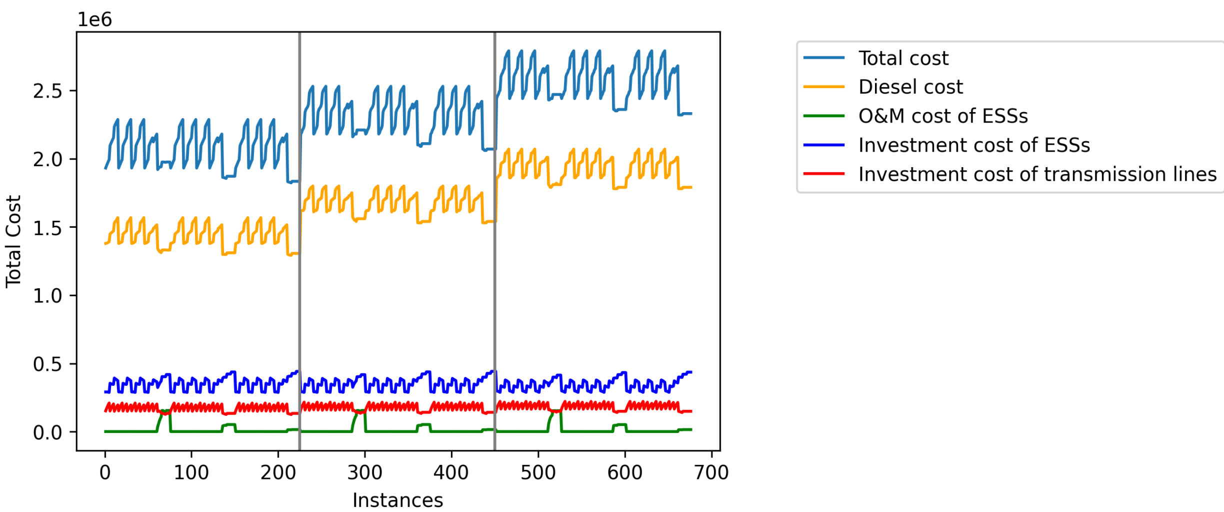

Figure 2.12 All cost parameters

Table 2.3 Cost averages for all load profiles ($)

	Low Load	Mod Load	High Load
Diesel cost	1,430,541	1,665,823	1,926,250
O&M cost for battery	12,820	13,121	13,245
O&M cost for PHS	956.44	943.93	930.52
Battery investment cost	65,983	67,759	66,221
PHS investment cost	382,747	380,512	376,096
Tr. line investment cost	170,231	177,193	184,118
Total cost	2,063,279	2,304,796	2,567,455
Diesel cost %	0.693	0.722	0.750

The location of PHS has mild effects on the system's total cost, which slightly increases for some instances as the PHS facility is closer to the load center. However, most of the instances yield similar total costs as the PHS location changes. Each graph in Figure 2.13 shows the costs which are averaged over the instances based on the location of PHS. The X-axis indicates the miles away from the wind farm. On average, battery investment increases as the PHS approaches the load center, however, PHS investment decreases. Average transmission line investment, average diesel cost, and average total cost also increase when PHS gets closer to the load center. It should be noted that graphs show slight changes, and since they contain the averages, these increases and decreases cannot apply for all of the instances.

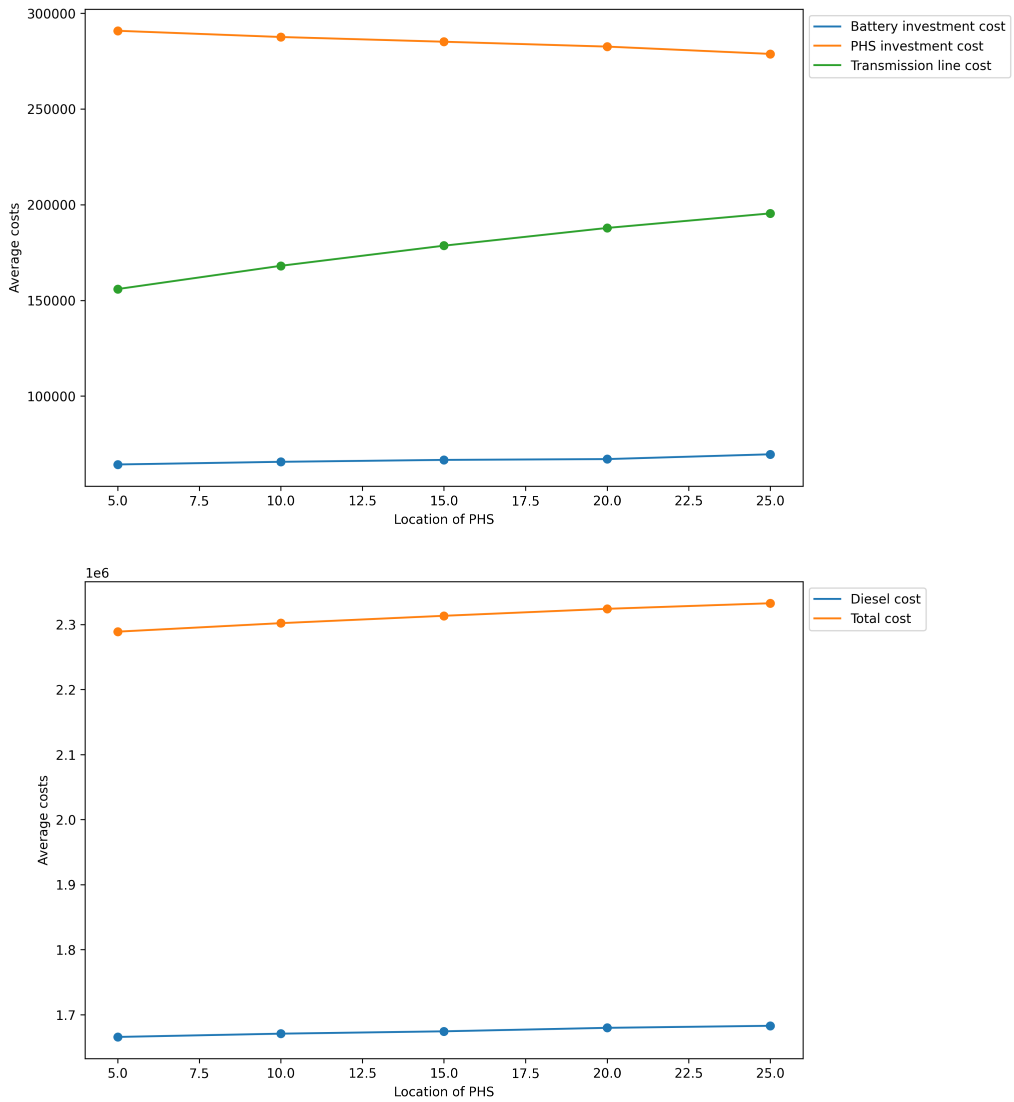

Figure 2.13 Effect of the location of PHS on the cost parameters and the total cost

The energy and power rate investments of ESSs have an obvious relation with the energy and power rate investment costs of PHS and battery. We also investigate if the other parameters have any effect on investments of ESSs. The location of the PHS, as mentioned above, has very little influence on the investment energy amounts of battery and PHS. Figure 2.14 illustrates the effect of O&M cost of battery changes on energy rate investment value of both ESSs. O&M cost for battery has three different parameters; 3,10, and 30 per MWh/$. As the O&M cost decreases, on the average, energy rate of battery investing increases, however, this decrease leads to less energy investment for PHS. As mentioned, load profile change does not affect significantly the investment amounts of ESSs. System rather prefer to fulfill this increased demand by raising the diesel consumption. First transmission line capacity is very high when there is no investment on the battery (see: Figure 2.16 yellow dots at the left). One reason of that is when there is no battery to store the energy next to the wind power, sending the generated electricity as much as possible is become important. The other point is when there is a PHS investment instead of battery, excess energy is sent to the PHS to be stored. Thus, more investment on the first transmission line is high when there is no battery investment.

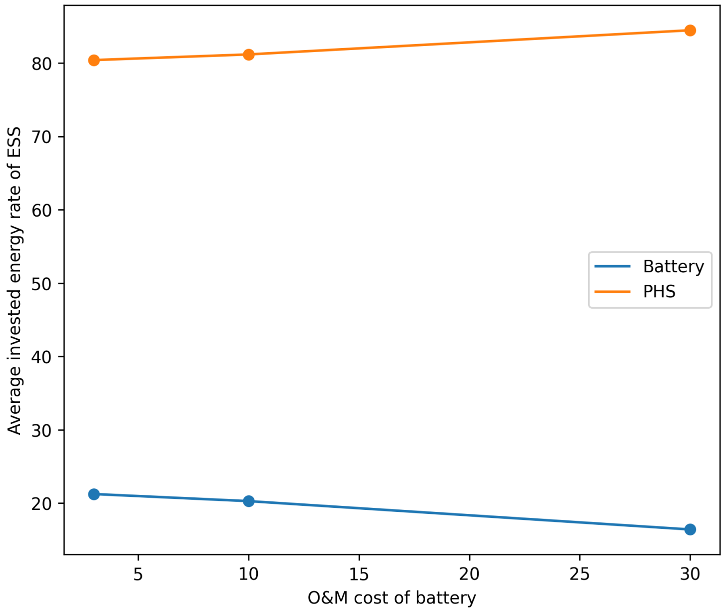

Figure 2.14 Effect of O&M cost parameters of battery on energy rate investments of ESSs

We investigate the investment rates of two transmission lines. First transmission line capacity is greater than the second transmission line capacity for most of the instances as it is seen in Figure 3.4. This is an expected result as in the most of the instances decide to construct PHS. Exceptions occur only for the instances which have a minimum investment cost of battery. When the battery investment cost gets its minimum value, it leads to more investment to battery than PHS. Moreover, for some of those instances, PHS is not invested at all, which makes the investment on the first transmission line insignificant. In this case, capacities of the transmission lines are equal, as we can also assume them as though it is a straight one. As a result, when the capacity investment of battery is a lot more than the amount of capacity invested for PHS, then, the second transmission line becomes more important. Otherwise, first transmission line investment is more critical, since there should be enough capacity to pass the generated and not used energy through the first line at a specific period to store it into PHS for later use.

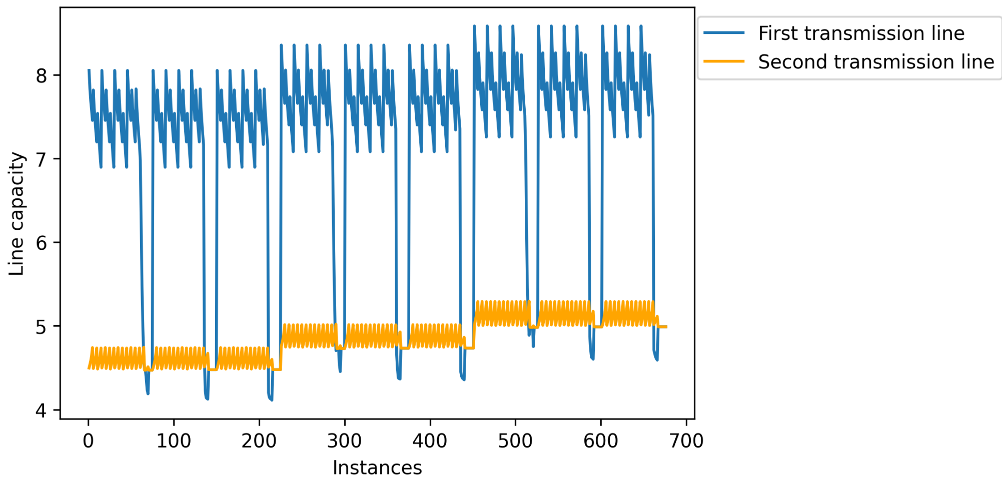

Figure 2.15 Invested capacity of two transmission lines

Likewise, Figure 2.16 emphasizes the relation between invested capacity of the first transmission line and energy (or power) rates of ESSs. To analyze the first transmission line may give us insightful results as it is needed both for carrying the energy to the load center, as well as storing the energy to PHS. Invested transmission line capacity decreases as invested energy rate for battery increases, and transmission line capacity increases as invested energy rate for PHS increases, for most of the instances. A similar pattern is shown between transmission line capacity and power rates.

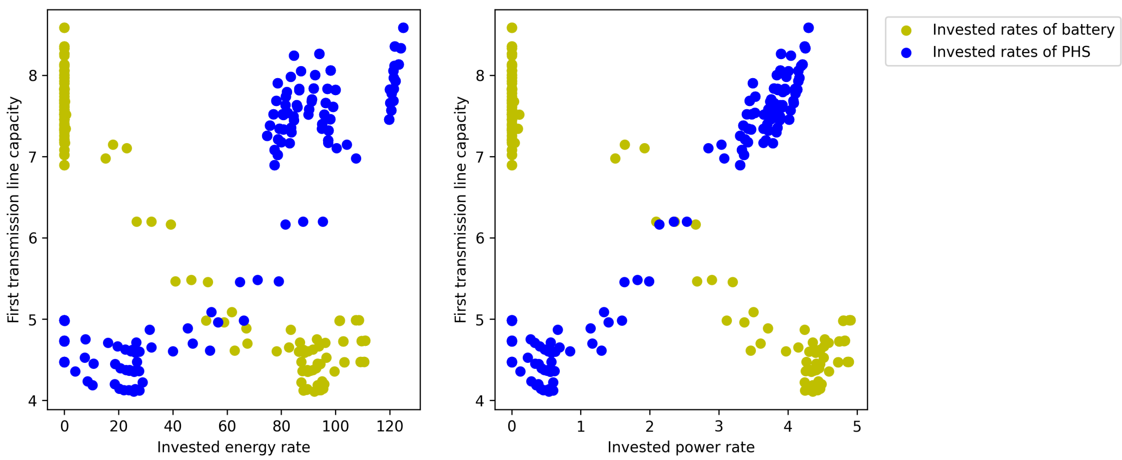

Figure 2.16 Effect of transmission line capacity on energy rate investments of ESSs

2.7.2 Only Battery Investment

In this section, we discuss the results of cases where only battery investment is allowed. Out of 45 instances, battery is invested in 36 instances. The remaining 9 instances are the ones that have the highest investment cost and the model rather prefer to use diesel generators to create electricity to satisfy the excess demand as well as fluctuations.

Similar to the setting with PHS, total cost and diesel cost are affected by the invested energy amount of the battery. More investment leads to less diesel usage and diesel cost, which is also directly related to the total cost. Figure 2.17 and 2.18 emphasize that the total cost and diesel cost increases as the energy rate investment of battery decreases. Figure 2.19 demonstrates all the cost components where first 15 instance has a low load, latter 15 represents the moderate load, and last 15 shows the high load profile. Total cost and diesel cost follow similar patterns over the instances. These costs go up as the load profile changes. However, investment cost of ESS and investment cost of transmission line remain quite similar as the load profile changes. Since invested rate of battery does not heavily depend on the load profile, O&M cost of battery also is not affected by the load profile. Table 2.4 also shows that total cost and diesel cost increase over the load profile. However, investment in battery amounts yields pretty close results. Also, transmission line investment slightly increases as the load profile increases.

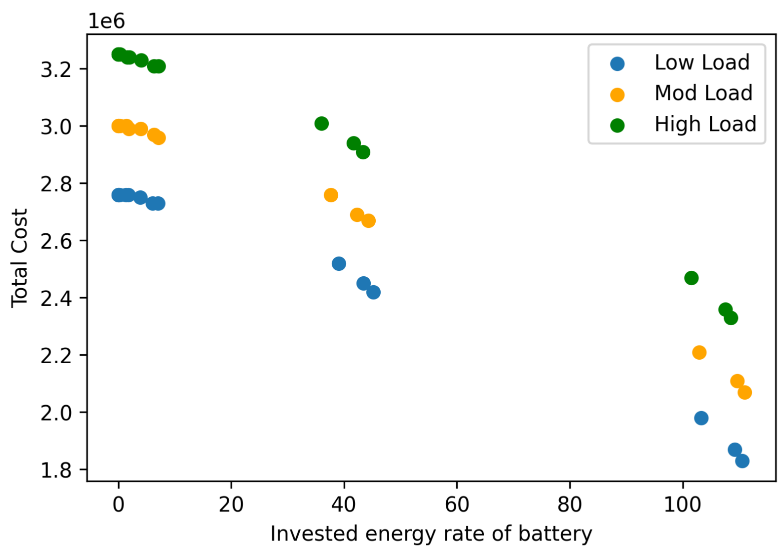

Figure 2.17 Effect of battery energy rate on total cost

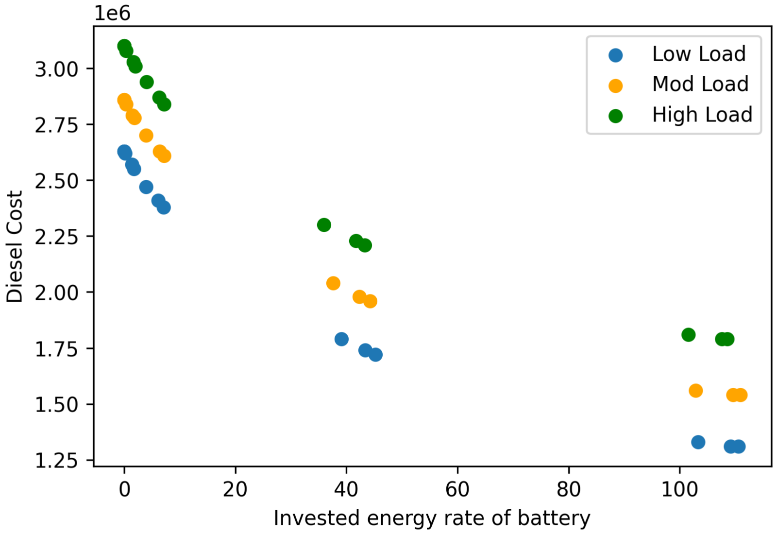

Figure 2.18 Diesel cost effect on total cost

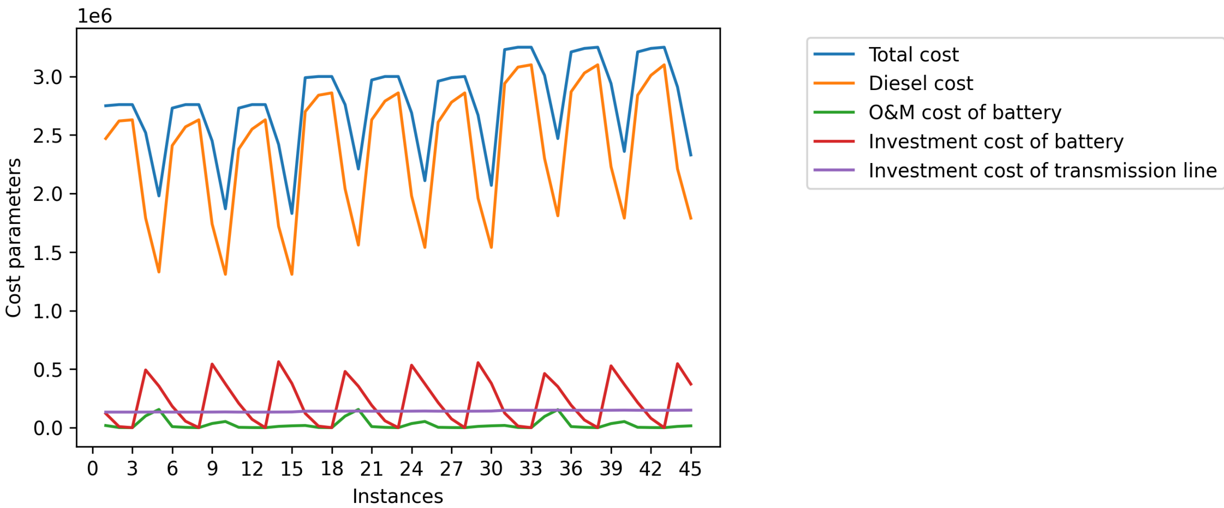

Figure 2.19 All cost parameters

Table 2.4 Cost averages for all load profiles ($)

	Low Load	Mod Load	High Load
Diesel cost	2,139,333	2,370,000	2,613,333
O&M cost for battery	27,029	26,982	26,672
Battery investment cost	223,579	223,292	221,268
Tr. line investment	133,278	141,001	148,685
Total cost	2,522,666.	2,761,333.	3,010,000
Diesel cost %	0.868	0.858	0.848

The energy and power rate investments of battery are mainly affected by energy and power rate investment costs of battery. As the investment cost increases, invested rates decrease and yet battery is not invested at all for the cases which have extreme investment costs. On average, the invested energy rate of battery increases when the O&M cost parameter decreases. However, investment decisions are made and dominated by investment costs. In Figure 2.20, investment cost of battery increases and decreases depends on the instances. Total investment cost of battery is high when the investment cost is lower, because there is more investment when the cost is low. Also, less total cost is observed when the battery storage investment is high.

In this problem setting, there is only one transmission line. Highest capacity investments are observed when the load profile is high, and this capacity investments decrease as the load profile decreases which is shown in Figure 2.20. Another observation is about energy rate investment costs. When the invested energy rate increases, the invested capacity of the transmission line also increases for all three load profile. As the total generated and stored energy increases, total transmission line capacity also increases so that the required energy can be transmitted to the load center.

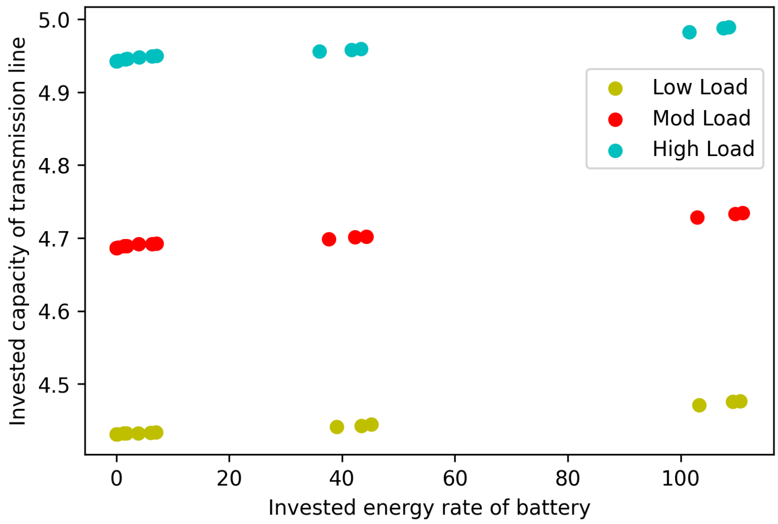

Figure 2.20 Investigation of transmission line capacity and invested energy rate of battery while considering the load profile

2.7.3 Comparison of two Settings

In this section, two settings that consist of one type (only battery) and two types (battery and PHS) of ESS are compared. Total costs of two settings vary between \$1.83M-\$3.25M and \$1.82M- \$2.79M, respectively. The values in Table 2.5 represent the averages costs over instances for both settings. On average, total cost and diesel cost are higher when there is only a battery installation option. It is mainly observing because constructing the battery is relatively more expensive than constructing PHS, thus for the instances with the high investment cost of battery, either very small size of battery is invested or nothing is invested. This leads to an increase in diesel cost and total cost for the setting with one type of ESS. Similarly, there is less average total invested transmission line capacity in the one type of ESS setting since total stored energy capacity is also less than the setting with two ESS setting. As a result, the investment costs of the ESSs are the key determinants of the total system cost. These costs also affect the other variables of the system such as invested transmission line capacity and diesel generator usage. As the total storage investment decreases, the invested capacity of the transmission line decreases, total and diesel cost increases. The percentage of diesel cost is also higher at one type of ESS setting since there is less investment on the battery mainly because of its costs.

The observations show that due to the very expensive investment and operating costs of the battery technology, PHS still seems the most efficient technology in terms of total system cost for the off-grid systems. Battery, however, still a viable option especially when its distinctive feature is taken into account; location independence. Moreover, with the predicted dropped investment costs of battery technology, it might be more cost-efficient than PHS technology in the future.

Table 2.5 Cost averages for all instances of two settings (\$)

Costs	Battery & PHS	Only battery
Diesel cost	1,675,555	2,374,222
O&M cost for battery	13,044	26,894
O&M cost for PHS	943	-
Battery investment cost	66,176	222,713
PHS investment cost	380,357	-
Tr. line investment cost	177,305	140,988
Total cost	2,313,447	2,764,819
Diesel cost %	0.722	0.858

Table 2.6 Comparison of two SMIPs (with 10 and 25 scenarios)

Total cost ($M)		Energy rate of battery		Energy rate of PHS		Power rate of battery		Power rate of PHS	
2.44	2.47	0	0	124.985	120.86	0	0	4.29682	4.25652
2.6	2.63	0	0	93.9937	92.02	0	0	3.89716	3.86100
2.74	2.76	0	0	78.6961	77.25	0	0	3.49218	3.43203
2.44	2.47	0	0	124.985	120.86	0	0	4.29682	4.25652
2.6	2.63	0	0	93.9937	92.02	0	0	3.89716	3.86100
2.74	2.76	0	0	78.6961	77.25	0	0	3.49218	3.43203
2.44	2.47	0	0	124.985	120.86	0	0	4.29682	4.25652
2.6	2.63	0	0	93.9937	92.02	0	0	3.89716	3.86100
2.74	2.76	0	0	78.6961	77.25	0	0	3.49218	3.43203
2.44	2.47	0	0	124.985	120.86	0	0	4.29682	4.25652
2.6	2.63	0	0	93.9937	92.02	0	0	3.89716	3.86100
2.63	2.65	0	0	84.6778	82.38	0	0	4.0403	3.97885
2.43	2.46	22.9691	23.6049	100.322	96.83	1.92266	2.00	2.84574	2.73398
2.47	2.5	101.547	100.42	0	0.00	4.80222	4.76	0	0
2.47	2.5	101.547	100.42	0	0.00	4.80222	4.76	0	0

2.7.4 Scenario Comparison

SMIP is solved with 10 different scenarios and analyzed in the previous sections. Number of scenarios that are used to solve the model has a critical role on the solution time which increases exponentially as the number of scenarios becomes larger. In this section, we provide some information about 10-scenario SMIP and compare it with some of the instances which are solved with 25 and 50-scenario SMIPs.

As it was mentioned before, we have 675 different instances to be solved for the setting with two ESSs. On average, one instance is solved in between 40-60 minutes for the 10-scenario case. However, when the number of scenarios is changed to 25 and 50, this solution time increases dramatically. Approximately, a solution is provided for one instance in between 80-100 minutes for 25-scenario case and between 6-7 hours for 50-scenario case. When this is the case, increasing the number of scenarios creates great difficulties in terms of solution time. Nonetheless, the results are quite similar as the number of scenarios become larger. We randomly pick 15 instances from the 25 and 50-scenario cases and solve the models in order to verify consistency and similarity with the 10-scenario case. As an indicator, we consider the investment decisions of ESSs and total cost. For all instances, investment decisions do not change, more precisely if it is not invested in the 10-scenario case, then also the same decisions are taken in the 25 and 50-scenario cases for that particular instance. In Table 2.6 and 2.7, there are 15 instances and some of the variables obtained by solving SMIP with both 10, 25 and 50 scenarios. Left columns indicate 10-scenario case and right columns consist of the 25 and 50-scenario cases, respectively. We observe tiny differences between the total costs where 25 and 50-scenario cases yield greater total costs and fewer investment rates for the ESSs. This experiment reveals that the results of the three scenarios are not very different from each other. Therefore, it seems more reasonable to apply the experiments with 10 scenarios, especially when the solution time is considered.

Table 2.7 Comparison of two SMIPs (with 10 and 50 scenarios)

Total cost ($M)		Energy rate of battery		Energy rate of PHS		Power rate of battery		Power rate of PHS	
2.44	2.48	0	0	124.985	123.98	0	0	4.29682	4.25448
2.6	2.64	0	0	93.9937	93.1543	0	0	3.89716	3.84171
2.74	2.77	0	0	78.6961	76.9543	0	0	3.49218	3.41485
2.44	2.48	0	0	124.985	123.98	0	0	4.29682	4.25448
2.6	2.64	0	0	93.9937	93.1543	0	0	3.89716	3.84171
2.74	2.77	0	0	78.6961	76.9543	0	0	3.49218	3.41485
2.44	2.48	0	0	124.985	123.98	0	0	4.29682	4.25448
2.6	2.64	0	0	93.9937	93.1543	0	0	3.89716	3.84171
2.74	2.77	0	0	78.6961	76.9543	0	0	3.49218	3.41485
2.44	2.48	0	0	124.985	123.98	0	0	4.29682	4.25448
2.6	2.64	0	0	93.9937	93.1543	0	0	3.89716	3.84171
2.63	2.66	0	0	84.6778	82.6938	0	0	4.0403	3.95631
2.43	2.46	22.9691	22.8392	100.322	100.322	1.92266	1.94666	2.84574	2.78135
2.47	2.5	101.547	101.485	0	0	4.80222	4.75168	0	0
2.47	2.5	101.547	101.485	0	0	4.80222	4.75168	0	0

2.8 Conclusion

In this chapter, an electricity system for an island where the PHS and battery storage sizing is studied. A mixed-integer linear programming model is used. Two experiments are conducted: with both storage systems and with only battery storage system. The main results of the experiment are as follows:

1) Importance of the investment and O&M costs of the storage technologies on the system cost is undeniable. Efficiencies of the storage technologies may also affect the investment rates and thus, the total cost.
2) When we consider the total system cost, it yields the minimum costs when there is a high investment on battery alongside lower investment on PHS. However, these decisions are obtained when the costs for battery (both investment and O&M) are unrealistically low. The current technological trends seem unpromising to achieve those cost levels. Therefore, PHS will continue to dominate the storage systems for a foreseable future.
3)When there is a balance between wind and load (as we decrease the load to be able to see the ESSs investment effects), on average, between 12%-16% of the yearly electricity is provided by constructed ESSs. Generated wind energy which is directly sent to the load center contributes approximately 61%-65% to the yearly electricity demand. Diesel generators share is around 19%-24% to fulfill the demand per year.
4) For that island, renewable generation dominates the supplied electricity, but still diesel generator (which contains around 75% of the total yearly system cost) has a considerable share on the electricity supply. This share is expected to be higher since real demand is decreased for the sake of the experiment.
5) The island that we have load and generation data, generates electricity through wind energy which is supported by PHS. It was announced that this island closes

the renewables share of 55% in 2019. In our model we conclude that 73-81% is the share of the renewables per year. One reason of this is can be the decreased load, and second one is we allow one more storage system. Another differences may arise because of our assumptions (e.g, transmission line length and PHS is constructed on the middle of the line because it is constructed near by the generation side in the real setting, etc.)
6) We have 3 different decreased load profile, however this experiments shows that when the load profile increases, there could not be further investment on ESSs' capacities. This means, when the real demand data is used, again the investments of ESS could possibly remain similar, but diesel usage could compensate the demand.

3. Grid Systems

In this chapter, we consider a more comprehensive system, i.e, the transmission grid that we shortly refer to as the grid system. Unlike the island system where the location decision is immediate, in grid systems, these decisions also become important. These systems are also complicated as they must necessarily contain various conventional generators that have various types constraints for generation start-up, shut down, and ramp up and down decisions. These systems are also complicated by the number of alternative PHS locations. Another complicating factor in these problems is the availability of different transmission technologies that have varying energy loss and cost structures. This issue becomes particularly important in large grids where some electricity is tranmmitted over long distances such as 1,000 kms or longer. Except for the last factor the model that we develop here considers previous factors.

It is almost impossible to solve large grid systems by using exact methods in which sizing and siting decisions have to be made. In the literature, there are several methods applied to overcome this complexity. For example, Pandžić et al. [2014] propose a three-stage mixed-integer problem for a transmission network that considers siting, sizing, and operational decisions independently. In the first part, a mathematical model is solved separately for all days. They investigate the nodes where storage is constructed and then the storage locations are determined based on a threshold value. The second stage is the same as the first one, but this time locations of the storage systems are known. They solve the model for each day by assigning the sizes of the storage units which are identified at the previous stage. At the last stage, the model is solved for each day for the entire year with the known locations and sizes of storage units. The importance of this stage is to understand the effect of the number of storage units on the system cost. They use a modified version of IEEE-RTS 96 test system where 19 wind farm is added to test their approach. Wind speed data is obtained from NREL western wind and it is converted to the wind power data. IEEE test systems are being used in the literature as they are public and offer standard data which are very useful while comparing the approaches.

Fernández-Blanco et al. [2016], study a siting and sizing problem of storage devices where the objective is to minimize the operating and investment cost of ESS for a transmission network. The objective function also includes a societal cost that is related to the spillage of renewable energy. Western electricity coordinating council (WECC) system which has 240-bus and 448-line is used to test their proposed method. The renewable generation and load are generated as five representative days. In the case study, 1, 5, 10, and 15 locations are determined as the maximum number of locations in which the storage devices can be located. The most preferred locations over the experiment are the ones that are closer to wind, biomass, and geothermal generation points. Also, some of the preferred buses are adjacent to the transmission lines that have more risk to have congestion. Dvijotham et al. [2014] aim to find optimal siting and sizing of ESS in a transmission network that includes renewable and traditional generators. To determine the locations and sizes of ESS, they develop a greedy heuristic.

Pudjianto et al. [2013] consider a whole-systems approach to minimize the overall cost of the new investments in generators and storage units. In addition, additional transmission line capacity and other operating costs are also considered. They compare bulk and distributed storage for different installation cost levels. Qi et al. [2015], consider a transmission network planning problem while including the ESS where the optimal transmission line capacities, sizes, and locations of ESS are determined in order to minimize the total expected cost. Two costs are taken into consideration where the first one is building costs and the second one is energy loss cost. Energy loss cost occurs due to friction loss, overflow loss, and curtailment loss. There are wind farms which have no connection to the main grid and the aim is to connect those farms to a single load center. In their first model, they solve a mixed-integer second-order-conic program (MISOPC) to find the optimal investment decisions of ESS and junction sites under the assumption that there is no limit on the storage capacity. In the second part, they derive a closed-form upper bound to find the optimal ESS sizes. In Fiorini et al. [2017], a transmission network with renewable energy is studied in which the aim is to minimize the production cost while finding the sizing and the location of the batteries. They also investigate the most stressed lines in the transmission network. They develop a ranking method for reducing the line congestion to decide the locations of the batteries. They show that locating the batteries close to the wind farms is not the best option to relieve the congestion for the lines connected to wind farms. Instead, to locate the batteries considering the stressed transmission lines promises to be more beneficial.

In this chapter, we propose an MILP model where the aim is solve a modest sized grid system, such as that of relatively large island or a small country. The grid in-

Table 3.1 Flexibility characteristics of conventional generators

	Start-up time	Start-up cost (USD/MW instant start)	Minimum load (% Pnom)	Avg. Ramp rate (% Pnom/minute)	Min. uptime	Min. downtime
Hard coal	2-10h	>100	25-40%	1.5-4%	48h	48h
Lignite	4-10h	>100	50-60%	1-2%	48h	48h
CCGT	1-4h	55	40-50%	2-4%	4h	2h
OCGT	5-11min	<1-70	40-50%	8-12%	10-30min	30-60min
ICE	5min	<1	20% (per unit)	>100%	<1min	5min

cludes two types of storage types, namely battery and PHS, conventional electricity generation system, and wind power. The aim is to determine the size and location of ESSs, capacity of transmission lines while minimizing the total cost. This cost consists of ESS investment and operational cost, investment cost of transmission lines, and operating cost of conventional generators. The most important difference between the model that we develop here and the previous one is the presence of conventional generators, whose different start-up, show-down, and ramp rate decisions, require various complicated constraints. Sometimes accurate representations of these constraints may even be infeasible in our modeling structure and therefore, needs to be approximated or rough-cut.

3.1 Conventional generators

According to Irena [2019] minimum load, ramp rate, and, start-up time are the flexibility characteristics of conventional generators. The values and the ranges of the characteristics are shown in Table 3.1. Hard coal-fired, lignite-fired, open cycle, and combined cycle gas turbine power plants are the main power generators which satisfy most of the world's electricity demand. In our model, we use hard coal-fired as conventional generators. lines, instead.

3.2 Problem formulation

In the second chapter, we use two problem formulations. Both are used in a two-stage algorithm. The first formulation is used in the first stage of the algorithm and the second formulation is used in the second stage of the algorithm. Below, the first problem formulation is shown which is called "P1".

Let $G = (B, K)$ indicate the graph of a power network, where B represents the set of buses (nodes) and K represents the transmission lines (edges). Buses can have conventional generators, renewable generators, and can be a load center. A bus can also include all of the elements at the same time.

Indices and Sets:

$i \in I$: Set of storage types

$t, t' \in T$: Set of time slots

$k \in K$: Set of transmission lines

$b, b' \in B$: Set of buses

$g \in G$: Set of generator units

$K_b \subset K$: Subset of transmission lines which are connected to bus b

$G_b \subset G$: Subset of generators which are connected to bus b

Parameters:

G^R_{bt}: Wind energy generation at bus b at time t,

D_{bt}: Demand at bus b at time t

rd_g: Ramp down rate for generator g

ru_g: Ramp up rate for generator g

G^{min}_g: Minimum output generator g can provide

G^{max}_g: Maximum output generator g can provide

C^{pen}: Unit penalty cost of not satisfying the demand

C^{TR}_k: Unit transmission cost of building line k

C^{SU}_g: Start-up cost of generator g

C^{OM}_g: Operating and maintenance cost of generator g

C^{nl}_g: No-load cost of generator g

C^e_i: Energy related investment cost of storage type i

C_i^p: Power related investment cost of storage type i

C_i^{OM}: Operating and maintenance cost of storage type i

E_i^{max}: Maximum energy rate that can be invested of storage type i

P_i^{max}: Maximum power rate that can be invested of storage type i

η_i^c: Charging efficiency of storage type i

η_i^d: Discharging efficiency of storage type i

L_g: Lead time for generator type g start-up

Decision Variables:

$$x_{bgt} = \begin{cases} 1, & \text{if conventional generator } g \text{ connected to bus } b \text{ is on at time } t, \\ 0, & \text{otherwise.} \end{cases}$$

$$y_{bgt} = \begin{cases} 1, & \text{if conventional generator } g \text{ at bus } b \text{ starts up at time } t, \\ 0, & \text{otherwise.} \end{cases}$$

$$z_{bgt} = \begin{cases} 1, & \text{if conventional generator } g \text{ at bus } b \text{ shuts down at time } t, \\ 0, & \text{otherwise.} \end{cases}$$

$$v_{bgt} = \begin{cases} 1, & \text{if conventional generator } g \text{ at bus } b \text{ is at lead time period at time } t, \\ 0, & \text{otherwise.} \end{cases}$$

G_{bgt}^C= Energy generated by generator g at bus b at time t

E_{ib}= Energy rate of storage type i at bus b

P_{ib}= Power rate of storage type i at bus b

X_k^{max}= Maximum capacity of transmission line k

S_{ibt}= Energy level at storage type i at bus b at time t

S_{ibt}^{ch}= Charging rate of storage type i at bus b at time t

S_{ibt}^{dis}= Discharging rate of storage type i at bus b at time t

X_{bkt}^{in}= Inflow to bus b through line k at time t

X_{bkt}^{out}= Outflow to bus b through line k at time t

L_{bt}= Dump load at bus b at time t

Y_{bt}= Penalty term if demand cannot be satisfied at bus b at time t

P(1)

$$Min \sum_{i\in I}\sum_{b\in B}(C_i^e E_{ib} + C_i^p P_{ib}) + \sum_{k\in K} C_k^{tr} X_k^{max} + \sum_{i\in I}\sum_{b\in B}\sum_{t\in T} C_i^{OM} S_{ibt}^{dis} + \sum_{b\in B}\sum_{t\in T} C^{pen} Y_{bt} + \sum_{b\in B}\sum_{g\in G_b}\sum_{t\in T}(C_g^{SU} y_{bgt} + C_g^{OM} G_{bgt} + C_g^{nl} x_{bgt}) \tag{3.1}$$

subject to;

$$y_{bgt} - z_{bgt} = x_{bgt} - x_{bg,t-1}, \qquad \forall b\in B, g\in G_b, t\in T \tag{3.2}$$

$$y_{bgt} + z_{bgt} \le 1, \qquad \forall b\in B, g\in G_b, t\in T \tag{3.3}$$

$$L_g * y_{bgt} \le \sum_{t=t}^{t+L_g} v_{bgt}, \qquad \forall b\in B, g\in G_b, t\in T \tag{3.4}$$

$$G_g^{Cmin} * (x_{bgt} - v_{bgt}) \le G_{bgt}^C \le G_g^{Cmax} * (x_{bgt} - v_{bgt}), \qquad \forall b\in B, g\in G_b, t\in T \tag{3.5}$$

$$rd_g \le G_{bgt}^C - G_{bg,t-1}^C \le ru_g, \qquad \forall b\in B, g\in G_b, t\in T \tag{3.6}$$

$$G_{bt}^R + \sum_{g\in G_b} G_{bgt}^C - \sum_{k\in K_b} X_{bkt}^{out} + \sum_{k\in K_b} X_{bkt}^{in} + \sum_{i\in I} S_{ibt}^{dis} + Y_{bt} = D_{bt} + \sum_{i\in I} S_{ibt}^{ch}, \qquad \forall b\in B, t\in T \tag{3.7}$$

$$X_{bkt}^{in} \le X_k^{max}, \qquad \forall b\in B, k\in K_b, t\in T \tag{3.8}$$

$$X_{bkt}^{out} \le X_k^{max}, \qquad \forall b\in B, k\in K_b, t\in T, \tag{3.9}$$

$$X_{bkt}^{in} = X_{b'kt}^{out}, \qquad \forall b, b'\in B, k\in K_b, t\in T \tag{3.10}$$

$$X_{bkt}^{out} = X_{b'kt}^{in}, \qquad \forall b, b'\in B, k\in K_b, t\in T \tag{3.11}$$

$$S_{ibt} \le E_{ib}, \qquad \forall i\in I, b\in B, t\in T \tag{3.12}$$

$$S_{ibt} = S_{i,b,t-1} + S_{ibt}^{ch}\eta_i^c - S_{ibt}^{dis}/\eta_i^d, \qquad \forall i\in I, b\in B, t\in T \tag{3.13}$$

$$S_{ibt}^{ch}\eta_i^c \le P_{ib}, \qquad \forall i\in I, b\in B, t\in T \tag{3.14}$$

$$S_{ibt}^{dis}/\eta_i^d \le P_{ib}, \qquad \forall i\in I, b\in B, t\in T \tag{3.15}$$

$$0 \le P_{ib} \le P_{i,max} * \sigma_{ib}, \qquad \forall i\in I, b\in B \tag{3.16}$$

$$0 \le E_{ib} \le E_{i,max} * \sigma_{ib}, \qquad \forall i\in I, b\in B \tag{3.17}$$

$$\sum_{i\in I}\sum_{b\in B} \sigma_{ib} \le N_{es} \tag{3.18}$$

$$x_{bgt}, y_{bgt}, z_{bgt}, v_{bgt} \in \{0,1\}, \qquad \forall b\in B, g\in G, t\in T \tag{3.19}$$

$$G_{bgt}^C \ge 0, \qquad \forall b\in B, g\in G, t\in T \tag{3.20}$$

$$S_{ibt}, S_{ibt}^{ch}, S_{ibt}^{dis} \ge 0, \qquad \forall i\in I, b\in B, t\in T \tag{3.21}$$

$$X_k^{max} \ge 0, \qquad \forall k\in K, \tag{3.22}$$

$$X_{bkt}^{in}, X_{bkt}^{out} \ge 0, \qquad \forall b\in B, k\in K_b, t\in T \tag{3.23}$$

$$L_{bt}, Y_{bt} \ge 0, \qquad \forall b\in B, t\in T \tag{3.24}$$

The objective function (3.1) minimizes the sum of ESS and transmission line investment costs, operation cost of storage units, and conventional generators related costs. The objection function consists of five parts. The first term denotes the total fixed cost per installed energy and power rate of the storage technologies. The second term includes the total cost of the transmission lines depending on their capacities. The third term is the operation and maintenance cost for the storage units and depends on their discharge rates. The fourth term is the total penalty cost that occurs when demand exceeds the total supply. The last three terms represent the total generation cost of conventional generators which consists of three parts: no-load cost, variable cost, and start-up cost. No-load cost is the hourly fixed cost which is considered as the cost without an output. This cost applies when the generator unit is working at a particular time. Variable cost depends on the amount of electricity generated. Start-up cost occurs each time the generator is started-up.

Equation 3.2 ensures that the generator can be either started up or shut down in a period, if the generator does not work at the previous period and works at the current period, or it works at the previous period and does not work at the current period. Constraint 3.3 states that in one period the generator cannot be started up and shut down at the same period. We need to include these two constraints in our model since we have start-up costs and operating costs of conventional generators. Constraint 3.4 ensures the lead time is passed after a conventional generator started up. Maximum and minimum generating units of the generators are shown in 3.5. If the conventional generator is in the lead time period or if the conventional generator is off, then the generator cannot generate electricity. Otherwise, the generator can generate electricity within the limits. Ramp-up and ramp-down limits of the conventional generators are introduced by 3.6. Equation 3.7 indicates the balance at any bus and ensures the demand is satisfied by conventional and renewable generators and storage systems through adjacent transmission lines. Maximum transmission line capacities are restricted in 3.8 and 3.9. Equation 3.10 and 3.11 show that energy received from any adjacent buses through transmission lines for a bus should equal the energy sent from adjacent buses through transmission lines. Equation 3.12 ensures that the storage level cannot exceed the energy rate for any period. In 3.13, storage level is updated for all periods, which depends on the previous level and charge or discharge units in the current period. Equations 3.14 and 3.15 are the power rate capacities for all periods. Minimum and maximum physical capacity restrictions for power and energy rates for storage types are shown in 3.16 and 3.17. The last constraint (3.18) restricts the number of storage to be deployed in the grid. Constraint sets (3.19)-(3.24) represent variable domains.

The second formulation is shown below as "P2". It does not include investment decisions. Thus, E_{ib}, P_{ib}, and X_k^{max} are taken as parameters. Also, the objection function does not contain first and second terms as in (3.1).

P(2)

(3.25)

$$Min \sum_{i \in I} \sum_{b \in B} \sum_{t \in T} C_i^{OM} S_{ibt}^{dis} + \sum_{b \in B} \sum_{t \in T} C^{pen} Y_{bt}$$

$$+ \sum_{b \in B} \sum_{g \in G_b} \sum_{t \in T} C_g^{SU} y_{bgt} + \sum_{b \in B} \sum_{g \in G_b} \sum_{t \in T} C_g^{OM} G_{bgt} + \sum_{b \in B} \sum_{g \in G_b} \sum_{t \in T} C_g^{nl} x_{bgt}$$

subject to;

(3.26) $$y_{bgt} - z_{bgt} = x_{bgt} - x_{bg,t-1} \quad b \in B \quad g \in G_b \quad t \in T$$

(3.27) $$y_{bgt} + z_{bgt} \leq 1 \quad b \in B \quad g \in G_b \quad t \in T$$

(3.28) $$L_g * y_{bgt} \leq \sum_{t=t}^{t+L_g} v_{bgt} \quad b \in B \quad g \in G_b \quad t \in T$$

(3.29) $$G_g^{Cmin} * (x_{bgt} - v_{bgt}) \leq G_{bgt}^C \leq G_g^{Cmax} * (x_{bgt} - v_{bgt}) \quad b \in B \quad g \in G_b \quad t \in T$$

(3.30) $$rd_g \leq G_{bgt}^C - G_{bg,t-1}^C \leq ru_g \quad b \in B \quad g \in G_b \quad t \in T$$

$$\sum_{g \in G_b} G_{bgt}^C + \sum_{r \in R_b} G_{brt}^R - \sum_{k \in K_b} X_{kt}^{out} + \sum_{k \in K_b} X_{kt}^{in}$$

(3.31) $$+ S_{ibt}^{dis} + Y_{bt} = D_{bt} + S_{ibt}^{ch} \quad b \in B \quad t \in T$$

(3.32) $$X_{kt}^{in} \leq X_k^{max} \quad k \in K \quad t \in T$$

(3.33) $$X_{kt}^{out} \leq X_k^{max} \quad k \in K \quad t \in T$$

(3.34) $$S_{ibt} \leq E_{ib} \quad i \in I \quad b \in B \quad t \in T$$

(3.35) $$S_{ibt} = S_{i,b,t-1} + S_{ibt}^{ch} \eta_i^c - S_{ibt}^{dis} / \eta_i^d \quad i \in I \quad b \in B \quad t \in T$$

(3.36) $$S_{ibt}^{ch} \eta_i^c \leq P_{ib} \quad i \in I \quad b \in B \quad t \in T$$

(3.37) $$S_{ibt}^{dis} / \eta_i^d \leq P_{ib} \quad i \in I \quad b \in B \quad t \in T$$

(3.38)

3.3 Data Description

The electricity grid system of Sardinia Island, Italy is investigated which is the second-largest island in the Mediterranean Sea. Sardinia has a favorable climatic condition to generate electricity from renewable sources such as wind and solar.

Table 3.2 Sardinia Island: Electricity consumption and generation information

City	Thermal	Wind	Load	Hydro	Population (%)	Wind (MW)	T/H cap.(MW)
1.Algero	0	0	1	0	7.063		
2.Cagliari	0	1	1	0	40.80	100	
3.Codrongianos	0	1	1	0	20.82	314	
4.Fiumesanto	1	0	1	0	0		640
5.Ittırı	0	0	1	0	0		
6.Olbia	0	0	1	0	9.9		
7.Oristano	0	1	1	0	5.10	168	
8.Ottana	1	0	1	0	0		140
9.Sarlux	1	0	0	0	0		575
10.Selargius	0	0	1	0	4.77		
11.Sulcis	1	1	1	0	4.45	90	590
12.Taloro	0	0	0	1	5.81		240
13.Villasor	0	0	1	0	1.16		

In Table 3.2 provided by Terna, the biggest thirteen cities are shown. Thermal stations have existed in Fiumesanto, Ottana, Sarlux, and Sulcis. 11 buses are considered as a load center. Also, Sardinia is connected to the Italian Peninsula and French Island of Corsica through HVDC lines which are generally being used to transmit excess generated electricity. As the island has limited interconnections to the mainland, renewable energy plays a crucial role to satisfy the electricity demand along with the traditional generators. According to the data provided by Terna, Cagliari and Sassari provinces have the greatest shares in electricity consumption in 2015 with 46% and 15%, respectively. Almost 30% of the generated electricity is exported to the Italian Peninsula and Corsica. Figure 3.1, shows that most of the electricity demand is supplied by the thermal generators, while around 30% of it accounts for renewable sources. Keeping in mind that 30% of the generated energy is sent to the mainland and Corsica, if the reliability of renewable sources is increased, then the share of non-renewable generations can be reduced in Sardinia. High-reliability levels can be achieved by the energy storage systems integration in the grid.

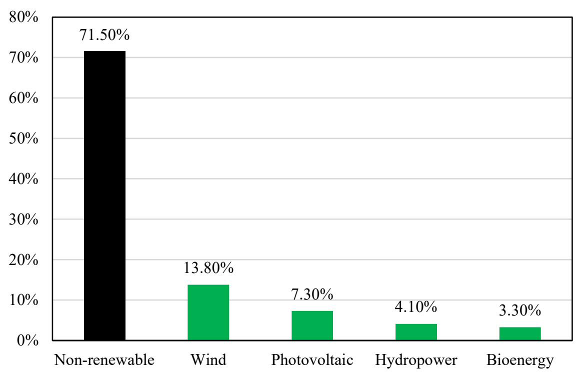

Figure 3.1 Structure of electricity supplied (TWh) in 2018 (Source: [Terna]).

The largest thermal plants are Fiumesanto, Ottana, Sarlux and Sulcis. The largest hydropower is located in Taloro with 240MW. Ramp rates are between 1.5-4% per minute. For coal-fired thermal plants, 2.5% ramp rate/minute is used for the experiments. Minimum outputs of the thermal generators are provided in Table 3.3. For coal-fired thermal stations, it is between 25-40% of nominal power. Start-up time is around 2 hours to 10 hours with a cost of less than $100/MW. The operating cost is around $20MWh. For hydropower, it is quite rapid to ramp up and down which is around 15% per minute. Start-up time is neglected as it takes only a few minutes to reach the nominal power. Minimum output is also neglected. Operating cost is around $10MWh.

As ESSs, Li-ion and PHS are chosen. For the experiments, moderate investment costs for ESSs from Table 2.1 are used. Also, variable costs, round-trip efficiencies, and transmission line construction costs are taken from Table 2.2.

Our experiment comprises of four wind farms with different installed powers. Particularly, wind farms shown in cities Cagliari, Oristano, Codrongiano, and Sulcis represent the aggregate of all small farms that are installed in the vicinity of these cities. Load centers are shown in Table 3.2 where all of the points are determined as load centers except Sarlux and Taloro.

Finally, we take 17 transmission lines that are readily available on the island. In Table 3.4, connected cities and transmission line numbers are shown. Since we want to solve a complete model, determination of the transmission line capacities is also considered. With the integration of storage systems, transmission lines capacities are expected to change. The original grid system is shown in Figure 3.2. Nodes take numbers from 1 to 13 as determined in Table 3.2.

Table 3.3 Technical characteristics of the coal-fired and hydropower generators.

	Coal-fired	Hydropower
Ramp rate (min/%)	1.5-4	15
Start-up cost ($\MWh)	100	0
Start-up time (hrs)	2	0
O&M cost ($\MWh)	20	10

Table 3.4 Connected cities in Sardinia Island.

Line #	Node 1	Node 2
1	Alghero	Fiumesanto
2	Alghero	Ittırı
3	Fiumesanto	Ittırı
4	Fiumesanto	Olbia
5	Codrongianos	Ittırı
6	Codrongianos	Olbia
7	Codrongianos	Oristano
8	Codrongianos	Ottana
9	Ottana	Taloro
10	Ittırı	Selargius
11	Ottana	Villasor
12	Oristano	Sulcis
13	Selargius	Villasor
14	Cagliari	Selargius
15	Cagliari	Villasor
16	Cagliari	Sulcis
17	Cagliari	Sarlux

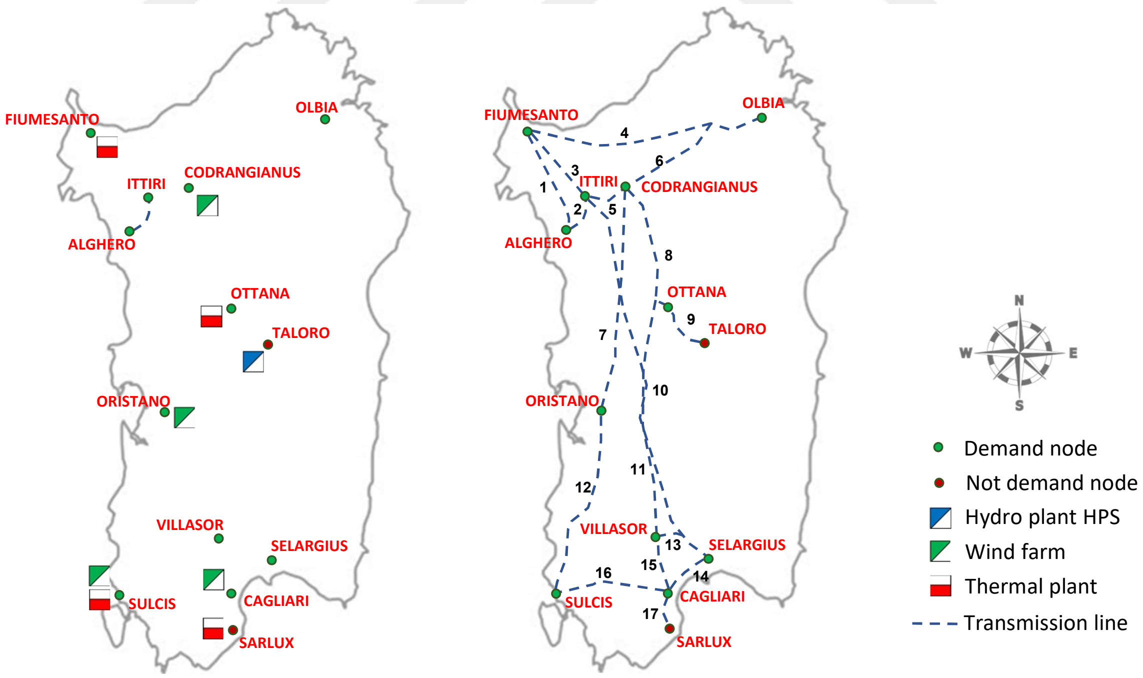

Figure 3.2 Original transmission network configuration for Sardinia Island.

.

3.3.1 Data description for wind and load

Sardinia Island's wind and load data are created based on the generated synthetic dataset from El-Hierro Island since the data of Sardinia for time periods are not available.

The average wind power is measured as 3.6 MWh while the installed wind power is 11.5 MW for El-Hierro Island. On average, wind turbines operate with a capacity of between 1/3 to 1/2 of the installed power. We generate wind data for the island of Sardinia on an hourly basis. We assume that the efficiency of the wind turbines are 50%. The installed wind powers for each bus are shown in Table 3.2 where the average maximum output of them reduces 50% and shown in Table 3.5. Multipliers for each node are used to adjust the El-Hierro data to Sardinia Island. Hence, we divided average maximum output of wind power in Sardinia Island to the average wind power (3.6 MWh) in El-Hierro island which is shown in the second row of the Table 3.5. Then, for each node that includes wind energy, we multiplied El-Hierro's data points with these multipliers to obtain the expected hourly wind data for Sardinia Island.

We generate the load data with a nearly the same method. Sum of the average loads calculated for each region of Sardinia Island covered in our experiment is 1015 MWh. Based on the population of the regions, the average electricity loads of regions vary between 414.12 and 11.8 MWh. But in El-Hierro Island, there is only one node with an average load of 5.03 MWh. So, in order to represent the load amount, we use multipliers for each city according to the El-Hierro's average load (see Table 3.5).

Table 3.5 Wind energy and load multipliers for each node.

		Algero	Cagliari	Codrangianos	Fiumesanto	Itturi	Olbia	Oristano	Ottana	Sarlux	Selargius	Sulcis	Taloro	Villasor
Ave.Max.Output (MWh)	Wind	-	50.00	157.00	-	-	-	49.45	-	-	-	45.00	-	-
Multiplier	Wind	-	13.89	43.61	-	-	-	13.74	-	-	-	12.50	-	-
Ave. Consumption (MWh)	Load	71.70	414.13	70.44	70.44	70.44	101.48	51.80	59.04	-	48.48	45.23	-	11.81
Multiplier	Load	14.25	82.33	14.00	14.00	14.00	20.17	10.30	11.74	-	9.64	8.99	-	2.35

3.4 Solution Methodology

As solving the problem for a grid system become more complex, a two-stage solution algorithm is proposed, as shown in Figure 3.3. In the model, there are two kinds of decisions to make which are investment and operational decisions. Investment decisions include energy storage siting and sizing as well as the transmission line capacity. Operational decisions include how much electricity is generated each period, how much demand is unsatisfied in each period, how much each ESSs charges or discharges in each period, what is the storage level in each period, and what is the status of conventional generators.

In the first stage, investment decisions are made in which P1 model is solved for each month separately. Then, the decisions for each month are investigated and averages of both investment decisions are taken to get the final decisions. Just for PHS, the average is taken if the storage size is greater than 100MWh which is taken as the technical installation limit for PHS. If the average is zero for ESS, then that ESS is not assigned to this bus. Similarly, if the average is zero or close to zero, the transmission line is not constructed between relevant nodes. Otherwise, storage systems' and transmission lines' capacities are saved.

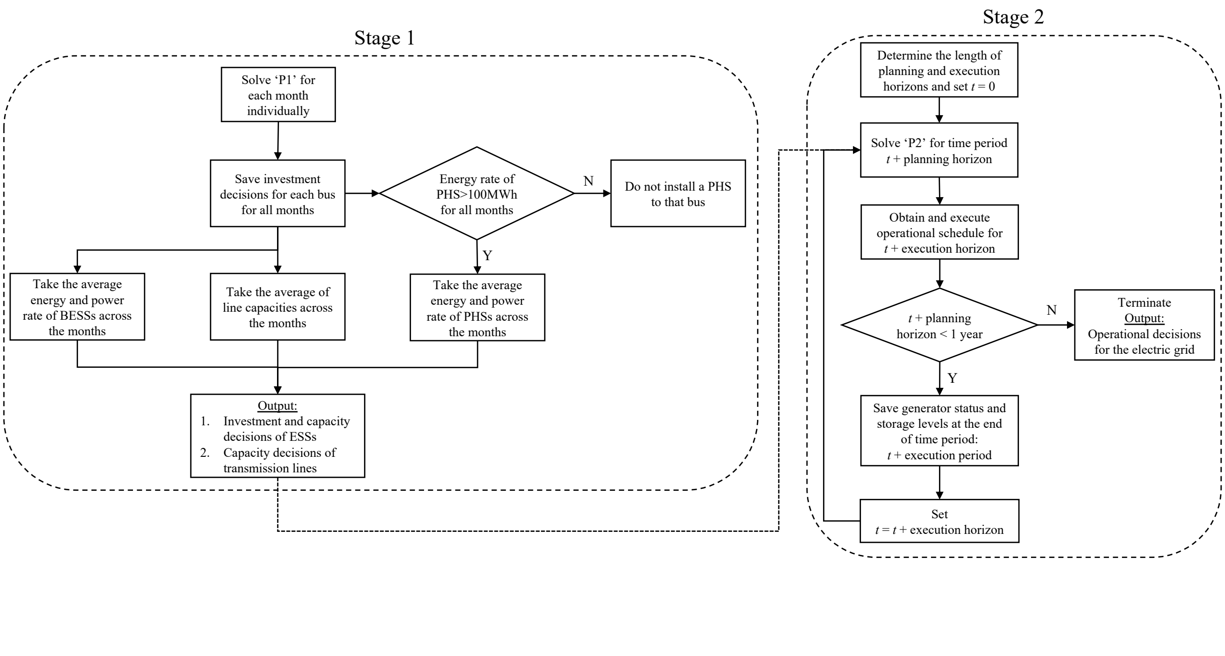

Figure 3.3 Two stage solution algorithm

After the determination of investment decisions, "P2" model is solved with a method called rolling horizon optimization for fixed location and size of ESSs, and fixed capacity of transmission lines. At this step, the model is solved for planning horizon. After solving the model, the operational decisions are saved just for only execution horizon Then, the last data points of the execution horizon are stored in order to be used as the initial data of the next period. Finally, planning and execution horizons are shifted. This algorithm continues until models are solved for each data point which is 8760.

3.5 Experimental Results

The numerical study includes two different experiments. In our first experiment, we allow both battery and PHS installations, how in the second experiment we only allow battery installation. Our main motivation behind the second experiment is that the PHS option can only be applied to geographies that are suitable to construct PHS. Hence, without allowing the PHS installation, we wanted to understand the general behavior of the model in cases where the geography is not appropriate to deploy PHSs but BESSs.

As explained, first the investment decisions are made by solving the model for 12 months separately. For the first experiment, investment decisions are first made for PHS and transmission lines and for the second one, battery and transmission lines investments are obtained. After obtaining the investment decisions, we solve the model hourly and for one year. So, the time slot of the model is 8760 hours. To have the operational decisions, we split the model into 365 parts. A model is solved for 48 hours, then the first 24 hours decisions are obtained and recorded. Then, we use the information as initial data for the next time period which is solved from t=24 to t=72. The initial data is required for the storage level and conventional generators status. This algorithm continues until we solve the model for all time periods, which is 8760 for our model. By taking the time shift as 24 hours, the model is solved 365 times.

3.5.1 First Experiment

In Table 3.6, energy and power rates for ESSs are shown for both experiments. For the first one out of 13 buses, PHS is constructed to 11 buses. The remaining two locations are Sarlux and Taloro where both are not load center but have thermal and hydropower stations. Among the regions, Codrongianos, which has the largest wind farm with 314MW, has the largest installed PHS. It is also the second most populated load center and provides electricity to the four neighboring regions when it is necessary. The second-largest PHS belongs to Cagliari, the most populated region of the island. The ratio of energy rate to power rate varies between 0.82 to 3.22.

Out of 17 transmission lines, 15 transmission lines are constructed according to the results, shown in Table 3.7. Between Codriangons and Oristano, the transmission line is not constructed. Codriangos has the largest wind power, and thus model chooses to construct the transmission lines to the regions which have neither wind power nor thermal stations. However, Oristano includes a wind farm. Besides, it also has a connection to Sulcis which has a thermal station with 590MW. So like this example, some transmission lines can be replaced by storage technologies.

At stage two, among the regions which have the thermal stations, throughout one year, Fiumesanto generates the electricity the most. It is logical because Fiumesanto has the greatest thermal station. None of the conventional generators are shut down throughout the year.

All generated wind energy is either stored or distributed to the load centers at each period, so there is no unused wind energy in this experiment.

Table 3.6 Energy and power rates for two experiments.

	Experiment 1		Experiment 2	
Node	Energy Rate (MWh)	Power Rate (MW)	Energy Rate (MWh)	Power Rate (MW)
Algero	343	198	75	20
Cagliari	698	352	510	107
Codrongianos	1153	357	480	67
Fiumesanto	223	161	21	10
Ittırı	538	203	100	18
Olbia	503	316	206	33
Oristano	618	435	333	34
Ottana	346	368	0	0
Sarlux	0	0	0	0
Selargius	367	228	121	32
Sulcis	100	25	0	0
Taloro	0	0	0	0
Villasor	260	315	24	10

Table 3.7 Transmission line capacities for two experiments.

	Experiment 1	Experiment 2
Line #	Tr. line cap.(MW)	Tr. line cap.(MW)
1	751	76
2	155	0
3	673	80
4	519	83
5	426	14
6	342	26
7	0	0
8	192	37
9	358	42
10	0	0
11	43	0
12	303	32
13	19	0
14	366	52
15	196	11
16	183	185
17	288	288

3.5.2 Second Experiment

In the second experiment, out of 13 buses, battery storage is constructed for 9 buses. Ottana, Sarlux, Sulcis, and Taloro are the regions without battery storage installation. Their common feature is that they all have electricity generation facilities. Similar to the first experiment, Cagliari and Codrangianos has the largest installed batteries which are the two regions with the most wind energy. The ratio of energy rate to power rate varies between 3.75 to 9.79.

Out of 17 transmission lines, 12 transmission lines are constructed according to the results, shown in Table 3.6. Between Algero-Ittırı, Codrangianos-Oristano, Ittırı-Selargius, Ottana-Villasor, and Selargius-Villasor, transmission lines are not invested. Villasor does not have a wind farm or electricity generation facility, it is only a load center. Thus, this region needs to get energy from its neighbors. According to results, it is only connected to Cagliari which provides enough energy to satisfy the demand. Similarly, Algero is a load center and gets the energy only from Fiumesanto.

For this experiment, again Fiumesanto is the leader of the electricity generation. None of the conventional generators are shut down throughout the year.

Almost 25% of the generated wind energy cannot be used and sent to the earth. It is mainly because of having less storage capacity or less transmission line capacities, and thus, generated electricity from renewables can not be used at some time periods.

3.5.3 Comparison of the Experiments

In both experiments, ESSs and transmission lines are invested at various places. However, mainly due to their costs, determined locations and installed capacities are different. In Figure 3.4, the sum of the capacities of ESSs for all buses and the sum of the capacities for all lines are shown for two experiments. PHS's capacity is almost 2.75 times larger than the battery's capacity. Likewise, invested transmission line capacities of the first experiment are five times larger than the second experiment.

Because of the reasonable investment and operating costs of the PHS, it is the most popular ESS in the world. Similarly for our example, due to the high costs of batteries, our model chooses to invest less in them. Therefore, the usage of renewable energy is reduced. This also affects the transmission line capacities. Since the stored amount of renewable energy reduces, energy transmission between cities also decreases. That leads to an increase in electricity generation from thermal stations.

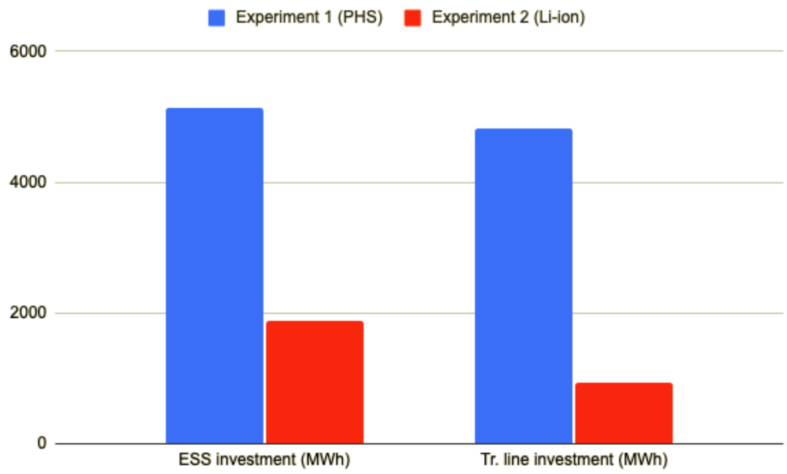

Figure 3.4 Investment decisions for two experiments

In Figure 3.5, the generation types and their percentage of usages for the whole year are shown. In our setting, demand can be met by conventional generators, wind power, and ESS. If the demand cannot be satisfied in any period, then this amount of demand is penalized. For the first experiment, 70.2% of the electricity is satisfied by conventional generators. However, in the second one, it increases to 75.3%. A small portion of the electricity is satisfied by ESSs for both experiments. As a result of the wider installation of transmission lines and ESSs, usage of wind energy is higher and conventional generators usage is lower in the first experiment.

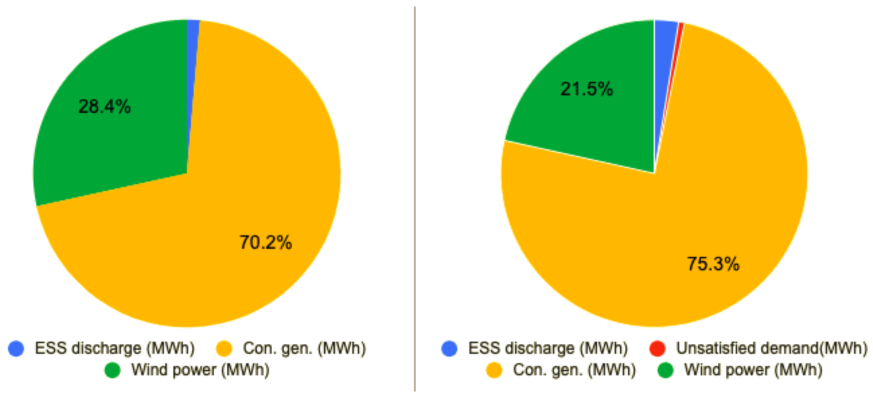

Figure 3.5 Percentages of electricity used based on generation type
Left: First experiment, Right: Second Experiment

Costs are also compared and investigated for two experiments. In Figure 3.6, the share of the cost components on total cost is shown. As discussed in the solution methodology, the total investment cost is found in the first stage and O&M cost for

ESS, start-up and O&M cost for generators, and penalty cost of not satisfying the demand are found in the second stage. Since the generators are never shut-down in the experiments, this cost is not included in the Figure 3.6. Also, the penalty cost for unsatisfied demand is kept larger than the other cost parameters to decrease the share of unsatisfied demand. For this reason, the penalty cost is also ignored in Figure 3.6 as it would not be logical to compare this cost to others.

In the first experiment, the greater share belongs to transmission line investment costs (47%) which are followed by ESSs' (PHS) investment cost in the total cost and conventional generators cost. In the second experiment, on the other hand, more than half of the total cost consist of generator O&M cost. Due to the less transmission line investment compared to the first experiment, only 17% of the total cost consist of transmission line investment cost. For both experiments, although shares of total ESS investment and O&M costs are close to each other (30% and 29% for investment and 0.05% and 2% for O&M cost) total investment amounts are different as also depicted in Figure 3.4.

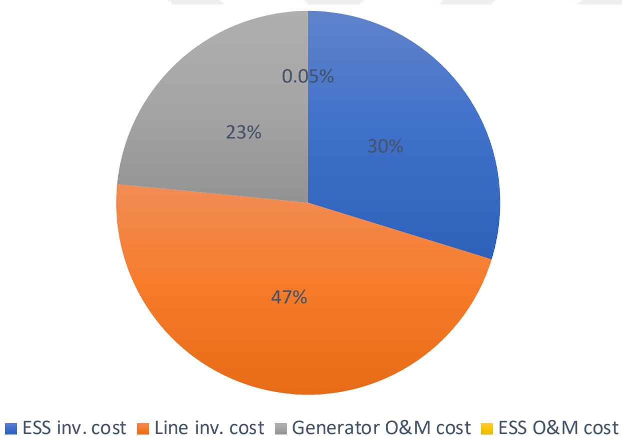

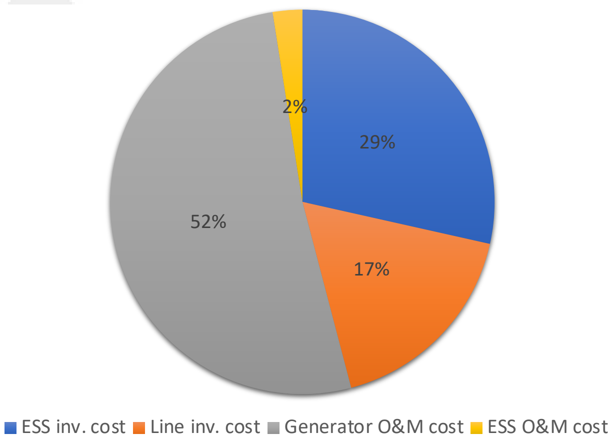

Figure 3.6 Percentages of cost components
Left: First experiment, Right: Second Experiment

When the costs are compared, the operating cost of ESSs for the second experiment is 5 times higher than the first one. In Figure 3.7, ESS's and transmission line's investment cost, and conventional generator's O&M costs are compared for two experiments. As ESSs at the first experiment are invested more than twice as much as ESSs in the second experiment, the investment cost is greater for the first one. Transmission line cost is also greater at the first experiment since both the capacities are larger and the number of invested transmission lines are higher. Finally, the O&M cost for conventional generations is very close to each other where the second experiment yields a slightly higher O&M cost.

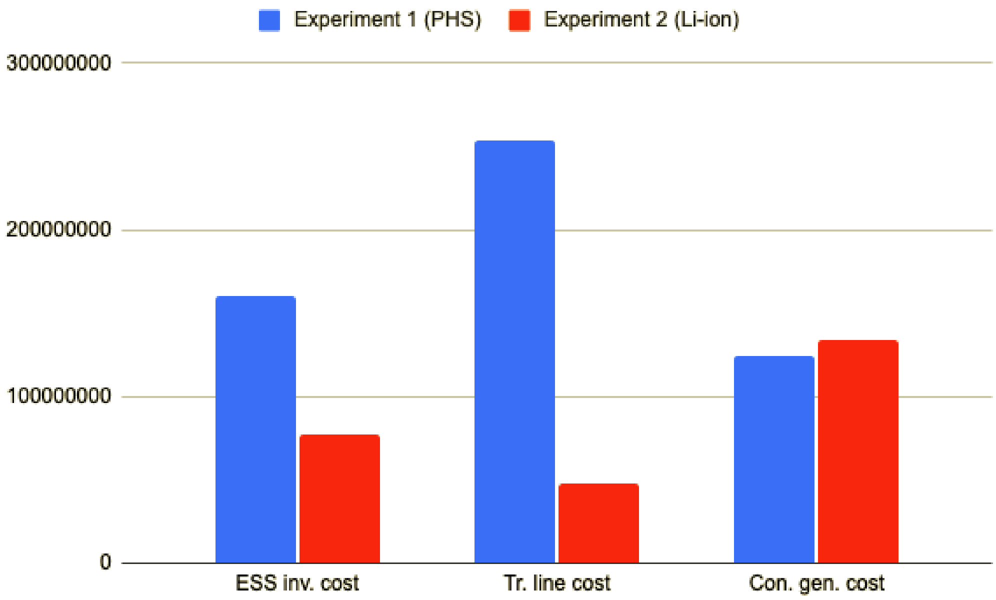

Figure 3.7 Investment costs and conventional generators' O&M cost for both experiment

The original transmission network configuration is shown in Figure 3.2, and this configuration is changed according to the solutions of both experiments. Since we have a choice to install ESSs to the grid, which has a positive effect on the usage of renewable sources, some of the transmission lines may not be invested. In the first experiment, compared to the original system, two transmission lines are not invested, however, in the second one, this number increases to five (see Table 3.8). More importantly, the second configuration splits into two smaller sub-networks. That means, two separate and independent transmission line networks are constructed when the ESS changes.

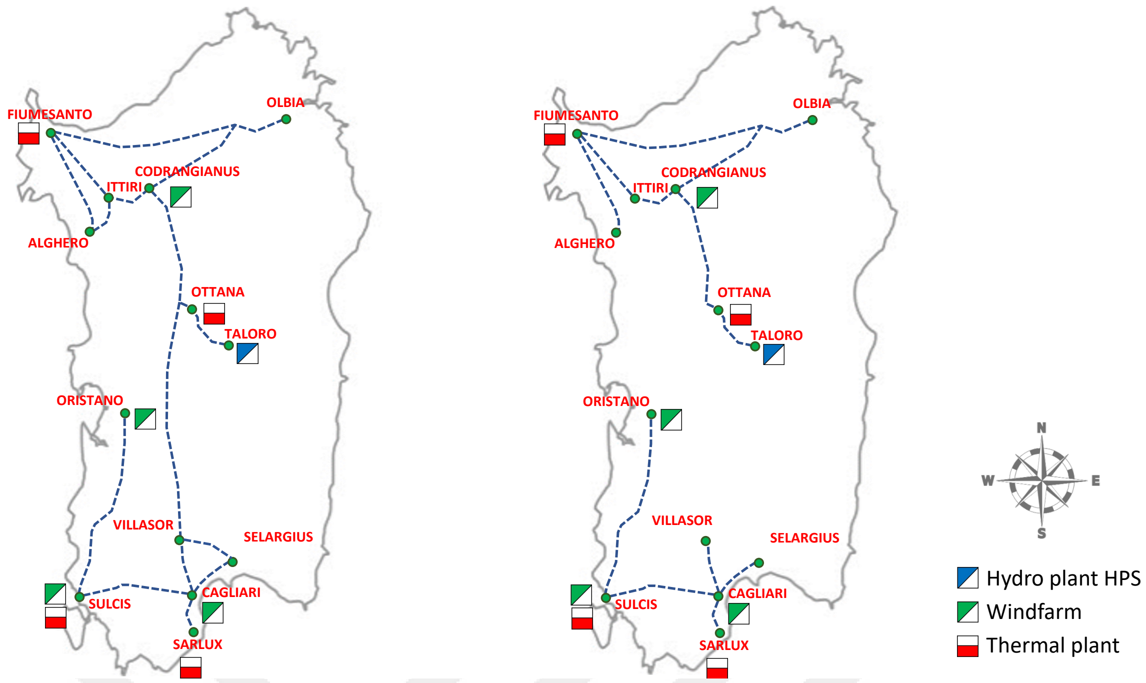

Figure 3.8 Transmission network configurations for the (Left) First experiment, (Right) Second experiment.

3.5.4 Sensitivity analysis on the second stage of the algorithm

As discussed in solution methodology, the second stage of the algorithm is solved for planning horizon of 48 hours and the solution is recorded for execution horizon of 24 hours. In our sensitivity analysis we specify the horizon length settings as [execution horizon-planning horizon] hours. We test two different set of sensitivity analysis. In group 1 runs, for a fixed planning horizon of 48 hours we solved the model for varying execution horizons as $[24-48]$, $[12-48]$, and $[6-48]$ hours. In group 2, for a fixed execution horizon of 24 hours we change the planning horizons as $[24-72]$, $[24-240]$, and $[24-480]$ hours. We note that the first run $[24-48]$ corresponds to our base case setting and we compare the quality of solutions with respect to that particular case. Although we report the solution time for each run, our main performance metric is the optimal objective function value.

In Table 3.8, the improvements in objective function value and solution times are represented. According to the results of the first group of runs, the greatest difference of objective function values is 2.6%. In the second test, the differences ranges between 1.1% and 4.4%. When the solution times are considered, the total cost which is reached with the original time slot provides a satisfying gap. The maximum gap which is 4.4% increases the solution time almost 20 times. So, the original time slot is sufficient to solve the mathematical model.

Table 3.8 Sensitivity analysis results on the execution and planning horizons.

	Group 1 runs			Group 2 runs		
Execution-Planning horizon (hours)	[24 – 48]	[12 – 48]	[6 – 48]	[24 – 72]	[24 – 240]	[24 – 480]
Improvement in obj. func. value	-	1.5%	2.6%	1.1%	1.2%	4.4%
Solution time (secs)	457	690	1920	660	2820	8500

3.6 Conclusion

In this study, the electricity grid system with renewable and conventional power plants for an island system is discussed. A MILP where the objective is minimizing the total system cost is developed to find the capacity of PHS and batteries and their location on the grid. Moreover, determining the capacities of the transmission lines between nodes is also included in the model. In order to have a realistic model, some conventional generators' properties are added to the problem. A two-stage algorithm is proposed to solve this model. In the first stage, investment decisions are determined by solving "P1" for each month. After determining the locations and sizes of the storage systems and transmission line capacities, a heuristic algorithm is used to find the operational decisions with a time-shifted method. Two experiments are conducted: in the first one PHS and battery storage can be invested, and in the second one, only battery storage can be invested. Even though the battery may be invested in the first experiment, battery investment is not observed due to their costs. The main results of this experiment are as follows:

- ESSs are not invested in the nodes which are not load centers but have conventional generator stations.
- In nodes where renewable energy production is high, the capacities of the installed ESSs are usually high.
- When PHS is allowed to be installed, there is no unused wind energy, they are either stored or distributed to the load centers.

- When only battery storage can be invested, %25 of the wind energy remains unused.
- When PHS and battery technology are compared, we see that PHS investments are larger than battery storage investments. Thus, the transmission line capacities are larger when PHS investments are done. The underlying reason for this is that the investment and O&M cost of PHS is more reasonable. The system with larger capacity storage requires more transmission line capacity.
- In the experiments with PHS installation, the transmission line has the greatest share among the cost components, however, in the experiments with battery storage installation, the O&M cost dominates the total system cost due to the high O&M cost of battery technologies.

4. ESSs with Solar Energy

In this chapter, an electricity system for an island with solar energy, which is one of the most common types of renewable energy, is discussed. Specifically, solar PVs are considered to generate electricity. The same mathematical model in Chapter 2 is used.

The production characteristics of solar energy and wind energy are very different from each other. Although a slight increase in wind power is observed in the evening hours on El-Hierro island data we have used earlier, it varies at each day and each month and has no specific daily and hourly production pattern in general. However, as we know, solar energy produces energy during daylight and this production gradually decreases after the sunset. It has a much more predictable production variability than wind power. Therefore, the aim is to observe the differences and similarities of these two renewable energy sources on the island electrical system which is explained in Chapter 2. The configuration is the same and only renewable energy source is switched to solar PV energy instead of wind energy. The main variables to be observed are the investment variables such as ESSs and transmission line investments. For this problem, Model P(1S) is solved.

In Figure 4.1, wind, solar, and consumption data hourly averages for one year at El-Hierro Island are shown. On average, wind and consumption data are more or less similar to each other in all hours. However, solar energy doubles the consumption data during the hours when the sun is at its peak. Wind energy can be expected to be stored in the early morning hours and released at noon when we look at the hourly averages. However, since the wind varies a lot from day to day, excess wind energy may be stored for one full day, while another daylight wind may cause the stored energy to be used all day. However, since solar energy is produced almost every day during the daytime and almost no energy is produced at night, the daily storage usage requirement is higher compared to a system with wind power. That is, the energy stored during daylight hours is usually released when there is no sun.

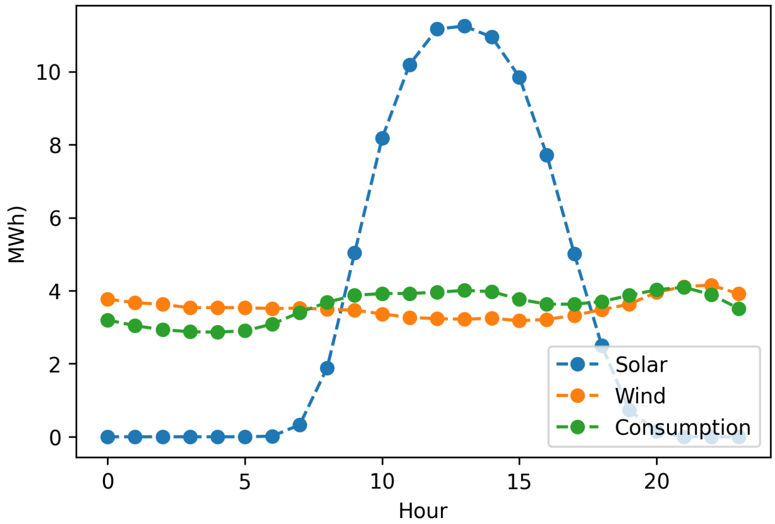

Figure 4.1 Wind, solar, and consumption hourly averages

4.1 Data description

For El-Hierro Island, solar PV data for hourly time periods is not available. For this reason, the dataset of solar PV production is gathered from Menorca Island. In order to fairly compare the wind and solar energy, solar PV data is recalibrated according to the total wind energy produced in a year on the island of El-Hierro. That means the yearly aggregate produced energy of both sources are equal to each other, but the solar generation profile is not that of El-Hierro which is off the coast of Western Sahara, but that of Spanish Islands in the Mediterranean. Therefore, the results should not perceived as valid for the island of El-Hierro. To create the synthetic solar PV data series, the same method applied for the load data is used.

The same synthetic load data for El-Hierro Island is used for the experiments.

All other parameters are taken from the chapter two including investment and O&M costs, efficiencies of ESSs, and diesel cost.

4.2 Experimental Design

As in the previous chapter, the experiments involve different ESSs investment costs and O&M costs for battery technology which is shown in 2.1. As we observe in the result of Chapter 2 experiments that the PHS location and load profile do not have much of an impact on both the total cost and installation decisions, they are not included in this experiment. Only two different location alternatives are included which are the closest and the farthest point to the load center. In the experiments, moderate consumption data is used, where the wind energy produced and the consumption are equal in a total of one year. All other parameters are the same as the ones in Chapter 2. So, the model is solved for 90 instances; there are fifteen ESSs investment costs, three O&M costs, and two PHS locations in the experiment.

4.3 Experimental Results

Out of 90 instances, battery and PHS are invested in 26 and 78 instances, respectively. In 14 instances, both battery and PHS are invested. Instances which have the lowest investment cost are the majority of cases with battery placement.

Instances with the highest objective function values are those where PHS and battery installation are the most expensive and PHS is close to the load center. Only PHS installation is observed in these instances. Instances with the highest objective function values are those where the battery installation and O$M cost are the cheapest. In these instances, only battery installation is observed. After these instances, the lowest total costs are observed in the instances of PHS with the lowest installation cost.

First of all, unlike the system with wind power, no significant relationship is observed between the average total and average diesel costs of the instances when solar power is used (Figure 4.2). Likewise, the total invested energy rate of ESSs does not directly affect the total cost as shown in Figure 4.3. As shown in Table 4.1, diesel cost accounts for 56 percent of the total cost. In addition, transmission line and ESS investments are relatively higher than other costs.

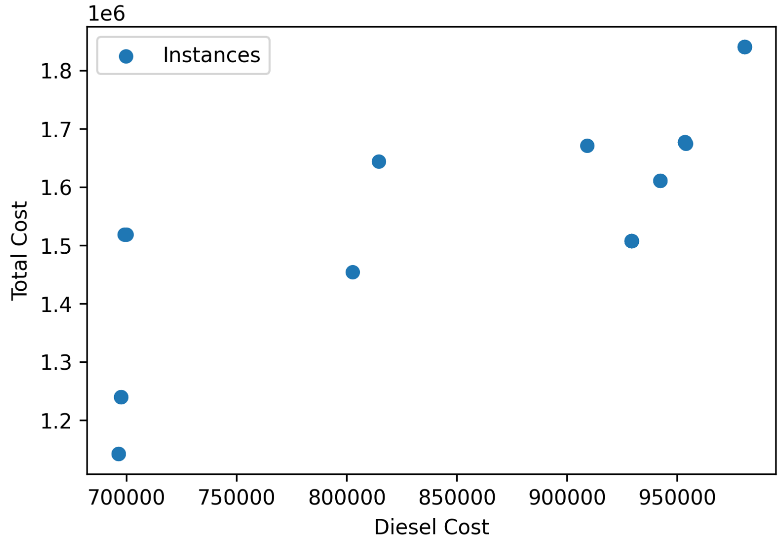

Figure 4.2 Diesel cost effect on total cost

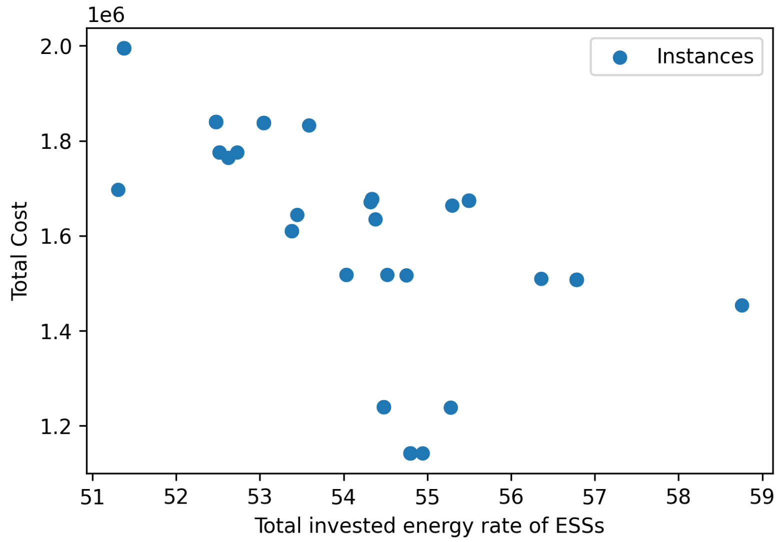

Figure 4.3 Effect of sum of battery and PHS energy rate on total cost

Table 4.1 Cost averages($)

	Mod. Load
Diesel cost	903,254
O&M cost for battery	38,635
O&M cost for PHS	2,508
Battery investment cost	49,711
PHS investment cost	398,808
Tr. line investment cost	227,323
Total cost	1,620,241.87
Diesel cost %	0.56

The location of the PHS has an impact on this problem as well. As the PHS gets closer to the load center, we see that the total and diesel costs increase slightly. Also, when PHS is invested close to the load center, transmission line investment cost increases. In the instances where PHS is invested, there is usually energy transfer from the solar farm to the PHS. For this reason, when the PHS is invested, the capacity of the line between the PHS and the wind farm is generally higher than the other line (PHS to load center). This results in an increase in transmission line cost as the distance between the wind farm and PHS increases. This is the main reason for the increase in total cost in these instances.

Finally, the investment of both storage types is investigated separately, as the relations with the total amount of invested ESSs and total cost and diesel cost are not very clear. In Figure 4.4 at the left-hand side, the relation between invested energy and power rates of ESSs and the total cost is shown. We can observe that total cost increases when PHS investment increases and total cost decreases when BESS investment increases in general. On the right-hand side, diesel cost is taken instead of total cost and both upper and lower figures provide a more clear pattern. Again when the investment of BESS increases, diesel cost decreases, and when the investment of PHS increases, diesel cost increases. At first glance, we see that diesel cost increases as the PHS investment increases, which is an unexpected and surprising result. However, when we look at the data points more carefully, we see in the right upper and lower figures that the diesel cost decreases when the PHS investment increases in the instances where only PHS is invested as ESSs, which are 51MW and above installations. All of the PHS investments of 51 MW (energy rate) and below are invested with the battery.

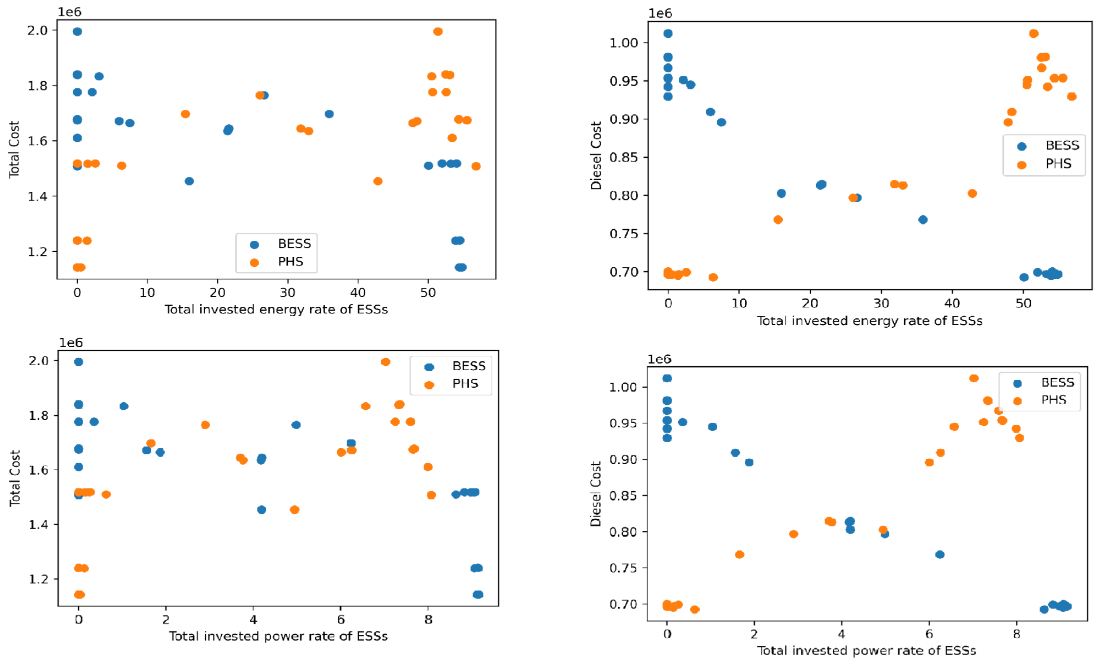

Figure 4.4 Effect of sum of battery and PHS energy rate on total cost

4.4 Comparison of two island systems: Wind and Solar

In this section, two different island systems are compared. While the first one uses wind energy as a renewable source, the other one has solar PV with the same yearly total generation amount with wind. In order to have a fair comparison, 90 instances explained above are used for both systems.

Invested energy rates are generally higher when wind power is used. In Figure 4.5, both BESS and PHS investment energy rates are shown. It is clear that, except in some instances, wind energy requires more energy rate and thus greater capacity than solar PV energy. This might make sense because the variability of the wind is much greater than that of the solar. The wind may be strong for days in a row and produce energy every day that may remain unused and has to be stored. In order to store this excess energy, the main required investment is the energy rate. Similarly, wind may be light for several days and in order to meet the demand with a reduced cost, higher energy capacity is required. However, exact the opposite is observed in power rate investments. An island system with solar PV needs more power rate investments for ESSs than an island system with the wind as seen in Figure 4.6. In the solar PV system, the battery and PHS power rates are almost twice that of the wind system. One of the most important reasons for this is that the output variability of the solar is low and storage systems are usually charged and discharged during the day. Therefore, more power rate is needed for storage systems.

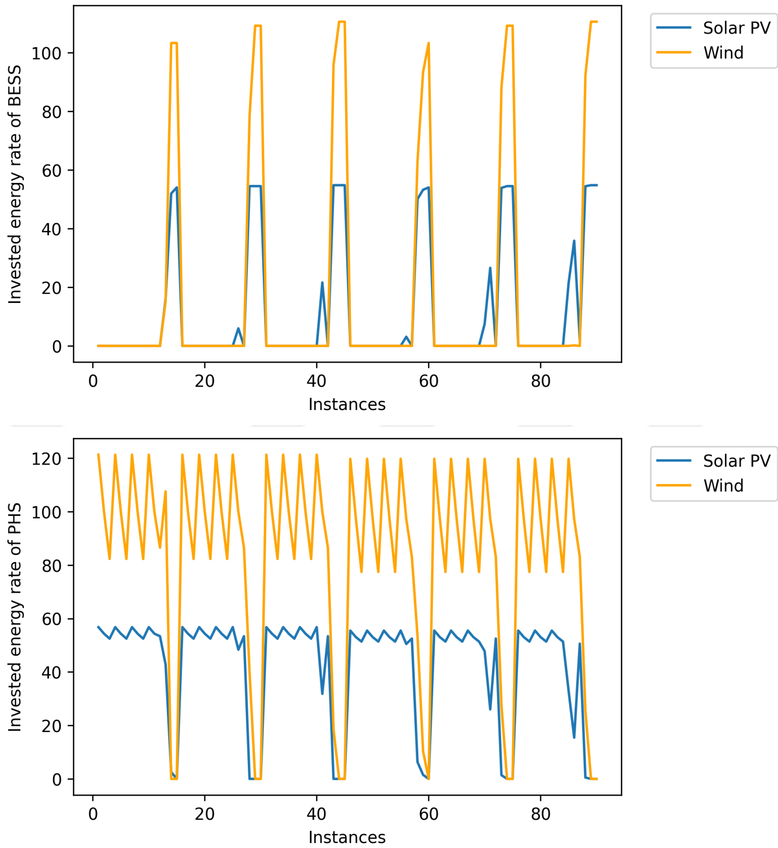

Figure 4.5 Invested energy rates at each instances for BESS and PHS for wind and solar system

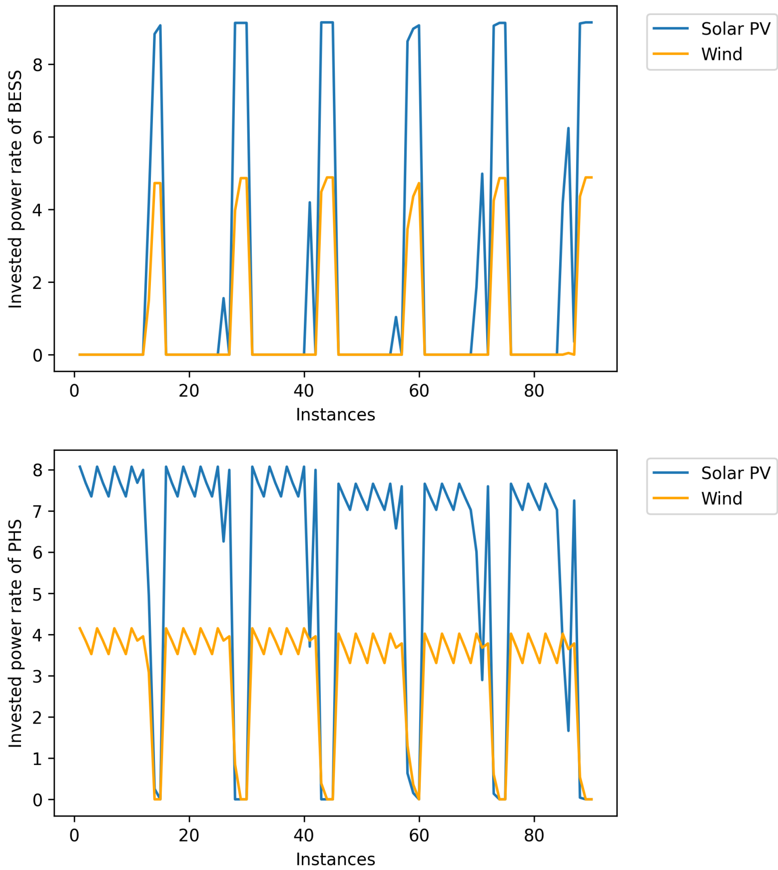

Figure 4.6 Invested power rates at each instances for BESS and PHS for wind and solar system

In the system where solar energy is used, more investment is made in transmission lines in almost every instance compared to the wind system, also shown in Figure 4.7. As discussed above, this is largely due to the output variability difference between the two renewable energy sources. Firstly, since PHS is installed in most instances and energy is transferred to PHS through lines, generally, the 1st lines have higher capacity. Since solar energy has a daily pattern that tends to store more, the transmission line capacity increases in the system with solar energy. Since the wind energy system is more variable and stores relatively less energy, transmission line capacities are relatively lower. Similarly, transmitted energy during a day from renewables to load center is higher in solar energy, which increases the invested transmission line capacity.

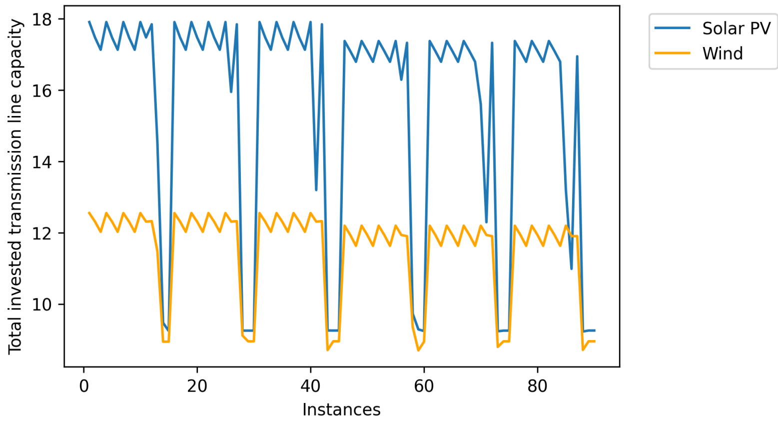

Figure 4.7 Total invested transmission line capacities for wind and solar system

4.4.1 Cost Comparison

Total system cost, diesel cost, investment costs, and O&M for both systems are compared. All instances averages for all costs are shown in Table 4.2. Taking the average of all instances, the total cost is approximately 18% lower for the solar PV system than the wind system. Also, in Figure 4.8, it is shown that in all instances total system cost of the wind system is higher than the solar system. Diesel usage is also lower in the solar system, reduced by almost 37% compared to the wind system. In Figure 4.9, it is shown that for all instances, diesel cost is higher in wind systems. Diesel usage percentage is 56 for solar systems and 73 for wind systems. We can say that solar system' renewable source usage is higher. One of the reasons for this is that it can generally meet its electricity needs during the day from solar PVs. As a result of this, as will be mentioned below, transmission line investments are higher than the wind system.

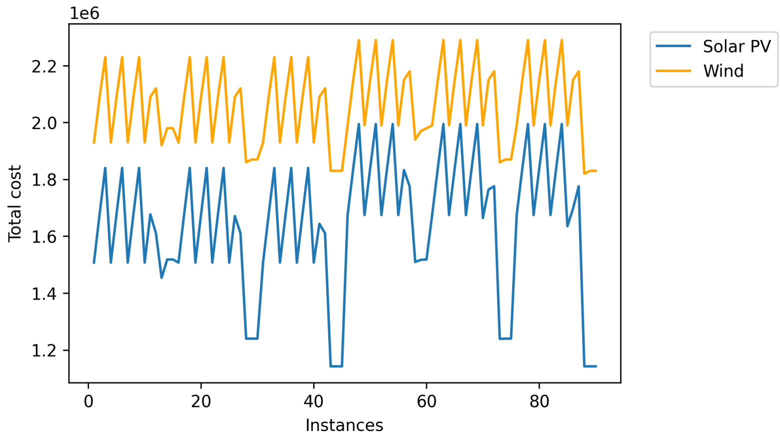

Figure 4.8 Total costs by instances for wind and solar system

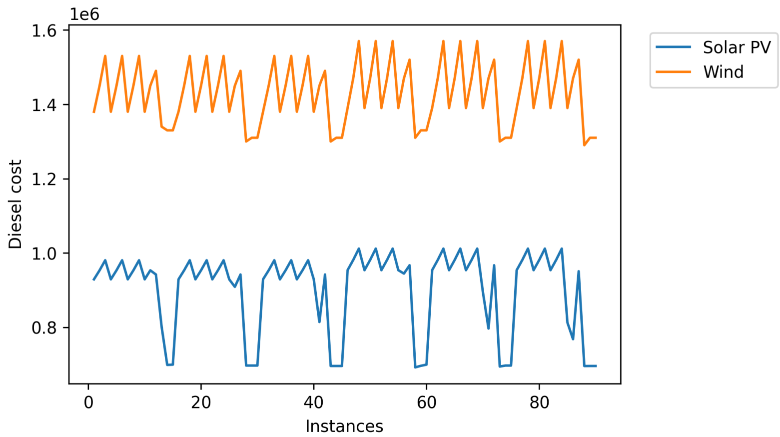

Figure 4.9 Diesel costs by instances for wind and solar system

In 26 instances battery storage is invested in the solar system, however, this number decreases to 19 for the wind system. When we examine the instances one by one, we see that in all instances where the battery storage is installed in the wind system, the battery storage is installed for the solar system as well. However, in these instances, the installed energy rate in the wind system is higher and the power rate is lower. Apart from those instances, there are 7 more instances where battery installations are done in the solar system. In conclusion, battery storage installation cost for solar system is higher than wind system, on the average, but not for all instances. PHS investment cost is higher in almost all instances for the solar system. In 78 and 79 instances PHS is invested in wind system and solar system, respectively. Again, the total investment cost of PHS is higher in the solar system. For all instances, comparison of investment costs of solar and wind system for battery technology and PHS are shown in Figure 4.10 and 4.11, respectively. Both storage system investment cost is shown in Figure 4.12, and most of the instances, solar PV system's

ESSs energy and power rate investments and thus, the ESSs investment costs are higher.

O&M cost is also higher in the solar system. Since O&M cost depends on the storage discharge rate, we can say that in the solar system ESSs charge and discharge more frequently than wind system.

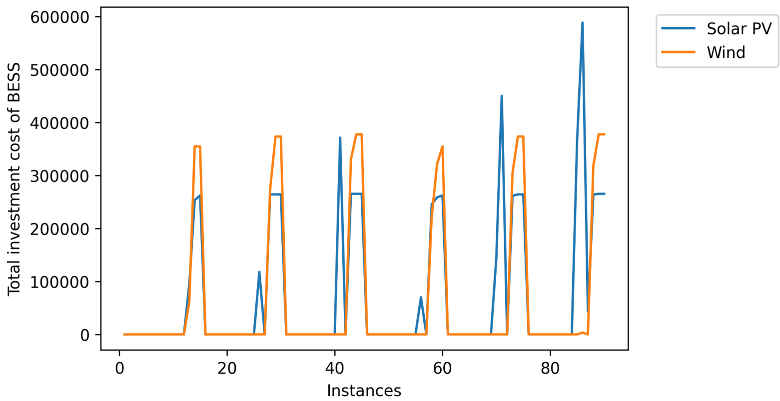

Figure 4.10 Battery investment costs for wind and solar system

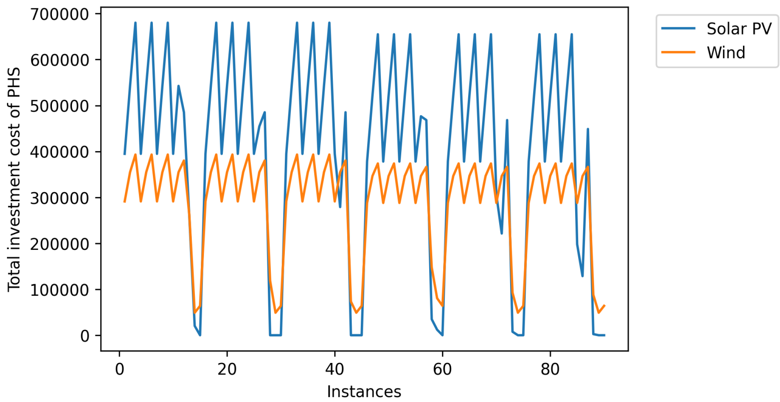

Figure 4.11 PHS investment costs for wind and solar system

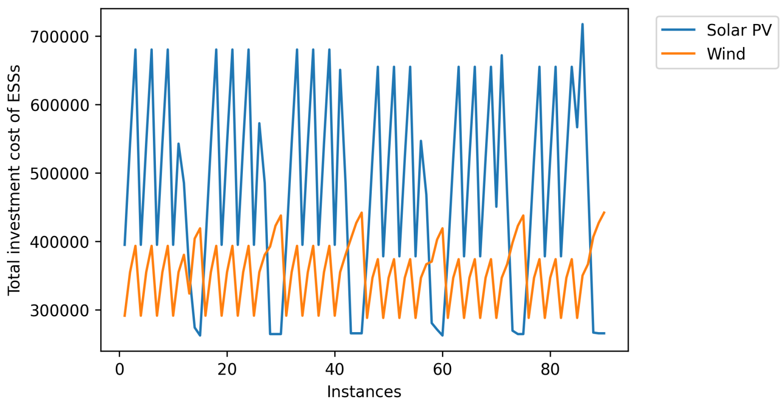

Figure 4.12 ESSs investment costs for wind and solar system

Finally, transmission line cost is higher than wind system for all instances in solar system, also shown in Figure 4.13. This cost increases sharply when the PHS is located close to the load center.

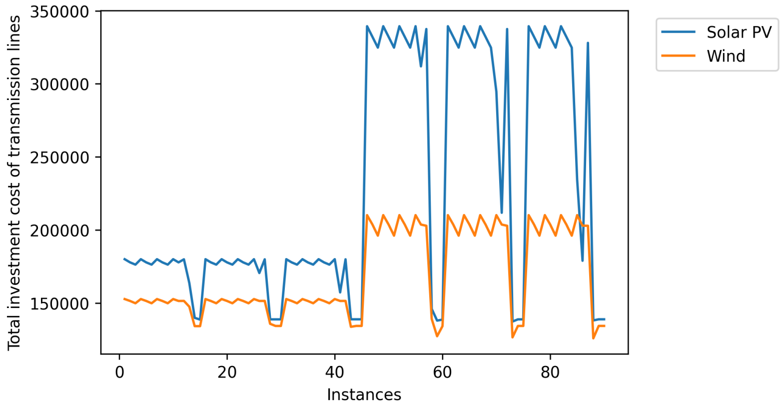

Figure 4.13 Transmission line investment costs for wind and solar system

Table 4.2 Cost averages($) for Solar PV and Wind power

	Solar PV	Wind
Diesel cost	903,254	1,439,222
O&M cost for battery	38,635	21,152
O&M cost for PHS	2,508	1,010
Battery investment cost	49,711	46,667
PHS investment cost	398,808	302,139
Tr. line investment cost	227,323	172,176
Total cost	1,620,241	1,982,368
Diesel cost %	0.56	0.73

4.5 Conclusion

In this chapter, we consider an island system with solar power and a diesel system. It is identical to the electricity system that is considered in Chapter 2. The total yearly output of both renewable sources is equal to each other. The investment decisions, location of PHS, and cost components are interpreted according to experiments. Also, similarities and differences of these two renewable energy sources on the island system are observed. As a result, similar to the wind system, ESSs investment amounts and decisions are highly correlated with the costs of ESSs. Location of PHS affects the transmission line investment; when the PHS gets closer to the load center, the transmission line investment and its cost increase. Given the output characteristics of both renewable sources, the solar system requires more power rate compared to the wind system, however, the wind system requires more energy rate than the solar system. As a result, the solar system's renewable energy usage is higher and thus, the diesel usage is lower.

5. Conclusion

An energy transformation towards renewable sources is inevitable due to increased energy needs and limited conventional sources, but most importantly, for local environmental and global warming concerns. However, the pace of this transformation rests critically on the ultimate cost of renewable sources that have highly variable and intermittent generation profiles that needs to be smoothed out by electricity storage systems which may also account for a major part of their cost. Among the energy storage systems, the technology with the highest installed power in the world is PHSs, and has been around since hydroelectric power. However, PHSs depend highly on the geography and themselves be quite controversial given their demand for valuable land. BESSs are also used in large-scale electricity systems, and especially lithium-ion batteries are at the forefront of the fastest-growing energy technologies provided the increased adoption of renewable sources. BESSs are particularly required for some level of production smoothing at the generation site, which otherwise may lose considerable production capacity during peak times. Therefore, such systems must contain BESSs at the local sites as well as PHSs that help better match supply with the demand at the system level.

This dissertation is concerned with finding the optimal location and sizing of ESSs with renewable energy sources in an electricity systems. As ESSs, especially PHS and battery technologies are discussed, which are at the forefront of storage technologies, which are discussed at length in the introductory chapter along with the other relevant background information about renewable energy sources, electricity systems, application areas of ESSs, and ESSs types are discussed.

In the second chapter, the electrical system of an island with a single transmission line is considered. In this system, electricity is supplied by a wind farm and diesel generator and the former is sent to the load center via a transmission line along which a PHS opportunity is also available. Since the operational decisions are highly difficult to incorporate accurately, an MILP is formulated under Sample Average Approximation approach. This model is solved for the optimal sizing of two different storage technologies considering the hourly wind generation and electricity consumption data of El-Hierro Island of Spain in the Atlantic Ocean. A total of 675 instances are created for a detailed what-if analysis. These instances are determined by considering different investment costs for ESSs and transmission lines, different O&M costs for ESSs, three different load profiles, and different PHS locations. Due to PHSs' lower cost it is not surprising to see larger amounts of energy is is invested for PHS. In majority of cases, higher investments in ESSs are also characterized by lower total cost which means that the storage systems are attractable options for island systems where diesel is used as an alternative. In this setting the impact of location of PHS is negligible.

In the third chapter, a transmission grid system is examined. The nodes in this system can be generation and load centers or both. Generator units can be both a set of conventional generators and wind farms. What makes this problem more difficult is also the consideration of conventional generation restrictions such as on/off status and ramp-up and down constraints. The purpose of this problem is to optimally locate and size the PHS and battery storage technologies.

However, the problem is much smaller than many realistic grid systems, current computational technologies are not very effective at solving it. In addition, considering hourly operational control makes the model very difficult, if not impossible, to solve. Therefore, we proposed a two-stage heuristic method to solve this problem of location and sizing model. In the first phase, the investment decisions such as ESSs locations and sizes and transmission line capacities are made. With investment fixed investment decisions, operating decisions are determined, and objection function value is reached in the second phase. In the experiments, Sardinia Island's transmission grid system is investigated which includes 17 transmission lines connecting 13 nodes. Two different experiments are carried out; in the first one, PHS and battery storage investment are allowed, but only PHS investment could be invested due to the reasonable investment costs, and in the second, only battery storage investment is allowed. The results reveal that PHS is invested almost 2.5 times larger than battery storage capacity which reduces more conventional generator's output and increases renewable sources' output. This leads to lower total system costs when PHS is invested compared to battery storage. Also, transmission line capacities are larger in the first experiment since more capacity is needed to store or discharge the energy from PHS. Thanks to ESSs investments wind energy usage reaches 100% and 75% for the first and second experiment, respectively. Change in ESSs type even may change the system configuration. The experiments show that the network is connected in the system with PHS, however, two separate networks are observed when the battery storage is used. All of these results are based on the heuristic solutions of our system, however, the ability to economically invest in

BESSs might lead to sub-grids that are sort of partitions within the entire grid.

The fourth chapter investigates an island system that is identical to the system in Chapter 2. This time, wind power is switch to solar PV power. Wind and solar PV yearly outputs are equalized in order to be able to make a comparison among the two systems. Systems are similar to each other in terms of investment decisions, however, it is revealed that the system with wind power requires more energy rate, whereas solar PV requires more power rate. This result stems from different output characteristics of both renewable sources. Location of PHS affects the transmission line cost and investment energy and power rates. When PHS gets closer to the load center costs increase and investment decreases. In comparison to the system with wind generation, the location of PHS has more impact on the system with solar power.

While we aim to provide a rather comprehensive treatment of the problem, our work opens up new avenues for research, some are immediate and some require further elaboration. One of the major assumptions of our models is that storage systems may have arbitrary energy and power rates. While it may be a plausible assumption for BESSs, only a discrete set of capacity pairs may be feasible for PHSs. Hence, a model including such decisions through a discrete framework is needed. A second immediate future work is a thorough study of computational approaches for the grid systems. While a commercial optimizer can solve a considerably small island system, they fail simply due to massive memory requirements. It is important to test a comprehensive set of heuristics on a wide variety of grid systems.

To investigate the issues relating to ESSs this work has assumed that the generation units are already established with known capacities. An integrated approach can be devised that also includes the investment decisions on renewable generators and disinvestment of conventional generators integrated with the storage and transmission line decisions. Thus, in addition to reducing the total investment and operating cost of the entire system, the efficiency of renewable resources and storage systems can also be increased. This would be a major undertaking that also require effective solution techniques.

While this dissertation an some of future work consider a single investment decision opportunity, in truth, energy systems require a long term approach. Most generators, conventional or renewable, as well as transmission lines are expensive investments and they serve a long time. Therefore, replacement of conventional sources with the renewable ones cannot be achieved overnight, which entails excessive costs. Therefore, multi-period framework for investment and disinvestment decisions is necessary for the grid systems where conventional generators that are already installed will be slowly replaced by renewable sources over the years. In addition, potential future improvements in energy storage technologies, especially batteries, may also be incorporated in such a modeling framework as well as the changing adoption levels of distributed storage developments, i.e, increased use of electric vehicles, which apart from its obvious function may also be used as a small storage system for a household.

Finally, all these approaches are from that of a single decision maker which designs and controls the entire system. In reality, most grid systems are characterized by multitude of ownership structures. Most commonly, there are large number of production companies that may own a few of the production capacities and make production decisions based on the price formation dynamics in the electricity market. Such firms would also be responsible for ESS decisions at their locations. Transmission lines may also be operated by a single or a few firms, who may also need to make energy storage decisions in the system as a way to better match supply with demand. There are also companies that may own the distribution grid networks, i.e. at a city or a region which are termed as demand nodes. Such companies already utilize some storage facilities that are needed for voltage regulation and preventing short term black-outs. However, they may also consider storage facilities for the sole purpose of efficient matching of the demand and supply, which is not relevant in our context as it would be a better decision not to employ any ESSs at the load centers. While the governments may dictate certain decisions hence increasing the value of our approaches that aim to find the global optimal solutions, they nonetheless cannot do so verbatim, but only may develop policies or incentives that help obtain a good system-wide solution.

BIBLIOGRAPHY

Global energy storage database | energy storage systems. https://www.sandia.gov/ess-ssl/global-energy-storage-database/. (Accessed on 10/12/2020).

Gyrobus: The flywheel-powered public transportation | amusing planet. https://www.amusingplanet.com/2019/02/gyrobus-flywheel-powered-public.html. (Accessed on 10/12/2020).

Round-up: 60mwh japan project, northern ireland's 10mw array and imergy goes for africa teleco | energy storage news. https://www.energy-storage.news/news/round-up-60mwh-japan-project-northern-irelands-10mw-array-and-imergy-goes-f. (Accessed on 10/12/2020).

Operating plants | beacon power. https://beaconpower.com/operating-plants/, 2014. (Accessed on 09/02/2020).

ABB. Abb wins orders of over $300 million for world's first 1,100 kv uhvdc power link in china. https://new.abb.com/news/detail/13922/abb-wins-orders-of-over-300-million-for-worlds-first-1100-kv-uhvdc-power-link-in-china. (Accessed on 10/12/2020).

C. Abbey and G. Joós. A stochastic optimization approach to rating of energy storage systems in wind-diesel isolated grids. *IEEE Transactions on power systems*, 24(1):418–426, 2008.

U. E. I. Administration. Use of electricity. https://www.eia.gov/energyexplained/electricity/use-of-electricity.php. (Accessed on 10/12/2020).

A. A. Akhil, G. Huff, A. B. Currier, B. C. Kaun, D. M. Rastler, S. B. Chen, A. L. Cotter, D. T. Bradshaw, and W. D. Gauntlett. *DOE/EPRI 2013 electricity storage handbook in collaboration with NRECA*. Sandia National Laboratories Albuquerque, NM, 2013.

A. A. Akhil, G. Huff, A. B. Currier, B. C. Kaun, D. M. Rastler, S. B. Chen, A. L. Cotter, D. T. Bradshaw, and W. D. Gauntlett. Doe/epri electricity storage handbook in collaboration with nreca. *Sandia national laboratories*, 2015.

H. Alharbi and K. Bhattacharya. Stochastic optimal planning of battery energy storage systems for isolated microgrids. *IEEE Transactions on Sustainable Energy*, 9(1):211–227, 2017.

G. Alva, Y. Lin, and G. Fang. An overview of thermal energy storage systems. *Energy*, 144:341–378, 2018.

J. S. Anagnostopoulos and D. E. Papantonis. Pumping station design for a pumped-storage wind-hydro power plant. *Energy Conversion and Management*, 48(11):3009–3017, 2007.

BPEnergy. Bp statistical review of world energy. *London, UK*, 2021.

K. Brokish and J. Kirtley. Pitfalls of modeling wind power using markov chains. In *2009 IEEE/PES Power Systems Conference and Exposition*, pages 1–6. IEEE, 2009.

P. D. Brown, J. P. Lopes, and M. A. Matos. Optimization of pumped storage capacity in an isolated power system with large renewable penetration. *IEEE Transactions on Power systems*, 23(2):523–531, 2008.

A. Carpinone, M. Giorgio, R. Langella, and A. Testa. Markov chain modeling for very-short-term wind power forecasting. *Electric Power Systems Research*, 122: 152–158, 2015.

E. D. Castronuovo, J. Usaola, R. Bessa, M. Matos, I. Costa, L. Bremermann, J. Lugaro, and G. Kariniotakis. An integrated approach for optimal coordination of wind power and hydro pumping storage. *Wind Energy*, 17(6):829–852, 2014.

P. Chen, T. Pedersen, B. Bak-Jensen, and Z. Chen. Arima-based time series model of stochastic wind power generation. *IEEE transactions on power systems*, 25(2): 667–676, 2009.

S. Chen, H. B. Gooi, and M. Wang. Sizing of energy storage for microgrids. *IEEE Transactions on Smart Grid*, 3(1):142–151, 2011.

E. A. Committee. Bottling electricity: storage as a strategic tool for managing variability and capacity concerns in the modern grid. *A report by the Electricity Advisory Committee*, 2008.

J. Conti, P. Holtberg, J. Diefenderfer, A. LaRose, J. T. Turnure, and L. Westfall. International energy outlook 2016 with projections to 2040. Technical report, USDOE Energy Information Administration (EIA), Washington, DC (United States . . . , 2016.

W. E. Council. World energy resources 2016. *World Energy Council, London, UK*, 2016.

M. Densing. Dispatch planning using newsvendor dual problems and occupation times: Application to hydropower. *European Journal of Operational Research*, 228(2):321–330, 2013.

K. Dvijotham, M. Chertkov, and S. Backhaus. Storage sizing and placement through operational and uncertainty-aware simulations. In *2014 47th Hawaii international conference on system sciences*, pages 2408–2416. IEEE, 2014.

J. Eyer and G. Corey. Energy storage for the electricity grid: Benefits and market potential assessment guide. *Sandia National Laboratories*, 20(10):5, 2010.

J. M. Eyer, P. C. Butler, and J. J. Iannucci Jr. Estimating electricity storage power rating and discharge duration for utility transmission and distribution deferral: a study for the doe energy storage program. Technical report, Sandia National Laboratories, 2005.

R. Fernández-Blanco, Y. Dvorkin, B. Xu, Y. Wang, and D. S. Kirschen. Optimal energy storage siting and sizing: A wecc case study. *IEEE transactions on sustainable energy*, 8(2):733–743, 2016.

H. L. Ferreira, R. Garde, G. Fulli, W. Kling, and J. P. Lopes. Characterisation of electrical energy storage technologies. *Energy*, 53:288–298, 2013.

L. Fiorini, G. A. Pagani, P. Pelacchi, D. Poli, and M. Aiello. Sizing and siting of large-scale batteries in transmission grids to optimize the use of renewables. *IEEE Journal on Emerging and Selected Topics in Circuits and Systems*, 7(2):285–294, 2017.

P. Fraser. Distributed generation in liberalised electricity markets. In *Second international symposium on distributed generation: power system and market aspects (Stockholm, 2-4 October 2002)*, pages 1G–12, 2002.

K. Garus. Hvdc platform sylwin alpha is complete | offshore wind industry. https://www.offshorewindindustry.com/news/hvdc-platform-sylwin-alpha-complete, 07 2014. (Accessed on 10/12/2020).

D. M. Gioutsos, K. Blok, L. van Velzen, and S. Moorman. Cost-optimal electricity systems with increasing renewable energy penetration for islands across the globe. *Applied energy*, 226:437–449, 2018.

T. Gonen. *Electrical power transmission system engineering: Analysis and design*. CRC press, 2011.

I. Hadjipaschalis, A. Poullikkas, and V. Efthimiou. Overview of current and future energy storage technologies for electric power applications. *Renewable and sustainable energy reviews*, 13(6-7):1513–1522, 2009.

P. Harsha and M. Dahleh. Optimal management and sizing of energy storage under dynamic pricing for the efficient integration of renewable energy. *IEEE Transactions on Power Systems*, 30(3):1164–1181, 2014.

B. P. Hayes, A. Wilson, R. Webster, and S. Z. Djokic. Comparison of two energy storage options for optimum balancing of wind farm power outputs. *IET Generation, Transmission & Distribution*, 10(3):832–839, 2016.

W. He and J. Wang. Optimal selection of air expansion machine in compressed air energy storage: A review. *Renewable and Sustainable Energy Reviews*, 87:77–95, 2018.

F. Hocaoglu, O. Gerek, and M. Kurban. The effect of markov chain state size for synthetic wind speed generation. In *Proceedings of the 10th International Conference on Probablistic Methods Applied to Power Systems*, pages 1–4. IEEE, 2008.

IEC. Electrical energy storage. https://www.iec.ch/whitepaper/pdf/iecWP-energystorage-LR-en.pdf. (Accessed on 10/13/2020).

Irena. Innovation landscape brief: Flexibility in conventional power plants. https://www.irena.org/-/media/Files/IRENA/Agency/Publication/2019/Sep/IRENA_Flexibility_in_CPPs_2019.pdf?la=en&hash=AF60106EA083E492638D8FA9ADF7FD099259F5A1, 2019. (Accessed on 03/15/2021).

P. Kanakasabapathy and K. S. Swarup. Bidding strategy for pumped-storage plant in pool-based electricity market. *Energy conversion and Management*, 51(3):572–579, 2010.

R. Kempener and E. Borden. Battery storage for renewables: Market status and technology outlook. *International Renewable Energy Agency, Abu Dhabi*, page 32, 2015.

H.-Y. Kim. Statistical notes for clinical researchers: assessing normal distribution (2) using skewness and kurtosis. *Restorative dentistry & endodontics*, 38(1):52–54, 2013.

J. H. Kim and W. B. Powell. Optimal energy commitments with storage and intermittent supply. *Operations research*, 59(6):1347–1360, 2011.

M. Kopp, D. Coleman, C. Stiller, K. Scheffer, J. Aichinger, and B. Scheppat. Energiepark mainz: Technical and economic analysis of the worldwide largest power-to-gas plant with pem electrolysis. *International Journal of Hydrogen Energy*, 42 (19):13311–13320, 2017.

M. Korpaas, A. T. Holen, and R. Hildrum. Operation and sizing of energy storage for wind power plants in a market system. *International Journal of Electrical Power & Energy Systems*, 25(8):599–606, 2003.

L. Kuznia, B. Zeng, G. Centeno, and Z. Miao. Stochastic optimization for power system configuration with renewable energy in remote areas. *Annals of Operations Research*, 210(1):411–432, 2013.

X. Luo, J. Wang, M. Dooner, and J. Clarke. Overview of current development in electrical energy storage technologies and the application potential in power system operation. *Applied energy*, 137:511–536, 2015.

T. T. Mai, P. Jadun, J. S. Logan, C. A. McMillan, M. Muratori, D. C. Steinberg, L. J. Vimmerstedt, B. Haley, R. Jones, and B. Nelson. Electrification futures study: Scenarios of electric technology adoption and power consumption for the united states. Technical report, National Renewable Energy Lab.(NREL), Golden, CO (United States), 2018.

A. Malheiro, P. M. Castro, R. M. Lima, and A. Estanqueiro. Integrated sizing and scheduling of wind/pv/diesel/battery isolated systems. *Renewable Energy*, 83: 646–657, 2015.

Z. Melhem. *Electricity transmission, distribution and storage systems.* Elsevier, 2013.

K. Mongird, V. V. Viswanathan, P. J. Balducci, M. J. E. Alam, V. Fotedar, V. S. Koritarov, and B. Hadjerioua. Energy storage technology and cost characterization report. Technical report, Pacific Northwest National Lab.(PNNL), Richland, WA (United States), 2019.

H. Nfaoui, H. Essiarab, and A. Sayigh. A stochastic markov chain model for simulating wind speed time series at tangiers, morocco. *Renewable Energy*, 29(8): 1407–1418, 2004.

A. Nourai, V. Kogan, and C. M. Schafer. Load leveling reduces t&d line losses. *IEEE Transactions on Power Delivery*, 23(4):2168–2173, 2008.

H. Pandžić, Y. Wang, T. Qiu, Y. Dvorkin, and D. S. Kirschen. Near-optimal method for siting and sizing of distributed storage in a transmission network. *IEEE Transactions on Power Systems*, 30(5):2288–2300, 2014.

D. Pudjianto, M. Aunedi, P. Djapic, and G. Strbac. Whole-systems assessment of the value of energy storage in low-carbon electricity systems. *IEEE Transactions on Smart Grid*, 5(2):1098–1109, 2013.

W. Qi, Y. Liang, and Z.-J. M. Shen. Joint planning of energy storage and transmission for wind energy generation. *Operations Research*, 63(6):1280–1293, 2015.

C. A. S. Rangel, L. Canha, M. Sperandio, and R. Severiano. Methodology for ess-type selection and optimal energy management in distribution system with dg considering reverse flow limitations and cost penalties. *IET Generation, Transmission & Distribution*, 12(5):1164–1170, 2017.

Y. Rebours and D. Kirschen. What is spinning reserve. *The University of Manchester*, 174(175), 2005.

S. Rehman, L. M. Al-Hadhrami, and M. M. Alam. Pumped hydro energy storage system: A technological review. *Renewable and Sustainable Energy Reviews*, 44: 586–598, 2015.

h. . https://www.ren21.net/reports/global-status-report/. m. . . y. . . n. . A. RenGSR, title = Renewables Global Status Report - REN21.

M. Ross, R. Hidalgo, C. Abbey, and G. Joós. Energy storage system scheduling for an isolated microgrid. *IET renewable power generation*, 5(2):117–123, 2011.

R. Rudervall, J. Charpentier, R. Sharma, et al. High voltage direct current (hvdc) transmission systems technology review paper. *Energy week*, 2000:2, 2000.

A. D. Sahin and Z. Sen. First-order markov chain approach to wind speed modelling. *Journal of Wind Engineering and Industrial Aerodynamics*, 89(3-4):263–269, 2001.

I. Sarbu and C. Sebarchievici. A comprehensive review of thermal energy storage. *Sustainability*, 10(1):191, 2018.

A. Shamshad, M. Bawadi, W. W. Hussin, T. Majid, and S. Sanusi. First and second order markov chain models for synthetic generation of wind speed time series. *Energy*, 30(5):693–708, 2005.

R. Sioshansi, P. Denholm, T. Jenkin, and J. Weiss. Estimating the value of electricity storage in pjm: Arbitrage and some welfare effects. *Energy economics*, 31(2):269–277, 2009.

Statista. Eu-28: renewable electricity generation share 2018. https://www.statista.com/statistics/862421/renewable-electricity-generation-source-shares-european-union-eu-28/, 2018. (Accessed on 10/13/2020).

B. Steffen and C. Weber. Optimal operation of pumped-hydro storage plants with continuous time-varying power prices. *European Journal of Operational Research*, 252(1):308–321, 2016.

J. Tang, A. Brouste, and K. L. Tsui. Some improvements of wind speed markov chain modeling. *Renewable Energy*, 81:52–56, 2015.

Terna. Home - terna spa. https://www.terna.it/en. (Accessed on 02/18/2021).

T. Weitzel and C. H. Glock. Energy management for stationary electric energy storage systems: A systematic literature review. *European Journal of Operational Research*, 264(2):582–606, 2018.

P. Yang and A. Nehorai. Joint optimization of hybrid energy storage and generation capacity with renewable energy. *IEEE Transactions on Smart Grid*, 5(4):1566–1574, 2014.

M. Zidar, P. S. Georgilakis, N. D. Hatziargyriou, T. Capuder, and D. Škrlec. Review of energy storage allocation in power distribution networks: applications, methods and future research. *IET Generation, Transmission & Distribution*, 10(3):645–652, 2016.